

AD _____

Award Number: DAMD17-97-1-7211

TITLE: Cell-Cell Adhesion and Insulin-Like Growth Factor I
Receptor in Breast Cancer

PRINCIPAL INVESTIGATOR: Marina A. Guvakova, Ph.D.
Ewa Surmacz, Ph.D.

CONTRACTING ORGANIZATION: Thomas Jefferson University
Philadelphia, Pennsylvania 19107

REPORT DATE: September 1999

TYPE OF REPORT: Annual

PREPARED FOR: U.S. Army Medical Research and Materiel Command
Fort Detrick, Maryland 21702-5012

DISTRIBUTION STATEMENT: Authorized for Release;
Distribution Unlimited.

The views, opinions and/or findings contained in this report are those of the author(s) and should not be construed as an official Department of the Army position, policy or decision unless so designated by other documentation.

20000828 225

REPORT DOCUMENTATION PAGE

Form Approved
OMB No. 074-0188

Public reporting burden for this collection of information is estimated to average 1 hour per response, including the time for reviewing instructions, searching existing data sources, gathering and maintaining the data needed, and completing and reviewing this collection of information. Send comments regarding this burden estimate or any other aspect of this collection of information, including suggestions for reducing this burden to Washington Headquarters Services, Directorate for Information Operations and Reports, 1215 Jefferson Davis Highway, Suite 1204, Arlington, VA 22202-4302, and to the Office of Management and Budget, Paperwork Reduction Project (0704-0188), Washington, DC 20503

1. AGENCY USE ONLY (Leave blank)

2. REPORT DATE

September 1999

3. REPORT TYPE AND DATES COVERED

Annual

(15 Aug 98 -14 Aug 99)

4. TITLE AND SUBTITLE

Cell-Cell Adhesion and Insulin-Like Growth Factor I Receptor in Breast Cancer

5. FUNDING NUMBERS

DAMD17-97-1-7211

6. AUTHOR(S)

Marina A. Guvakova, Ph.D.

Ewa Surmacz, Ph.D.

7. PERFORMING ORGANIZATION NAME(S) AND ADDRESS(ES)

Thomas Jefferson University
Philadelphia, Pennsylvania 19107

8. PERFORMING ORGANIZATION
REPORT NUMBER

E-MAIL:

Marina.Guvakova@mail.tju.edu

9. SPONSORING / MONITORING AGENCY NAME(S) AND ADDRESS(ES)

U.S. Army Medical Research and Materiel Command
Fort Detrick, Maryland 21702-5012

10. SPONSORING / MONITORING
AGENCY REPORT NUMBER

11. SUPPLEMENTARY NOTES

12a. DISTRIBUTION / AVAILABILITY STATEMENT

Authorized for Release;
Distribution Unlimited.

12b. DISTRIBUTION CODE

13. ABSTRACT (Maximum 200 Words)

The structural disintegration of normal epithelium is an early manifestation of cancer in mammary gland. Yet our knowledge on mechanisms controlling breast epithelial cell adhesion is still rudimentary. The increased content of the insulin-like growth factor I receptor (IGF-IR) and its close homologue the insulin receptor (IR) has been well documented in human breast cancer specimens. In this study we investigated how these hormone receptors modulate cell adhesion in breast carcinoma cells.

Previously we developed MCF-7 human breast cancer cells overexpressing the IGF-IR. The major achievement of this work is the establishment of a new model consisting of MCF-7-derived cells overexpressing the IR that allowed the comparison of IR and IGF-IR functions. Our results strongly confirmed the specificity of the IGF-IR in promoting the large non-invasive tumor aggregates on biological matrix. For the first time we demonstrated that in breast cancer cells IGF-IR tyrosine kinase modulates the intercellular balance of β -catenin, the element of E-cadherin/catenin cell-cell adhesion complex.

We continued to explore anti-tumor potentials of the antiestrogens and found that a synthetic steroid analog ICI 182,780 is a potent inhibitor of non-invasive breast tumor aggregates in three-dimensional culture.

14. SUBJECT TERMS

Breast Cancer

15. NUMBER OF PAGES

65

16. PRICE CODE

17. SECURITY CLASSIFICATION
OF REPORT

Unclassified

18. SECURITY CLASSIFICATION
OF THIS PAGE

Unclassified

19. SECURITY CLASSIFICATION
OF ABSTRACT

Unclassified

20. LIMITATION OF ABSTRACT

Unlimited

NSN 7540-01-280-5500

Standard Form 298 (Rev. 2-89)
Prescribed by ANSI Std. Z39-18
298-102

FOREWORD

Opinions, interpretations, conclusions and recommendations are those of the author and are not necessarily endorsed by the U.S. Army.

N/A Where copyrighted material is quoted, permission has been obtained to use such material.

N/A Where material from documents designated for limited distribution is quoted, permission has been obtained to use the material.

M. G. Citations of commercial organizations and trade names in this report do not constitute an official Department of Army endorsement or approval of the products or services of these organizations.

N/A In conducting research using animals, the investigator(s) adhered to the "Guide for the Care and Use of Laboratory Animals," prepared by the Committee on Care and use of Laboratory Animals of the Institute of Laboratory Resources, national Research Council (NIH Publication No. 86-23, Revised 1985).

N/A For the protection of human subjects, the investigator(s) adhered to policies of applicable Federal Law 45 CFR 46.

M. G. In conducting research utilizing recombinant DNA technology, the investigator(s) adhered to current guidelines promulgated by the National Institutes of Health.

M. G. In the conduct of research utilizing recombinant DNA, the investigator(s) adhered to the NIH Guidelines for Research Involving Recombinant DNA Molecules.

M. G. In the conduct of research involving hazardous organisms, the investigator(s) adhered to the CDC-NIH Guide for Biosafety in Microbiological and Biomedical Laboratories.



PI - Signature 9/12/99
Date

TABLE OF CONTENTS

| | Page |
|--|-------------|
| Front Cover | 1 |
| Report Documentation Page | 2 |
| Foreword | 3 |
| Table of Contents | 4 |
| Introduction | 5 |
| Body/Technical Report | 5 |
| Appendix/Key Research Accomplishments | 14 |

INTRODUCTION

The **general aim** of this study is to understand how the physiological molecules such as hormones and synthetic compounds such as antiestrogens regulate the structure and function of human mammary epithelium. The integrity of the epithelial tissue is critical for normal breast physiology, whereas malfunction of cell adhesion is a manifestation of malignant transformation in breast epithelial tissue. The **major purpose** of this work is to investigate whether the IGF-IR – the specific hormone receptor, whose content is significantly increased in primary human carcinomas -- affects intercellular adhesion. Exploring potentials of the synthetic steroid and non-steroid antiestrogenic compounds in regulating breast epithelial cell adhesion is an **additional objective**. This **study is primarily focused** on the development of new human breast cancer cell lines and their analysis in different experimental settings in vitro. The results of this investigation will shed light on mechanisms of breast carcinoma and potentiality of therapeutic approaches against this disease in human.

BODY

The PI dedicated 100% of her working time to the continuation of this project and obtained the following data in accordance with the proposed Statement of Work.

PART I. Development and characterization of MCF-7 breast cancer cells overexpressing the human insulin receptor (hIR) (started and completed)

1st year report conclusions: Overexpression of the IGF-IR in MCF-7 human breast cancer cells correlates with the ability of carcinoma cell to form large (>300 µm in diameter) compact multicellular aggregates on Matrigel, an analog of the basal membrane. IGF-IR tyrosine kinase activity is required for the development of this type of aggregates.

AIM 1. To investigate whether the effect of the human IGF-IR on breast cancer cell aggregation is specific.

The IGF-IR shares 70% homology with the IR, which content is also increased in human breast cancer specimens (Milazzo et al., 1992). A certain degree of an overlap in IR and IGF-IR biological activities has been observed (Steele-Perkins et al., 1988). The question raised in this study is whether in breast epithelial cells the overexpressed IR promotes cell aggregation in a similar manner as the IGF-IR does?

Major experiments and results:

1. The hIR cDNA was obtained from Dr. R. Baserga's laboratory at the Thomas Jefferson University. **The full-length hIR was cloned into Hind III and Ecor V restriction sites of the mammalian expression vector pcDNA3** (Invitrogen), which drives the inserted cDNA by the CMV promoter and contains the neomycin resistance gene. The cloning of the insert was verified by multiple restriction digestion and DNA sequencing.
2. **MCF-7 human breast cancer cells with low physiological IR expression were transfected with the new pcDNA3/hIR plasmid** using the calcium phosphate precipitation (Guvakova and Surmacz, 1997a). The stable neomycin-resistant clones were selected in 2 mg/ml G418,

Geneticin (Gibco BRL). To avoid false negative detection of the incorporated in the genome exogenous hIR cDNA, the polymerase chain reaction (PCR) was omitted. Instead, fluorescence-activated cell sorting (FACS) was chosen based on its reliability (for reference please see 1st report, p.8-9). The IR alpha (α) (N-20) rabbit polyclonal antibody (pAb) (Santa Cruz) raised against the peptide corresponding to the amino terminus of the hIR α chain precursor was used. Surprisingly, this Ab bound poorly to either parental or transfected live cells. Possibly, the fixation/permeabilization of the cell membrane is required to detect IR α subunit with this Ab.

3. To solve the problem of IR detection, **the total amount of exogenous and endogenous IR was estimated in 34 transfectants by semi-quantitative assay using immunoprecipitation (IP) and western blotting (WB). Three stable MCF-7/IR clones expressing the highest levels of the hIR were selected for the further analysis.** The total level of the IR in those clones was approximated as $\sim 0.8-1.0 \times 10^6$ IR /cell, that was at least 20 times higher then endogenous IR in MCF-7 cells and comparable with the level of the IGF-IR in MCF-7/IGF-IR/WT cells (1st year report, p 9).

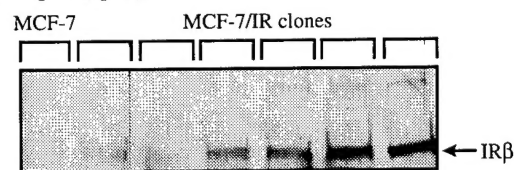


Fig. 1. The total level of the IR β subunit in MCF-7 cells and 6 randomly selected MCF-7/IR clones. The IR was IP with IR β mAb (Calbiochem) and WB with IR β pAb (Transduction Laboratories). The last clone on the right has about 1.0×10^6 IR/cell.

4. To verify that the overexpressed hIR is localized properly within a cell, **the indirect immunofluorescence (IF) light microscopy was performed.** In MCF-7/IR cells, both α - and beta (β)- subunits of the IR localize predominantly to cell membrane. Notably, stained α subunit was less visible than β subunit that may partially explain the negative results of FACS reported above.

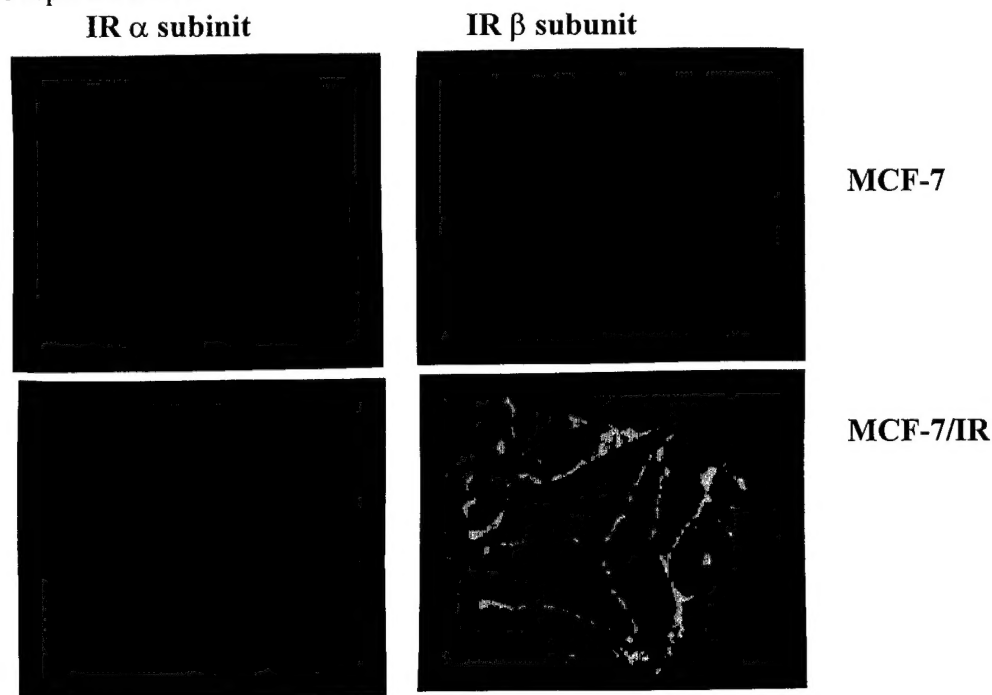


Fig. 2. Subcellular localization of the IR in MCF-7 transfectants visualized by the indirect IF with IR α pAb (N-20) (Santa Cruz) + IR β mAb (Ab-3) (Calbiochem). One double stained representative MCF-7/IR clone is shown. Images were processed using Adobe Photoshop.

5. To confirm the functional activity of the exogenous IR, **biochemical analysis of IR signaling pathways was performed in MCF-7/IR clones**. Because of similarity between the IGF-IR and the IR, characterization of IR signaling followed the scheme established for the IGF-IR (1st report, pp. 10-11). The major observations are: Insulin-induced tyrosine phosphorylation of IR β subunit as well as IR-associated IRS-1 was elevated remarkably in MCF-7/IR clones when compared to MCF-7 cells. The basal and insulin-induced tyrosine phosphorylation of the total pools of IRS-1 is notably augmented. Insulin-induced SHC phosphorylation is slightly higher in MCF-7/IR than in MCF-7 cells. Interestingly, only in one of MCF-7/IR clones, the basal and insulin-induced MAPK activity was increased compared to all other cells tested, however, biological relevance of such a peculiar feature was not pursued.

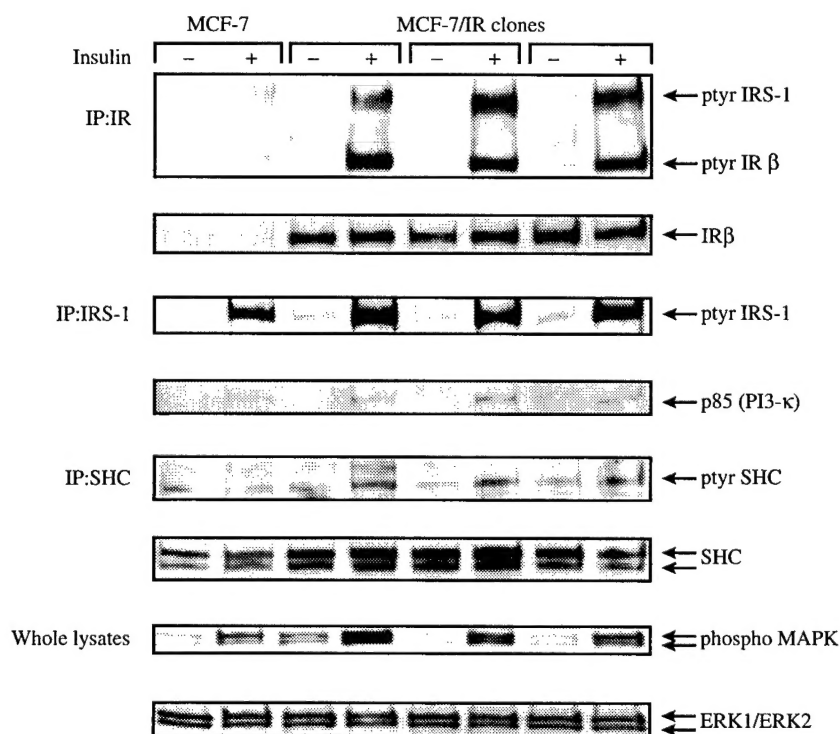


Fig. 3. IR signaling in MCF-7/IR clones compared to MCF-7 cells. Cells were serum-starved for 24h (Insulin -) and then stimulated with 50 μ g/ml insulin (Sigma) for 15 minutes (Insulin +). Either the whole cell lysates (to detect phosphorylated and total MAPKs) or IPs of the IR, IRS-1, SHC with the specific Abs were analyzed. In IPs, the tyrosine phosphorylated proteins (ptyr) were detected with PY20 mAb (Santa Cruz), the levels of the IR β , IRS-1-associated p85 (PI3-k), and the total SHC protein were detected with anti- IR β pAb (Transduction Laboratories), p85 (PI3-k) mAb (UBI), and SHC mAb (Santa Cruz) respectively.

6. **MCF-7/IR cell aggregation on Matrigel.** The aggregation of MCF-7/IR cells was compared with that in MCF-7/IGF-IR/WT and MCF-7 cells. Similar results were obtained in all repeats. 1) MCF-7/IR clones formed lesser aggregates than MCF-7/IGF-IR/WT cells. 2) Multicellular aggregates of MCF-7/IR clones were smaller in size than that formed by MCF-7/IGF-IR/WT cells. 3) Remarkably, MCF-7/IR cells can not firmly aggregate. They formed the loosely cohesive cellular groups characteristic for aggressive tumors.

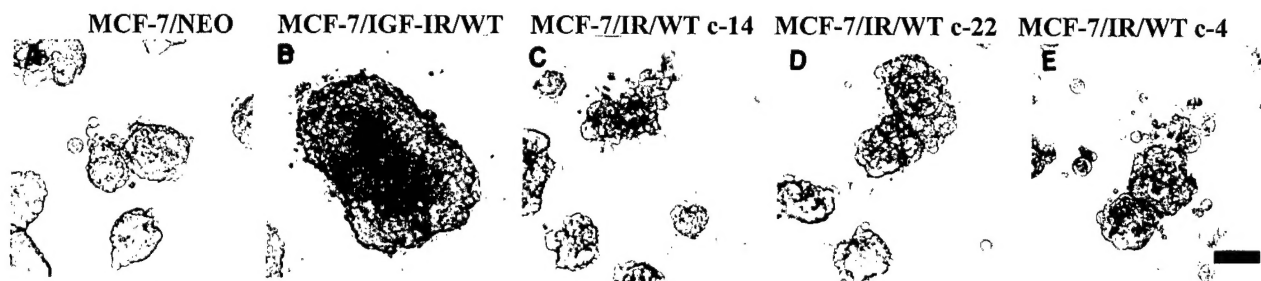


Fig. 4. Morphology of MCF-7/IR aggregates in 2 weeks after plating. Suspensions of 2×10^4 cells in the regular culture medium (DMEM/F12/5% CS) were placed on the top of Matrigel (Biocoat) composed of the elements of the extracellular matrix (ECM). On day 14 after plating, the morphology of aggregates was recorded and the amount of aggregates of the certain size was directly counted under a microscope with an ocular ruler. Representative phase-contrast micrographs are shown. Scale bar, 150 μ m.

| Size of aggregates | MCF-7/NEO | MCF-7/IGF-IR/WT | MCF-7/IR/WT c-14 | MCF-7/IR/WT c-22 | MCF-7/IR/WT c-4 |
|------------------------|-----------|-----------------|------------------|------------------|-----------------|
| $\geq 150 \mu\text{m}$ | 147 | 229 | 154 | 194 | 146 |
| $\geq 300 \mu\text{m}$ | 42 | 131 | 61 | 56 | 49 |

Table 1. Size and amount of aggregates in MCF-7/IR clones compared to other cells. The average amount of aggregates of each particular size is presented.

CONCLUSION 1: The overexpressed IR *per se* does not promote the development of large compact aggregates in E-cadherin positive breast cancer cells. Thus, the stimulatory effect of the IGF-IR on the same type of carcinoma aggregates is specific.

PART II. Characterization of E-cadherin/catenin complex in MCF-7 cells overexpressing either the wild or mutant IGF-IRs (continued and completed)

1st year report conclusions: Inactivation of the IGF-IR tyrosine kinase (through replacement of three tyrosines at positions 1131, 1135, 1136 by phenylalanines), mutation of the ATP-binding site (via substitution of tyrosine by arginine at position 1003), and deletion of the IGF-IR C-terminal 108 amino acids do not block physical association between the IGF-IR and E-cadherin. Interaction of these molecules, whether it is direct or indirect, is constitutive and independent on IGF-IR tyrosine kinase.

AIM 2. To identify molecular mechanisms by which the IGF-IR regulates function of E-cadherin/catenin adhesion complex.

To continue, I analyzed associations between the IGF-IR and α - or β - catenins, the cytoplasmic proteins that together with E-cadherin compose the adherence type junctions, the major structures responsible for the strength of cell-cell contacts. The study was performed in serum-starved untreated (UT) and IGF-I-stimulated MCF-7 cells overexpressing either the wild type (WT) or mutants of the IGF-IR described in the 1st report.

Major findings:

1. α -Catenin associated with all types of the IGF-IR including those with partially and completely inactivated tyrosine kinase. There was no change in the amount of IGF-IR-associated α -catenin in IGF-I-stimulated cells versus UT cells.
2. β -Catenin coupled with all forms of the IGF-IR tested, however, there was a reduction of β -catenin associated with the catalytically active IGF-IR in IGF-I-stimulated cells.
3. Functional inactivation of IGF-IR tyrosine kinase in dead kinase mutant (MCF-7/IGF-IR/YF3) prevented dissociation of β -catenin from the IGF-IR.

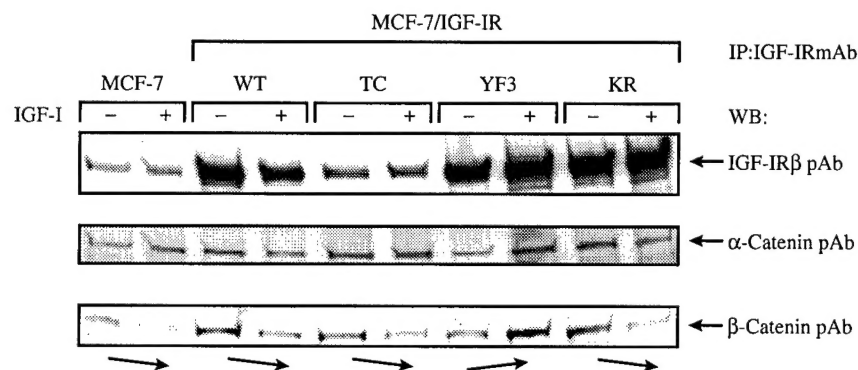


Fig. 1. The amount of α - and β -catenin associated with the IGF-IR in untreated and IGF-I-stimulated cells. Cells were serum-starved for 24h (IGF-I -), and then stimulated with 50 ng/ml IGF-I for 5 minutes (IGF-I +). 300 μ g of cell lysates was precipitated with anti-IGF-IR mAb (Ab-3) (Calbiochem). Blots were hybridized with anti-IGF-IR β pAb, then stripped and re-probed twice, first with anti- α -catenin, then with anti- β -catenin pAbs (Sigma). Note decreased amount of β -catenin indicated by arrow in the immunoprecipitates of all cells with active/partially active forms of the IGF-IR.

CONCLUSION 2: IGF-IR tyrosine kinase differentially regulates interaction between the IGF-IR and catenins. Association of α -catenin with the IGF-IR is not modulated by IGF-I, whereas the amount of IGF-IR-associated β -catenin is down regulated upon IGF-IR kinase stimulation.

PART III. Effect of antiestrogens Tamoxifen and ICI 182,780 on cell aggregation and function of E-cadherin/IGF-IR complex (continued and completed)

1st year report conclusion: A non-steroidal antiestrogen Tamoxifen (Tam) does not improve cell-cell aggregation of MCF-7-derived breast cancer cells, but reduces size of the aggregates indicating that Tam affects either the cell growth, or survival, or both processes.

Since Tam did not promote E-cadherin-mediated cell aggregation, the earlier planned control experiment with CAMA-1 (E-cadherin negative cell line) has been pared down.

AIM 3. To investigate molecular mechanism by which antiestrogens might control function of E-cadherin/IGF-IR complex and regulate three-dimensional (3-D) cell growth.

In monolayer, Tam inhibits cell growth and decreases tyrosine phosphorylation of the total pool of IRS-1 molecules (Guvakova and Surmacz, 1997b). Co-precipitated IRS-1 has been also identified in E-cadherin complex (Guvakova and Surmacz, 1997a). In this study, I investigated whether Tam altered the activation of E-cadherin-associated IRS-1 molecules as a potential mechanism regulating 3-D growth and survival. Furthermore, for the first time, the effect of a synthetic steroid antiestrogen ICI 182,780 (Zeneca) on non-invasive estrogen receptor positive (ER⁺) MCF-7/IGF-IR/WT and invasive estrogen receptor negative (ER⁻) MDA-MB-231 breast cancer cells in 3-D culture was assessed.

Major findings:

1. In ER⁺ cell lines, long term Tam treatment (3-4 days) blocked tyrosine phosphorylation of IRS-1 associated with E-cadherin complex, and that might cause down-regulation of 3-D growth.

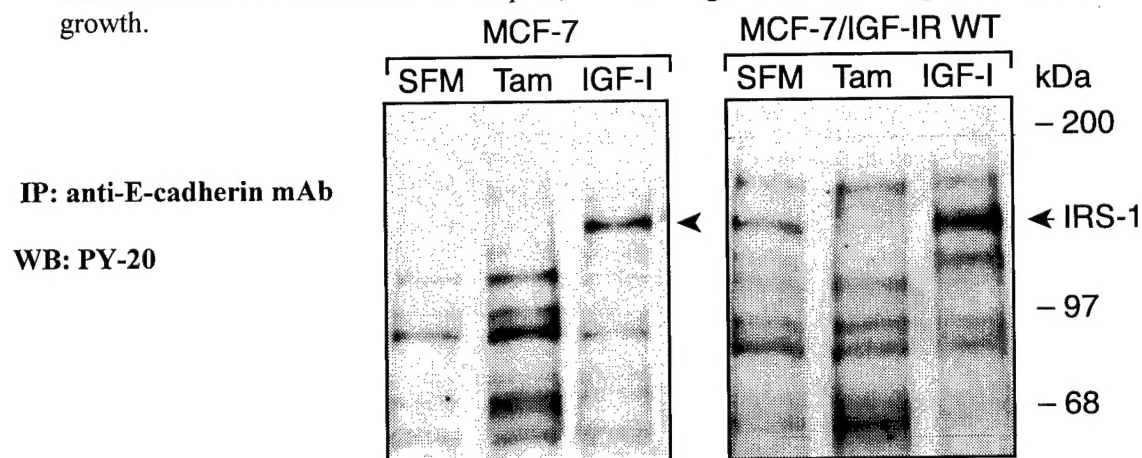


Fig 1. Tam inhibits tyrosine phosphorylation of E-cadherin-associated IRS-1. During 3 days cells were incubated either in serum-free medium (SFM) alone, or 10 nM Tam in SFM, or 50 ng/ml IGF-I in SFM. 500 μ g cell lysates were IP with 4 μ g of anti-E-cadherin mAb (Transduction Laboratories). E-cadherin-associated phosphoproteins were detected with PY 20 mAb. Position of IRS-1 indicated by arrow was confirmed by stripping and re-probing phosphotyrosine blots with anti-IRS-1 pAb (UBI). These blots are not shown.

2. A pure antiestrogenic compound ICI 182,780 was shown to reduce total IRS-1 expression and tyrosine phosphorylation, as well as block the basal and IGF-I-induced growth of ER⁺ MCF-7-derived cells in monolayer (Salerno et al., 1999 - collaborative project).
3. In 3-D culture, ICI 182,780 did not promote cell aggregation of either ER⁺ MCF-7/IGF-IR/WT or ER⁻ MDA-MB-231 cells. ICI 182,780, however, effectively inhibited growth of ER⁺ MCF-7/IGF-IR/WT compact aggregates on Matrigel (Fig. 2). This cytostatic action of the steroid antiestrogen is reminiscent the effect of a non-steroid compound Tam described earlier (1st report, p. 16).
4. ICI 182,780 had a poor blocking effect on the growth of the invasive ER⁻ MDA-MB-231 cells in Matrigel, at least at the concentration and under the treatment condition applied. Alternatively, a SFM itself might impair 3-D growth of ER⁻ MDA-MB-231 cells that made it difficult to distinguish the specific growth inhibitory effect of the drug.

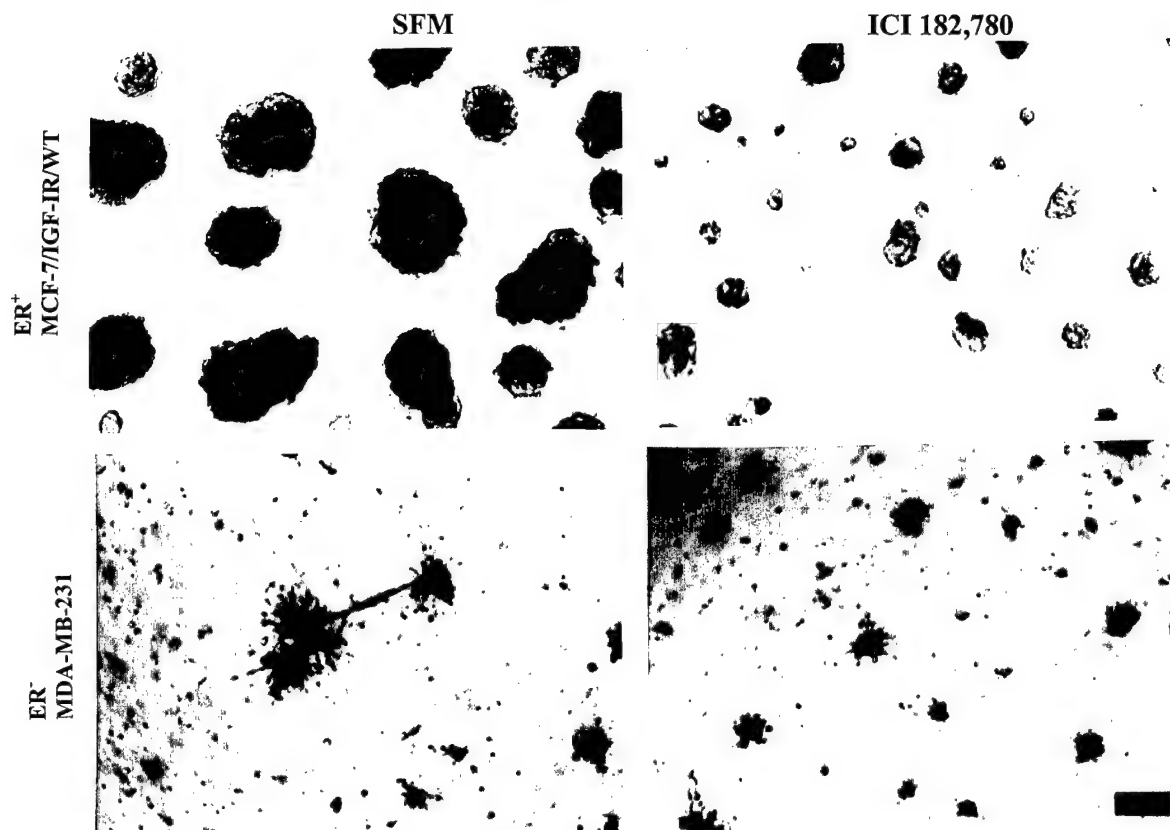


Fig. 2. ICI 182,780 inhibits 3-D growth of breast cancer cells on Matrigel. 2×10^4 cells were plated on Matrigel into 24-well plates. After 4 days of plating, when small aggregates were formed the culture medium (DMEM/F12/5%) was changed to SFM alone, or SFM supplemented with 100 nM ICI 182,780. The treatment was refreshed each 4th day during 2 following weeks prior to recording the results. Scale bar, 100 μ m.

CONCLUSION 3: Tamoxifen and ICI 182, 780 are equally effective in inhibiting ER⁺ breast tumor cell growth in monolayer and 3-D culture. The cytostatic action of those drugs counteracts ER- as well as IGF-IR/IRS-1-mediated growth signaling. Whether these antiestrogens affect the growth of ER⁻ tumor cells remains to be verified thoroughly.

PART IV. Characterization of invasive breast cancer cell lines (in progress)

In evaluation of the invasive potential of mammary carcinoma the useful criterion is the expression of E-cadherin along with catenins (Zchiesche et al., 1997). In the present study, the level of these adhesion molecules and the IGF-IR was analyzed in the invasive MDA-MB-231 and non-invasive MCF-7 and BT-474 carcinoma cells, as well as in MCF-10A normal breast epithelial cell line. For the first time, a potential effect of IGF-I on aggregation of the invasive breast tumor cells in 3-D culture was assessed.

Initial observations:

1. Invasive MDA-MB-231 cells lacked E-cadherin, contained little α -catenin, but comparable to non-invasive cell lines β -catenin. In MDA-MB-231 cells, IGF-IR expression was slightly lower than in MCF-7 cells and comparable with that in MCF-10A cells.

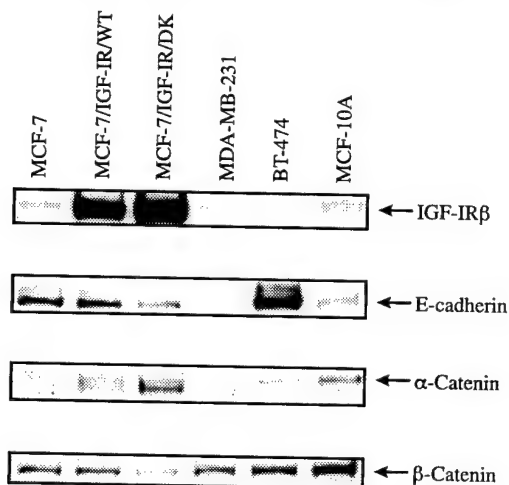


Fig.1. The levels of IGF-IR β subunit, E-cadherin, α - and β -catenin were detected in the correspondent IPs with anti-IGF-IR mAb, anti-E-cadherin mAb, and anti- α - and β -catenin pAbs, respectively. Note MDA-MB-231 cells substituted earlier proposed MDA-MB-436 cells with a similar E-cadherin/catenin profile.

2. Unexpectedly, IGF-I remarkably stimulated growth and invasion of MDA-MB-231 within the Matrigel suggesting pro-invasive potential of IGF-I in E-cadherin negative breast carcinoma cells.

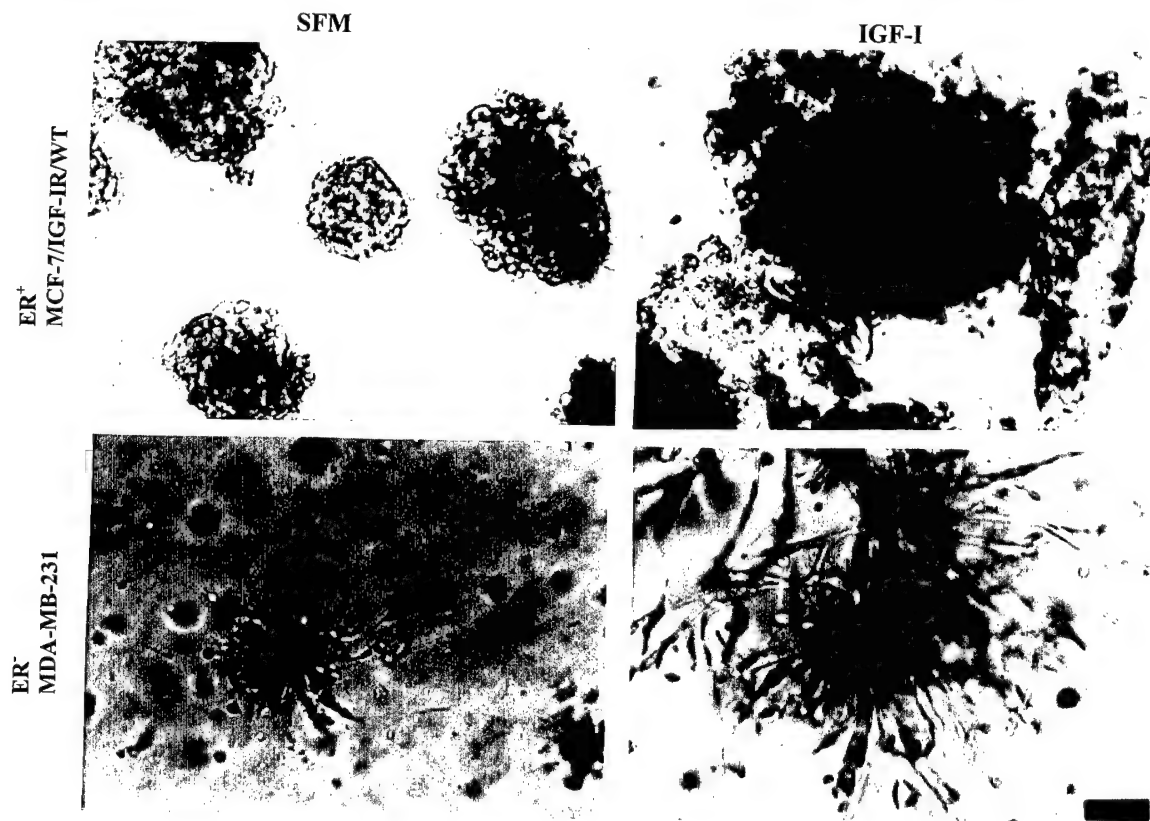


Fig. 2. IGF-I promotes invasive growth in ER⁻ MDA-MB-231 cells. 2×10^4 cells were plated on Matrigel into 24-well plates. After 4 days of plating, when small aggregates were formed the culture medium (DMEM/F12/5%) was changed to SFM alone, or SFM supplemented with 100 nM ICI 182,780. The treatment was refreshed each 4th day during 2 following weeks prior to recording the results. Scale bar, 200 μ m.

CONCLUSION 4: In E-cadherin negative breast carcinoma cells, IGF-I acting via the IGF-IR up-regulates invasive cell growth. Thus, it is anticipated that IGF-IR overexpression in this subset of tumor cells will increase invasiveness rather than cell-cell aggregation as it was predicted initially.

PART V. Discovering new functions of the IGF-IR in human breast carcinoma (in progress)

Numerous studies on cell proliferation and apoptosis suggest that the IGF-IR is essential for phenotypical transformation (Pezzino et al., 1996). However, a role of the IGF-IR in tumor progression goes beyond its growth promoting activity. In this work, **the novel function of the IGF-IR – its ability to depolarize breast epithelial cells - was revealed.** Although a loss of epithelial polarity is a well-known diagnostic criterion of malignant breast tumors (Bibbo, 1997), the impact of IGF-IR signaling in regulating cell polarity has never been investigated. Therefore, I dedicated extra time to study molecular and cellular mechanism of IGF-IR-mediated breast epithelial cell depolarization. **The results of this investigation have been documented in the paper recently published in the *Experimental Cell Research* (Guvakova and Surmacz, 1999).** Taking an advantage of the cell models developed in this study, I am currently investigating influence of the IGF-IR on breast cancer cell motility.

References:

- Bibbo, M. Comprehensive cytopathology, (1997), W. B. Saunders Company, pp 731-780.
- Guvakova, M. A. and Surmacz, E. (1997a). Overexpressed IGF-I receptors reduce estrogen growth requirement, enhance survival and promote E-cadherin-mediated cell-cell adhesion in human breast cancer cells. *Exp Cell Res.* 231, 149-162.
- Guvakova, M. A. and Surmacz, E. (1997b). Tamoxifen interferes with the insulin-like growth factor I receptor (IGF-IR) signaling pathways in breast cancer cells. *Cancer Res.* 57, 2606-2610.
- Guvakova, M. A. and Surmacz, E. (1999). The activated Insulin-like growth factor I receptor induces depolarization of breast epithelial cells characterized by actin filament disassembly and tyrosine dephosphorylation of FAK, Cas, and paxillin. *Exp. Cell Res.*, 251, 244-255.
- Milazzo, G., Giorgino, F., Damante G., Sung, C., Stampfer, M., R., Vigneri, R., Goldfine, I., D., and Belfiore, A. (1992). Insulin receptor expression and function in human breast cancer cell lines. *Cancer Res.*, 52, 3924-3930.
- Pezzino V., Papa, V., Milazzo, G., Gliozzo, B., Russo, P., and Scalia, P.L. (1996) Insulin-like growth factor-I (IGF-I) receptors in breast cancer. *Annals New York Academy of Sciences*, p189-201.
- Steele-Perkins, G., Turner, J., Edmon, J., C., Hari, J., Pierce, S., B., Stover, C., Rutter, W., J., and Roth, R., A. (1988). Expression and characterization of a functional human insulin-like growth factor I receptor. *J. Biol. Chem.*, 263, 11486-11492.
- Zschiesche, W., Schonborn, I., Behrens, J., Herrenknecht, K, Hartveit, F., Lilleng, P., and Birchmeier W. (1997). Expression of E-cadherin and catenins in invasive mammary carcinomas. *Anticancer Res.* 17, 561-567.

The Activated Insulin-Like Growth Factor I Receptor Induces Depolarization in Breast Epithelial Cells Characterized by Actin Filament Disassembly and Tyrosine Dephosphorylation of FAK, Cas, and Paxillin

Marina A. Guvakova¹ and Ewa Surmacz

Kimmel Cancer Institute, Thomas Jefferson University, 233 South 10th Street, B.L.S.B. 606, Philadelphia, Pennsylvania 19107

Insulin-like growth factor I (IGF-I) promotes the motility of different cell types. We investigated the role of IGF-I receptor (IGF-IR) signaling in locomotion of MCF-7 breast cancer epithelial cells overexpressing the wild-type IGF-IR (MCF-7/IGF-IR). Stimulation of MCF-7/IGF-IR cells with 50 ng/ml IGF-I induced disruption of the polarized cell monolayer followed by morphological transition toward a mesenchymal phenotype. Immunofluorescence staining of the cells with rhodamine-phalloidin revealed rapid disassembly of actin fibers and development of a cortical actin meshwork. Activation of phosphatidylinositol (PI) 3-kinase downstream of the IGF-IR was necessary for this process, as blocking PI 3-kinase activity with the specific inhibitor LY 294002 at 10 μ M prevented disruption of the filamentous actin. In parallel, IGF-IR activation induced rapid and transient tyrosine dephosphorylation of focal adhesion proteins p125 focal adhesion kinase (FAK), p130 Crk-associated substrate (Cas), and paxillin. This process required phosphotyrosine phosphatase (PTP) activity, since pretreatment of the cells with 5 μ M phenylarsine oxide (PAO), an inhibitor of PTPs, rescued FAK and its associated proteins Cas and paxillin from IGF-I-induced dephosphorylation. In addition, PAO-pretreated cells were refractory to IGF-I-induced morphological transition. Thus, our findings reveal a new function of the IGF-IR, the ability to depolarize epithelial cells. In MCF-7 cells, mechanisms of IGF-IR-mediated cell depolarization involve PI 3-kinase signaling and putative PTP activities.

© 1999 Academic Press

Key Words: insulin-like growth factor I receptor signaling; F-actin; phosphatidylinositol 3-kinase; focal adhesion; phosphotyrosine phosphatase.

INTRODUCTION

Differentiated epithelial cells form tightly adherent polarized sheets with a full complement of specific ad-

hesive junctions that stably link cells together and to the underlying biological substratum [1]. In the cell interior, various membrane junctions are connected by the cytoskeletal network, providing the strength and architecture required for the proper physiological function of the epithelial sheet [2]. Normal epithelial cells move as a coherent sheet in which each cell keeps contacts with its neighboring cells as well as with extracellular matrix [3]. The ability of cells to move individually appears to be an exclusive attribute of carcinoma cells. At present, however, little is known about how depolarization of epithelial cells is accomplished and regulated and what signals trigger this process.

The studies on chemotaxis and cell spreading suggest that insulin-like growth factor I (IGF-I) is a regulator of motility in normal and tumor cells [4–7]. In breast cancer cells, IGF-I-induced chemotactic migration has been reported to occur through the IGF-I receptor (IGF-IR) [8, 9]. Importantly, IGF-IR expression is 14 times higher and IGF-IR kinase activity is significantly increased in malignant compared with normal breast tissue. Furthermore, ligands of the IGF-IR, IGF-I, and IGF-II, are secreted by the surrounding mammary epithelium stromal cells [10]. The possibility that IGF-IR overexpression promotes depolarization and locomotive functions in breast epithelial cells has not been investigated.

The IGF-IR belongs to the tyrosine kinase receptor superfamily and is known to play an important role in normal and abnormal growth [11]. Ligand binding stimulates autophosphorylation of the IGF-IR β subunit, elevates its kinase activity, and leads to a recruitment of multiple signaling molecules: insulin receptor substrates 1 and 2 (IRS-1 and IRS-2), Shc, Crk, Gab1, Grb10, the p85 regulatory subunit of phosphatidylinositol 3-kinase (PI 3-kinase) [12]. Many of the known IGF-IR pathways convey mitogenic stimuli. IRS-1 molecule, for example, via its multiple tyrosine phosphorylation sites, recruits secondary signaling proteins containing Src-homology 2 (SH2) domains such as PI

¹ To whom reprint requests should be addressed. Fax: (215) 923–0249. E-mail: Marina.Guvakova@mail.tju.edu.

3-kinase, phosphotyrosine phosphatase 1D (PTP1D/SH-PTP2/Syp), and Src-family kinase Fyn, as well as adapter proteins Grb-2, Crk, and Nck that participate in the mitogenic Ras/Raf/MAPK (mitogen-activated protein kinase) cascade [13]. It still remains unknown whether IGF-IR signaling pathways controlling epithelial cell motility are similar to or different from those required for cell proliferation.

The structure of the epithelial cell monolayer is supported by the integrity of the actin-enriched cytoskeleton, and its reorganization is critical for regulating cell motility [14]. Previous studies have described two types of IGF-IR effects on the actin cytoskeleton: the appearance of actin-enriched circular ruffles along the margins of KB epidermoid carcinoma cells [15, 16], and the development of an actin meshwork in the extended neurites of neuronal cells [17]. In breast epithelial cells, the relationship between the IGF-IR and the actin cytoskeleton has not been defined.

In polarized epithelial cells, focal adhesion proteins are localized to the termini of the stress fiber-like actin filaments as well as to cell-cell junctions adjacent to circumferential actin bundles [18]. Hence, reorganization of the actin network may affect the dynamics of focal adhesion assembly and lead to modulation of cell-substratum interaction, cellular shape, and consequently cell motility. In different cell types, IGF-I has been shown to positively or negatively modulate tyrosine phosphorylation of focal adhesion proteins such as FAK, Cas, and paxillin [17, 19, 20]. However, in these studies the link between IGF-I modulation of focal adhesion protein phosphorylation and cell motility was not established. Whether IGF-IR signaling regulates activity of focal adhesion proteins in breast epithelial cells, what the mechanism of the regulation might be, and how it relates to cell motility remain unexplored.

In work presented here, we analyzed the effect of IGF-IR activation on locomotion of MCF-7-derived breast epithelial cells organized in a monolayer with particular focus on elucidation of IGF-IR signaling promoting cell motility.

MATERIALS AND METHODS

Cell culture and chemicals. MCF-7 human breast epithelial cells overexpressing the IGF-IR were derived by stable transfection with pcDNA3/IGF-IR plasmid [21]. All MCF-7-derived cells were grown in DMEM:F12 (1:1) containing 5% calf serum. To starve the cells of serum, they were incubated in phenol red-free, serum-free Dulbecco's modified Eagle's medium (DMEM) containing 0.5 mg/ml bovine serum albumin (BSA), 1 μ M FeSO₄, and 2 mM L-glutamine (SFM) for 24 h.

BSA, phenylarsine oxide (PAO), cytochalasin D (CD), and tetramethylrhodamine B isothiocyanate (TRITC)-conjugated phalloidin were purchased from Sigma. LY 294002 was from Calbiochem. Human recombinant IGF-I was purchased from Bachem.

Immunofluorescence light microscopy. Subconfluent cells grown on a glass coverslip were fixed with 3.7% formaldehyde in PBS for 15 min and permeabilized with 0.2% Triton X-100 in PBS for 5 min. To visualize actin filaments (F-actin) cells were stained with TRITC-conjugated phalloidin (1 μ g/ml) for 30 min and examined with a Zeiss Axiophot microscope. Changes in the intracellular distribution of FAK, Cas, and paxillin were assessed by labeling with the primary antibodies: anti-FAK (A-17) pAb (Santa Cruz Biotechnology), a mixture of anti-Cas B and F pAbs (gift of Dr. A. H. Bouton, University of Virginia), or anti-paxillin mAb (Transduction Laboratories) for 60 min. In some experiments, subcellular localization of FAK was visualized with the 2A7 mAb raised against C terminus of pp125 FAK (gift of Dr. J. T. Parsons, University of Virginia). Primary antibody detection was performed with lissamine rhodamine (LRSC)-conjugated goat anti-rabbit IgG (Jackson ImmunoResearch Laboratories) or fluorescein isothiocyanate (FITC)-conjugated goat anti-mouse IgG (Calbiochem). In controls, the primary antibody was omitted. Some samples were examined using the Zeiss Axiovert 100 MRC 600 confocal laser scanning (Bio-Rad) immunofluorescence microscope. Optical sections were taken at the ventral plane.

Immunoprecipitation and immunoblotting. Cells were lysed in protein lysis buffer (50 mM Hepes pH 7.5, 150 mM NaCl, 1.5 mM MgCl₂, 1 mM EGTA, 10% glycerol, 1% Triton X-100, 20 μ g/ml aprotinin, 2 mM Na orthovanadate, 1 mM phenylmethylsulfonyl fluoride). FAK, Cas, and paxillin were precipitated from the cell lysates (500 μ g of total protein) with specific antibodies: anti-FAK (A-17) polyclonal antibody (pAb) (Santa Cruz Biotechnology), anti-Cas monoclonal antibody mAb (Transduction Laboratories), and anti-paxillin mAb (Transduction Laboratories), respectively. Protein-antibody complexes were collected with either protein A- or anti-mouse IgG-agarose beads overnight. The precipitates were washed with HNTG buffer (20 mM Hepes pH 7.5, 150 mM NaCl, 0.1% Triton X-100, 10% glycerol), resolved by sodium dodecyl sulfate (SDS)-polyacrylamide gel electrophoresis, and transferred to nitrocellulose. Tyrosine phosphorylation and protein levels of FAK, Cas, and paxillin were assessed by immunoblotting with anti-phosphotyrosine mAb (PY-20) (Santa Cruz Biotechnology) or the specific antibodies as used for precipitations. The proteins were visualized by enhanced chemiluminescence detection (Amersham).

RESULTS

Activation of the IGF-IR Induces Depolarization of MCF-7 Cells

Serum-starved MCF-7 cells expressing moderate levels of the endogenous IGF-IR (6×10^4 receptors/cell) and MCF-7/IGF-IR cells with an 18-fold overexpression of wild-type IGF-IR both displayed a characteristic epithelial morphology with apicobasal polarity. The basal cell surfaces were adherent to the substratum, while lateral membranes of adjacent cells were attached to each other (Figs. 1A, 1B). In response to addition of 5–50 ng/ml IGF-I the cell monolayers underwent a dose-related morphological reorganization (data not shown). The most drastic changes occurred in 50 ng/ml IGF-I and were characterized by disruption of the epithelial sheet, loss of cell polarity, and development of a fibroblast-like phenotype by the majority of cells (Figs. 1C, 1D). Within 15 min cell-cell contacts loosened. By 60 min the cells partially detached from the plastic surface and rounded up slightly. Between 1 and 4 h of continuous IGF-I exposure the cells devel-

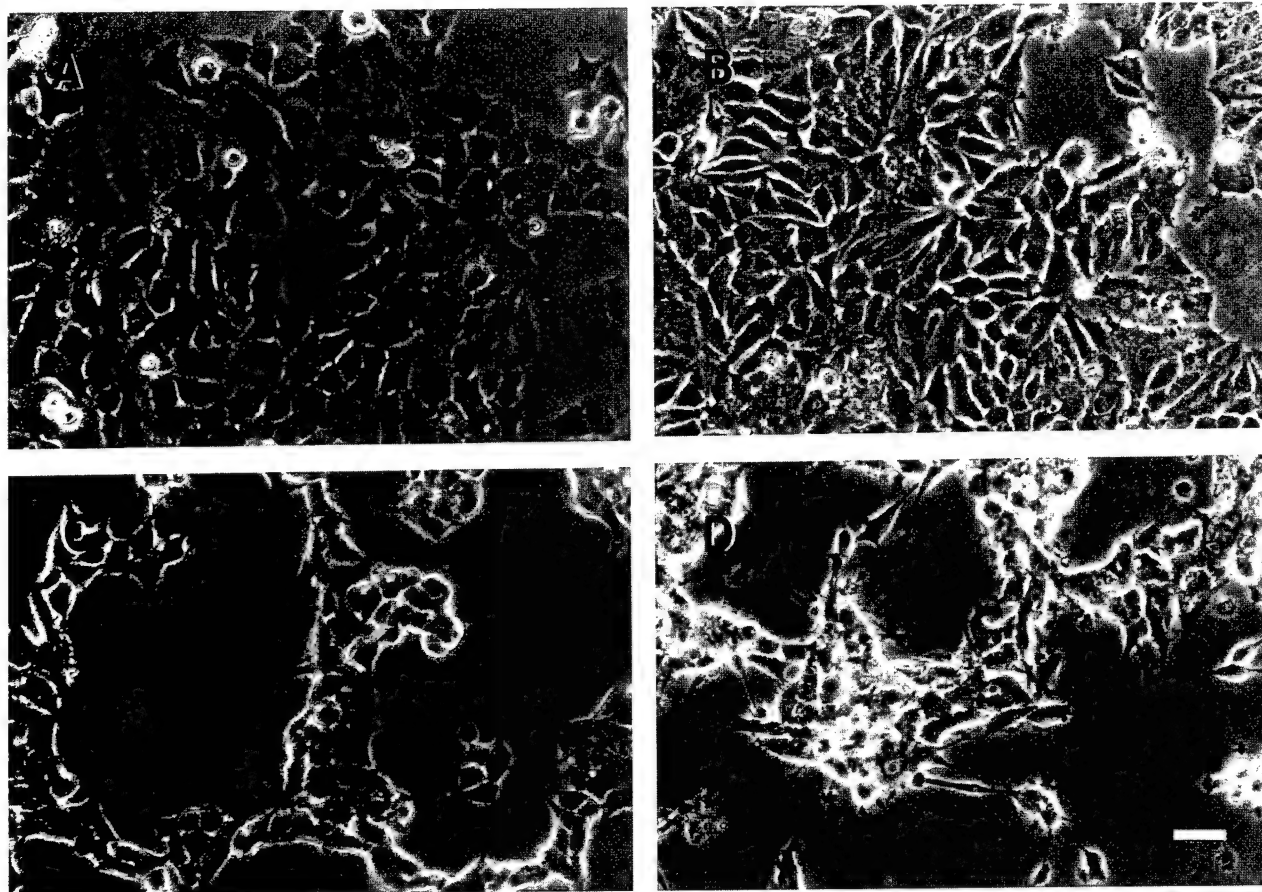


FIG. 1. IGF-IR activation stimulates depolarization and morphological transition in MCF-7-derived cells. The representative phase-contrast micrographs show the morphology of serum-starved MCF-7 (A) and MCF-7/IGF-IR (B) cells. In (C), MCF-7 and in (D), MCF-7/IGF-IR serum-starved cells were stimulated with 50 ng/ml IGF-I for 4 h. Bar = 100 μ m.

oped multiple lamellipodial structures, which are characteristics of motile cells. Both control and IGF-IR-overexpressing cells were affected by IGF-I; however, the extent of the modifications was more pronounced in MCF-7/IGF-IR than MCF-7 cells (compare Figs. 1C and 1D). Therefore, IGF-IR-overexpressing cells were chosen for analysis in all subsequent experiments.

IGF-IR Activation Induces PI 3-Kinase-Dependent Disassembly of the Actin Filaments

To determine if IGF-IR activation induces reorganization of the actin cytoskeleton, F-actin was visualized in serum-starved MCF-7/IGF-IR cells treated with 50 ng/ml IGF-I for various times (Figs. 2A–2D). Within 5 min, the IGF-I effect on the actin cytoskeleton was detected as a disappearance of circumferential actin bundles, disassembly of stress fiber-like filaments, and development of a widespread cortical actin meshwork (Fig. 2B). After approximately 15 min, accumulation of F-actin was observed at the cell margins within struc-

tures resembling microspikes or small membrane ruffles (Figs. 2C, 2E). Between 1 and 4 h, the cells developed multiple extended protrusions, and fine long actin filaments reappeared, traversing cytoplasm and terminating in the veil-like lamellipodia (Fig. 2D).

Activation of PI 3-kinase has been implicated in restructuring of the actin cytoskeleton in other cell types [18, 26]. We investigated the role of PI 3-kinase in IGF-IR-induced modification of F-actin using a synthetic compound LY 294002 that blocks PI 3-kinase specifically ($IC_{50} = 1.4 \mu$ M) and does not affect the activity of either IGF-IR or IRS-1 at concentrations up to 20 μ M (data not shown). When MCF-7/IGF-IR cells pretreated with 10 μ M LY 294002 for 30 min were stimulated with 50 ng/ml IGF-I for 30 min in the presence of the inhibitor, F-actin disassembly was prevented completely (compare Figs. 2E and 2F). The appearance of short actin bundles in membrane ruffles also was blocked. The actin cytoskeleton remained intact even 1 h after addition of IGF-I (data not shown).

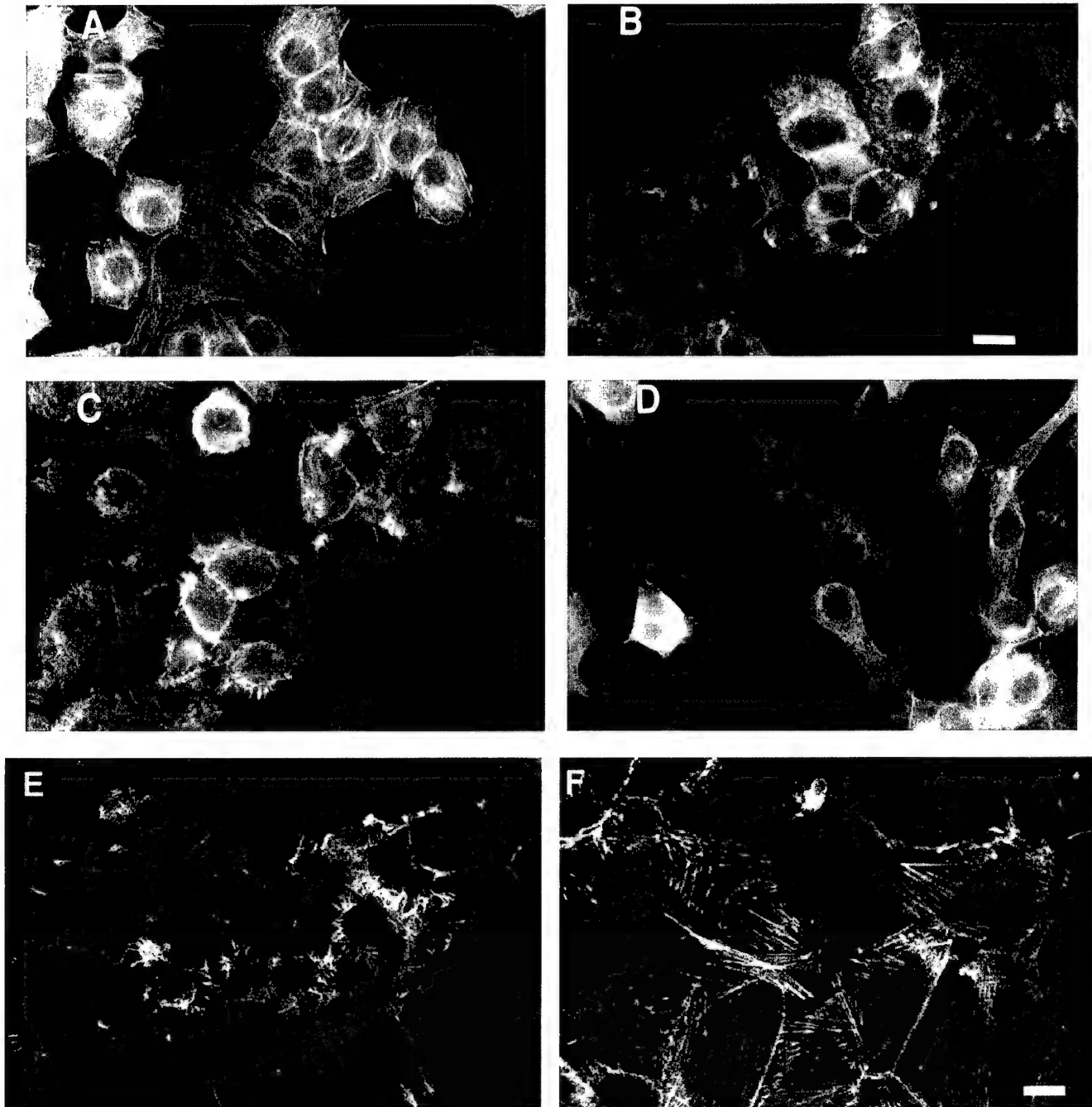


FIG. 2. IGF-I stimulation rapidly changes F-actin pattern in MCF-7/IGF-IR cells. The representative images of the selected time points show MCF-7/IGF-IR cells in which F-actin was visualized with TRITC-labeled phalloidin. Serum-starved cells (A); serum-starved cells stimulated with 50 ng/ml IGF-I for 5 min (B), 15 min (C), 30 min (E), and 4 h (D). (F) The cells were pretreated with 10 μ M LY 294002 for 30 min, followed by stimulation with 50 ng/ml IGF-I for 30 min. Bar = 20 μ m.

These results indicate that IGF-IR-activated PI 3-kinase signaling is critical for the initial step of IGF-IR-induced F-actin reorganization, namely, for the transient breakdown of actin filaments, as well as for subsequent F-actin rearrangement related to membrane protrusion.

The Activated IGF-IR Promotes Restructuring of Focal Adhesion Contacts

To investigate the relationship between changes in the actin filament network and organization of focal adhesions, conventional immunofluorescence light mi-

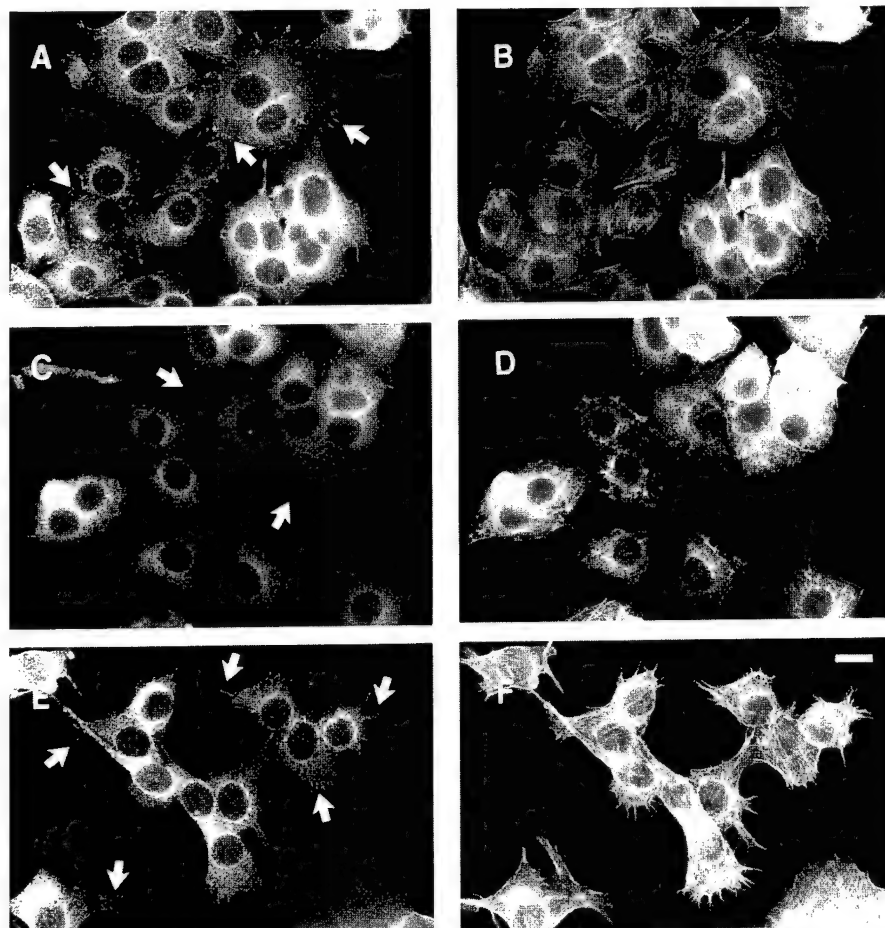


FIG. 3. Actin cytoskeleton reorganization is accompanied by redistribution of paxillin in IGF-I-stimulated MCF-7/IGF-IR cells. The representative images show cells costained with an anti-paxillin mAb (A, C, E) and TRITC-phalloidin (B, D, F). Serum-starved cells (A, B). Serum-starved cells treated with 50 ng/ml IGF-I for 5 min (C, D) and 60 min (E, F). Arrows in (A), (C), and (E) point to the position of the paxillin accumulations in membrane protrusions. Bar = 20 μ m.

croscopy was used. MCF-7/IGF-IR cells stimulated with 50 ng/ml IGF-I for various times were examined (Figs. 3A–3F). Costaining of F-actin and paxillin, a marker of focal adhesions, revealed that “arrowhead”-shaped paxillin clusters disappeared, along with actin filament disassembly, within 5 min of IGF-I stimulation (compare Figs. 3A, 3B and 3C, 3D). Approximately 1 h after IGF-I addition, when the fine actin filaments reappeared, elongated streaks of paxillin staining were observed in numerous membrane protrusions (Figs. 3E, 3F).

To investigate whether changes in paxillin localization paralleled redistribution of two other focal adhesion-associated proteins, FAK and Cas, MCF-7/IGF-IR cells were doubly stained with anti-paxillin mAb [Figs. 4A(a)–4F(a)] and either anti-FAK (A-17) [Figs. 4A(b), 4C(b), 4E(b)] or anti-Cas [Figs. 4B(b), 4D(b), 4F(b)] pAbs. In fully spread, serum-starved cells, FAK and Cas partially colocalized with paxillin in punctate arrays of dots along cell edges and in fine clusters dis-

tributed over the ventral surface of cells (Figs. 4A, 4B). Within 15 min of IGF-I stimulation, FAK, Cas, and paxillin were all stained in the cytoplasm. At this time point the cells were slightly rounded up and had only a few paxillin-positive focal contacts (Figs. 4C, 4D). After 1–4 h, FAK and Cas could not be detected clearly in membrane protrusions where paxillin streaks were abundant [Figs. 4E(b), 4F(b)]. Similar results with respect to the intracellular redistribution of FAK were observed with both the A-17 and 2A7 anti-FAK antibodies.

Activation of the IGF-IR Induces Rapid Tyrosine Dephosphorylation of Focal Adhesion Proteins: FAK, Cas, and Paxillin

Actin fiber disassembly was shown to correlate with a reduction of FAK tyrosine phosphorylation in CHO cells [22]. We examined the time course and extent of the FAK tyrosine phosphorylation in MCF-7/IGF-IR

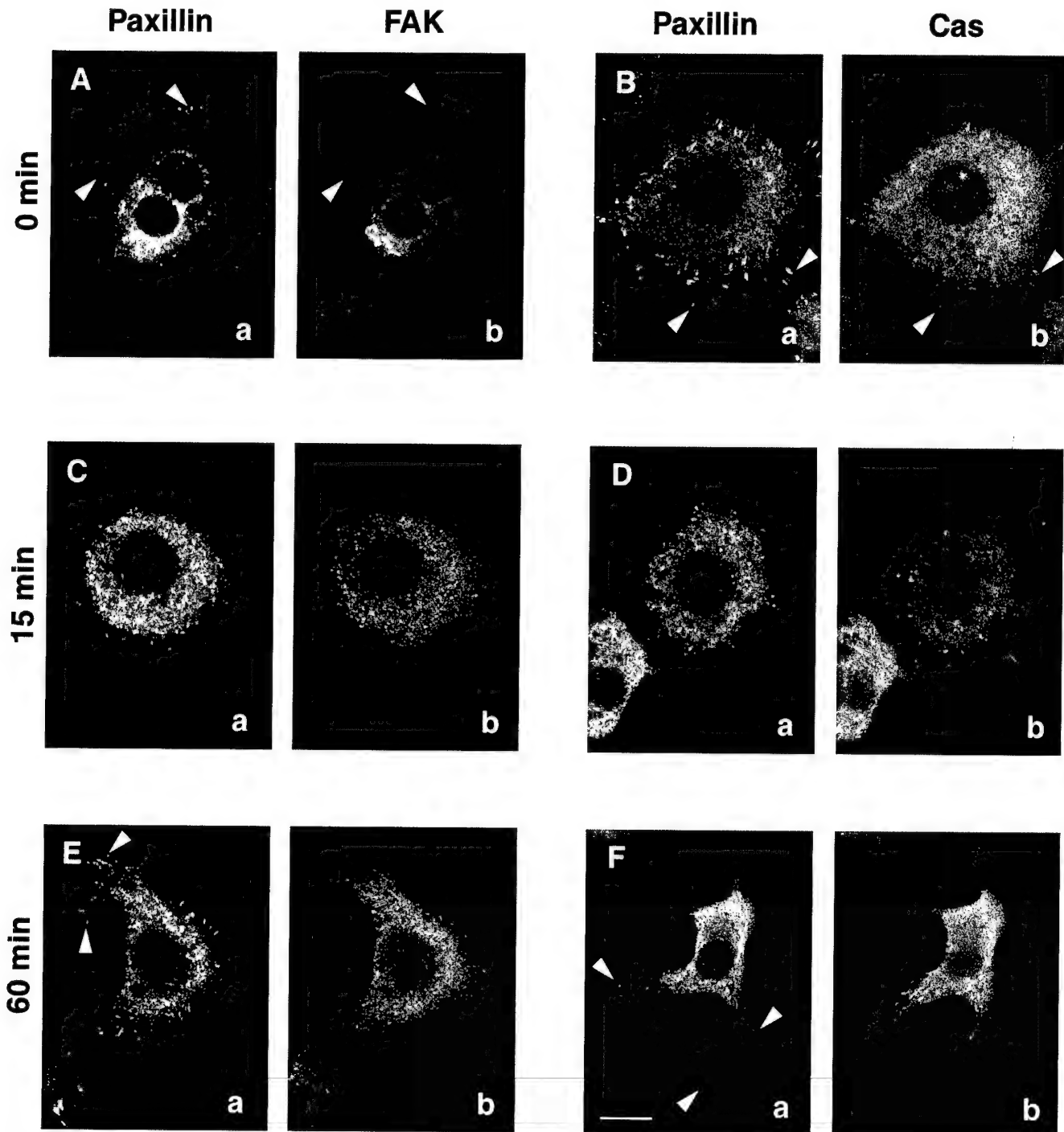


FIG. 4. IGF-I stimulation changes intracellular localization of FAK and Cas along with paxillin in MCF-7/IGF-IR cells. The representative confocal microscopy images demonstrate cells colabeled with anti-paxillin mAb [A(a), C(a), E(a)] and anti-FAK (N-17) pAb [A(b), C(b), E(b)]; cells colabeled with anti-paxillin mAb [B(a), D(a), F(a)] and a mixture of anti-Cas B and anti-Cas F pAbs [B(b), D(b), F(b)]. Serum-starved cells (A, B); serum-starved cells treated with 50 ng/ml IGF-I for 15 min (C, D) and 60 min (E, F). The representative areas of coincidental staining of paxillin with either FAK or Cas are marked by arrowheads in (A) and (B), respectively. In (E) and (F), arrowheads indicate the accumulation of paxillin in prolonged streaks localized to membrane protrusions. Bar = 20 μ m.

cells stimulated with IGF-I. In serum-starved cells, FAK was prominently tyrosine phosphorylated (Fig. 5A'). Within 5 min of IGF-I treatment, FAK became

dephosphorylated by 50% (Fig. 5A). The level of FAK phosphorylation remained low for at least 15 min, then was elevated almost to basal level by 1 h (Figs. 5A and

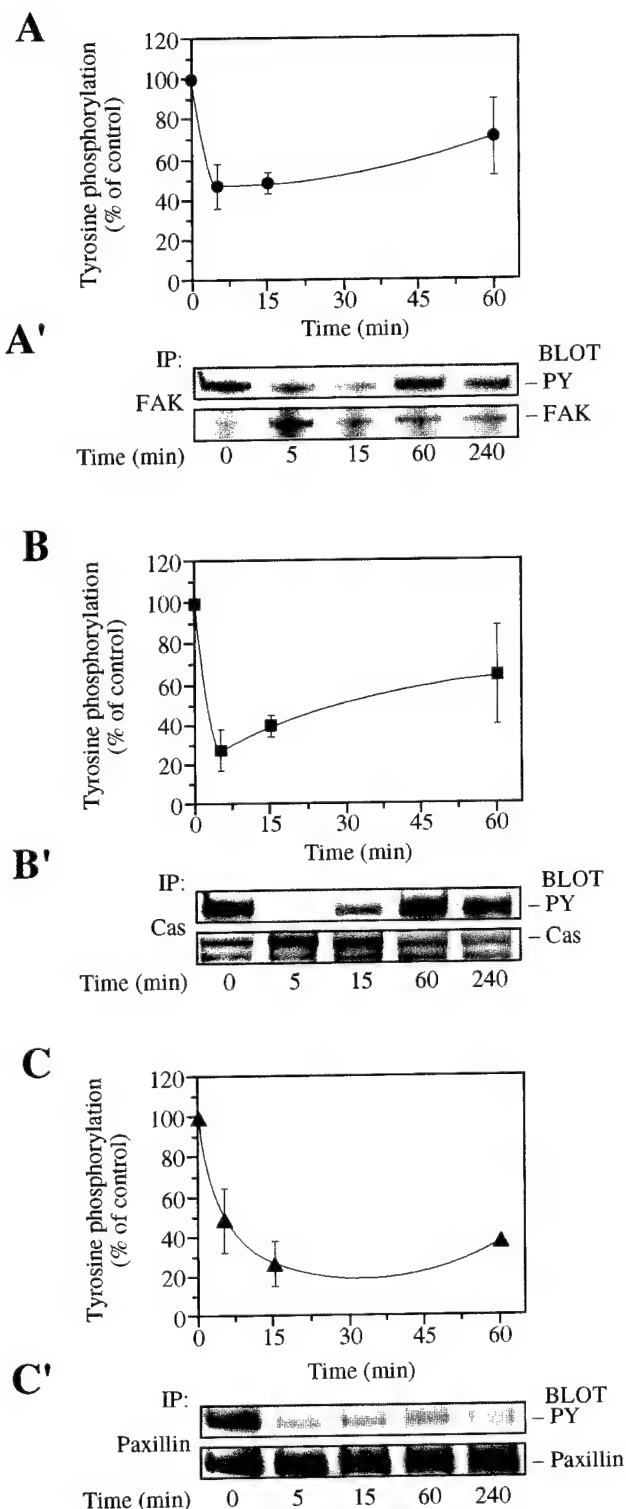


FIG. 5. IGF-IR activation induces rapid tyrosine dephosphorylation of FAK, Cas, and paxillin in MCF-7/IGF-IR cells. (A, B, C) Time courses of the relative tyrosine phosphorylation of FAK, Cas, and paxillin in response to 50 ng/ml IGF-I, correspondingly. The intensity of the bands of the phosphorylated proteins was measured by laser scanning densitometry. The value of tyrosine phosphorylation

5A', upper panel). To test the possibility that tyrosine dephosphorylation of FAK affected the phosphotyrosine content of FAK targets such as Cas and paxillin, we immunoprecipitated both these proteins from the same lysates as FAK.

In control serum-starved cells, the tyrosine phosphorylation level of Cas and paxillin was high (Figs. 5B', 5C', upper panels). After 5 min of IGF-I stimulation, the Cas tyrosine phosphorylation was reduced by more than 70% of the control level. Tyrosine dephosphorylation of Cas was transient, since within 15 min of IGF-I addition its phosphorylation was elevated, and by 1 h it almost reverted to the basal level (Figs. 5B, 5B'). Within 5 min of IGF-I stimulation, tyrosine phosphorylation of paxillin was reduced by 50%, and over the next 10 min it declined further to 30–40% of basal phosphorylation, remaining at this level for at least 4 h (Fig. 5C).

In the absence of IGF-I stimulation, the basal level of tyrosine phosphorylation of FAK, Cas, and paxillin in the parental MCF-7 cells was comparable to that in MCF-7/IGF-IR cells. However, no significant changes in tyrosine phosphorylation status of focal adhesion-associated proteins FAK, Cas, and paxillin were observed in MCF-7 cells treated with 50 ng/ml IGF-I for up to 4 h (data not shown).

PAO Prevents Tyrosine Dephosphorylation of FAK, Cas, and Paxillin and Inhibits Membrane Protrusion in IGF-I-Stimulated MCF-7/IGF-IR Cells

To investigate whether protein tyrosine phosphatase activity was required for the reduced tyrosine phosphorylation of FAK, Cas, and paxillin in response to IGF-I stimulation of MCF-7/IGF-IR cells, we attempted to block a putative IGF-IR-activated PTP. The trivalent arsenical compound PAO was selected for this purpose. PAO is a membrane-permeable PTP inhibitor that blocks tyrosine phosphatase activity in insulin signaling and upregulates tyrosine phosphorylation of FAK and paxillin in fibroblasts at concentrations of 1–5 μ M [23, 24].

In a series of control experiments we established that 5 μ M PAO had no effect on IGF-I-induced tyrosine phosphorylation of either the IGF-IR β subunit or IRS-1 (data not shown). Subsequently, we examined

for each protein in serum-starved cells (time point 0 min) was taken as 100%. Error bars show SEM, $n = 4$. (A', B', C') Representative blots demonstrate the various levels of the tyrosine phosphorylated FAK, Cas, and paxillin (upper panels) and the comparable amounts of these proteins in the correspondent samples (lower panels) before and after IGF-I stimulation at the indicated time points. In the lower panels of (A'), (B'), and (C'), the anti-phosphotyrosine blots were stripped and reprobed with the indicated antibodies.

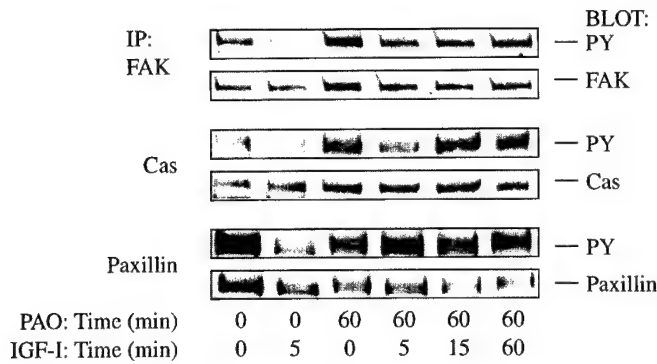


FIG. 6. PAO prevents tyrosine dephosphorylation of focal adhesion proteins in cells stimulated with IGF-I. Western blots show tyrosine phosphorylation and protein levels of the immunoprecipitated FAK, Cas, and paxillin in samples of serum-starved cells, serum-starved cells stimulated with 50 ng/ml IGF-I for 5 min, and serum-starved cells pretreated with 5 μ M PAO for 60 min and then stimulated with 50 ng/ml IGF-I for the time indicated.

the effect of PAO on IGF-I-induced dephosphorylation of focal adhesion proteins FAK, Cas, and paxillin (Fig. 6). Preincubation with PAO for 60 min resulted in slightly increased basal tyrosine phosphorylation only of FAK and Cas. The following stimulation of PAO-treated cells with IGF-I for up to 60 min did not reduce tyrosine phosphorylation of FAK, Cas, and paxillin, indicating that PTP activity is required for IGF-IR-mediated dephosphorylation of these molecules.

We further investigated whether PAO rescue of the focal adhesion proteins from IGF-I-induced dephosphorylation influenced IGF-IR-mediated changes in cell morphology. MCF-7/IGF-IR cells were incubated in either 5 μ M PAO in SFM or SFM alone for 60 min (Figs. 7A and 7D, respectively). Next, both cell monolayers were stimulated with 50 ng/ml IGF-I, and cell morphology was recorded after 15 and 60 min (Figs. 7B, E and 7C, F). After 60 min, PAO-treated cells formed lobopodium-like membrane advances resembling those displayed by serum-starved cells in response to a 15-min treatment with IGF-I (compare Figs. 7C and 7E). The outward extensions of lamellipodia typically seen in control cells after 60 min of IGF-I addition appeared to be blocked in PAO-pretreated cells, thereby suggesting at least a partial inhibition of morphological transition toward the motile phenotype.

DISCUSSION

The structural organization of a normal polarized epithelium restricts the separation and movement of individual cells. However, at early stages of malignant progression loss of epithelial polarity can promote cell motility and facilitate dissemination of cancer cells from epithelial tissue, thereby increasing the chance of a metastatic spread [25].

The increased level and enhanced autophosphorylation of the IGF-IR observed in malignant versus normal human breast tissues [10], as well as association of the IGF-IR with cell migration *in vitro* [8, 9], prompted our current investigations on the cellular and molecular mechanisms governing IGF-IR-mediated motility in breast cancer cells.

In the present work, we assessed the effects of IGF-IR overexpression on the events related to motility of MCF-7 breast epithelial cells. For the first time, we demonstrated that activation of the overexpressed IGF-IR causes depolarization of an epithelial cell monolayer. The magnitude of IGF-IR signaling as determined by the number of activated IGF-IRs appears critical for converting epithelial cells from a polarized to a motile phenotype, since a more striking morphological transformation occurred in MCF-7/IGF-IR (1.1×10^6 receptors/cell) than in the parental MCF-7 (6.0×10^4 receptors/cell) cells.

The drastic changes in morphology of IGF-I-stimulated MCF-7/IGF-IR cells point to the involvement of cytoskeleton restructuring in cell depolarization. In this study we analyzed reorganization of the actin cytoskeleton in MCF-7/IGF-IR cells stimulated with IGF-I for 4 h, and identified three distinct phases of F-actin reorganization: (1) actin filament disassembly followed by (2) accumulation of condensed short actin bundles along the cell periphery, and (3) reassembly of the long F-actin bundles.

We have demonstrated that disruption of circumferential and stress fiber-like actin bundles as well as cortical actin filaments—the cytoskeletal structures responsible for the architecture and strength of the multicellular epithelial sheet—is an early event associated with IGF-IR-induced depolarization. Disassembly of actin filamentous network appeared to be transient (5–15 min). How does the activated IGF-IR cause F-actin disassembly? One possibility is that the rapid breakdown of the actin filaments is caused by the activation of actin-severing proteins, like gelsolin, whose stimulation, in turn, requires the transient increase in intracellular Ca^{2+} [26]. In some cell types, IGF-I stimulates phosphatidylinositol turnover and intracellular Ca^{2+} release [27]. Whether a rise in Ca^{2+} and stimulation of the actin-severing proteins occur following IGF-IR activation in MCF-7 cells remains to be determined.

Another possibility might be an IGF-IR-mediated activation of the small GTP-binding protein Rac as well as other members of the Rho family. Recently, microinjection studies on Rho D, Rho G, TC10, Rnd 1, and Rnd 3 (RhoE) demonstrated that these proteins cause breakdown of the stress fibers and associated loss of cell adhesion in fibroblasts [28]. In mammary epithelial cells, Cdc42- and Rac-mediated actin reorganization has been disrupted by inhibition of the PI 3-kinase

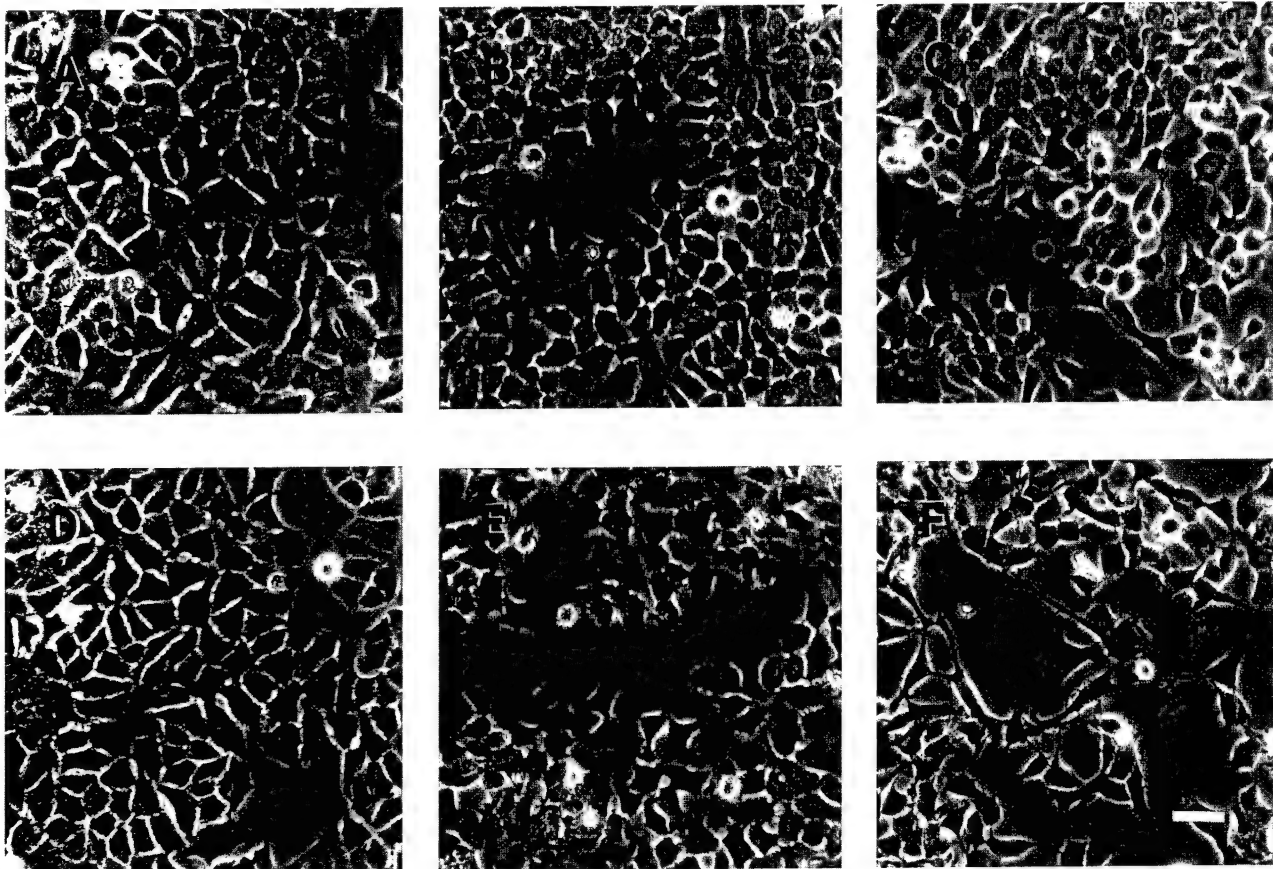


FIG. 7. PAO blocks morphological transitions in MCF-7/IGF-IR cells stimulated with IGF-I. The representative phase-contrast micrographs show the morphology of MCF-7/IGF-IR cells under different conditions. Serum-starved cells were pretreated with 5 μ M PAO in SFM for 60 min (A) and then stimulated with 50 ng/ml IGF-I for either 15 min (B) or 60 min (C). In parallel, serum-starved cells (D) were stimulated with 50 ng/ml IGF-I for either 15 min (E) or 60 min (F). Bar = 100 μ m.

[29]. In fibroblasts expressing the Ras oncogene, active PI 3-kinase has been implicated in the disruption of actin stress fibers via dissociation of cortactin, an F-actin crosslinking protein, from the actin-myosin II complex [30]. According to our previous data, the amount and activity of IRS-1-associated PI 3-kinase are higher in MCF-7/IGF-IR than in MCF-7 cells stimulated with IGF-I [21, 31]. In the study reported here, we tested the involvement of the PI 3-kinase in F-actin rearrangements in MCF-7/IGF-IR cells. Preincubation of the cells with the specific PI 3-kinase inhibitor LY 294002 abrogated IGF-I-induced F-actin disassembly, suggesting that IGF-IR/PI 3-kinase-dependent signaling triggers the rapid F-actin breakdown in MCF-7/IGF-IR cells.

The second phase of IGF-IR modulation of the actin cytoskeleton lasted approximately 1 h and was characterized by organization of the short F-actin bundles into microspike-like structures along the cell periphery. We speculate that IGF-IR regulation of actin-binding/bundling proteins is involved in microspike forma-

tion, which in turn might facilitate cell depolarization. This hypothesis is being tested currently.

The reappearance of the long actin filaments in the nascent lamellipodia apparently required actin polymerization, since addition of IGF-I along with cytochalasin, the drug that caps the plus end of actin filament and blocks actin polymerization, prevented lamellipodial extension (Guvakova, unpublished data). In many cell types, actin polymerization is closely linked with PI 3-kinase signaling [32], which also is required for lamellipodium formation and membrane ruffling [33]. Accordingly, we demonstrated that a block of PI 3-kinase activity inhibited IGF-I-induced membrane protrusion. This, however, does not rule out the possibility that the blockade of membrane extension is a secondary event, since the inhibition of PI 3-kinase also prevented F-actin disassembly, and the latter preceded lamellipodial protrusion in MCF-7/IGF-IR cells.

Previous studies have revealed that the breakdown of cell-cell adhesions plays an important role in epithelial-mesenchymal transition induced by different

growth factors [34, 35]. However, morphological cell transformation from polarized to nonpolarized phenotype is certainly related to modulation of cell–substratum interaction, and, therefore, mechanisms must exist to regulate the assembly and disassembly of cell–matrix junctions. We have shown here that IGF-IR activation induces rapid reorganization of focal adhesions. In response to IGF-I, “arrowhead”-shaped paxillin clusters in the static cell transformed into elongated streaks of paxillin at the periphery of membrane protrusions. The latter might function similarly to “transient focal contacts” of slowly moving cells described by Couchman and Rees [36]. Paxillin possesses multiple protein–protein interaction motifs [37] and, in contrast to FAK and Cas, is prominent in membrane protrusions. It is tempting to speculate that an exchange in paxillin molecular partners plays a key role in IGF-IR-mediated turnover of focal adhesions.

The effect of IGF-I on the tyrosine phosphorylation status of the focal adhesion proteins has been investigated in various cell models, and the reported influence of IGF-I on either FAK or paxillin appeared to be contrasting in different cells [17, 19, 20]. Recently, it was demonstrated that in IGF-I-stimulated Swiss 3T3 fibroblasts expressing very low levels of the IGF-IR there was an increase in FAK, Cas, and paxillin tyrosine phosphorylation [38]. In contrast to MCF-7 cells, however, serum-starved Swiss 3T3 cells lose their stress fibers and associated focal adhesions as well as tyrosine phosphorylation of FAK and paxillin [39]. Therefore, the contrasted cellular context and varying levels of IGF-IR expression in different cellular systems make it difficult to compare the results.

To clarify the relationship between IGF-IR stimulation, focal adhesion protein activity, and cell locomotion, we analyzed the time course of tyrosine phosphorylation of FAK, Cas, and paxillin in MCF-7 and MCF-7/IGF-IR cells exposed to IGF-I. In the MCF-7 parental cells, the relatively high basal phosphorylation of FAK, Cas, and paxillin was not reduced notably on IGF-I stimulation, whereas in MCF-7/IGF-IR cells, stronger IGF-IR activation triggered an acute tyrosine dephosphorylation of FAK and Cas. The kinetic profiles of FAK and Cas dephosphorylation were similar, consistent with the regulatory role of FAK in direct or indirect (via the activation of Src-family kinases) tyrosine phosphorylation of Cas [40, 41]. Alternatively, the activated IGF-IR might stimulate a PTP controlling the function of FAK, Cas, or Src-family proteins. In this respect it is interesting that a newly discovered dual-specificity phosphatase PTEN (MMAC1) interacts with FAK and reduces tyrosine phosphorylation of this kinase as well as Cas [42]. The SH3 domain of Cas also directly binds to proline-rich region of the cytoplasmic PTP1B [43] whose role in IGF-IR signaling remains obscure. In the present study, we found that another

FAK-associated phosphoprotein, paxillin, underwent tyrosine dephosphorylation in response to IGF-I. The recent discovery of the physical association between a nonreceptor PTP–PEST and paxillin suggests that paxillin itself or paxillin-binding partners, including FAK, might serve as PTP–PEST substrates [44]. Another enticing candidate for a role in IGF-IR-regulated PTP activity is PTP1D (also known as Shp2/SH-PTP2/Syp). This cytoplasmic PTP is activated by direct binding to the phosphorylated insulin receptor (IR), IGF-IR or IRS-1 [45], and is known to mediate insulin-induced dephosphorylation of FAK and paxillin in CHO cells overexpressing the IR [46]. Recent studies identified an important role for PTP1D in regulating cell spreading, migration, and cytoskeletal architecture in fibroblasts, presumably via control of FAK [47].

Despite the unknown identity of IGF-IR-activated PTP in our cell model, the experiments with PAO, a phosphotyrosine phosphatase inhibitor, support the idea that induction of a PTP is critical for depolarization in MCF-7/IGF-IR cells. PAO rescue of FAK, Cas, and paxillin, from IGF-I-induced tyrosine dephosphorylation was sufficient to block development of the motile membrane protrusions. Collectively, our findings suggest the IGF-IR as an upstream regulator of a PAO-sensitive PTP, which either directly or indirectly dephosphorylates FAK, Cas, and paxillin and disrupts focal contacts.

In summary, we have established that activation of the overexpressed IGF-IR in MCF-7 cells results in a loss of epithelial cell polarity associated with acute disassembly of the actin filaments, subcellular reorganization of paxillin-enriched focal contacts, and rapid tyrosine dephosphorylation of FAK, Cas, and paxillin. Both PI 3-kinase and PTP activities are required for the depolarization of MCF-7 breast cancer cells. Taken together, these results suggest that IGF-IR overexpression in mammary epithelial cells may have a significant impact in stimulating tumor cell motility.

We are grateful to Dr. Joseph A. DePasquale for valuable discussions during the work, to Dr. Karen Knudsen and Dr. Carol Marshall for the critical comments on the manuscript, to Todd Sargood and Dawn Fowler for help with image processing, and to Priya K. Hingorani for the expert assistance with confocal microscopy. We thank Dr. Amy H. Bouton and Dr. J. Thomas Parsons for the generous gift of the antibodies. M.A.G. is a recipient of a fellowship from the U.S. Army (DAMD 17-97-1-7211). This work was in part supported by NIH Grant DK48969 (E.S.)

REFERENCES

1. Davies, J. A., and Garrod, D. R. (1997). Molecular aspects of the epithelial phenotype. *BioEssays* **19**, 699–704.
2. Gumbiner, B. (1996). Cell adhesion: The molecular basis for tissue architecture and morphogenesis. *Cell* **84**, 345–357.
3. Danjo, Y., and Gipson, I. K. (1998). Actin ‘purse string’ filaments are anchored by E-cadherin-mediated adherens junctions.

- tions at the leading edge of the epithelial wound, providing coordinated cell movement. *J. Cell Sci.* **111**, 3323–3331.
4. Ando, Y., and Jensen, P. J. (1993). Epidermal growth factor and insulin-like growth factor I enhance keratinocyte migration. *J. Invest. Dermatol.* **100**, 633–639.
 5. Leventhal, P. S., and Feldman, E. L. (1997). Insulin-like growth factors as regulators of cell motility: Signaling mechanisms. *Trends Endocrinol. Metab.* **8**, 1–6.
 6. Brooks, P. C., Klemke, R. L., Schön, S., Lewis, J. M., Schwartz, M. A., and Cheresch, D. A. (1997). Insulin-like growth factor receptor cooperates with integrin $\alpha_v\beta_5$ to promote tumor cell dissemination in vivo. *J. Clin. Invest.* **99**, 1390–1398.
 7. Henricks, D. M., Kouba, A. J., Lackey, B. R., Boone, W. R., and Gray, S. L. (1998). Identification of insulin-like growth factor I in bovine seminal plasma and its receptor on spermatozoa: Influence on sperm motility. *Biol. Reprod.* **59**, 330–337.
 8. Kohn, E. C., Francis, E. A., Liotta, L. A., and Schiffmann, E. (1990). Heterogeneity of the motility responses in malignant tumor cells: A biological basis for the diversity and homing of metastatic cells. *Int. J. Cancer* **46**, 287–292.
 9. Doerr, M. E., and Jones, J. I. (1996). The roles of integrins and extracellular matrix proteins in the insulin-like growth factor I-stimulated chemotaxis of human breast cancer cells. *J. Biol. Chem.* **271**, 2443–2447.
 10. Resnik, J. L., Reichart, D. B., Huey, K., Webster, N. J. G., and Seely, B. L. (1998). Elevated insulin-like growth factor I receptor autophosphorylation and kinase activity in human breast cancer. *Cancer Res.* **58**, 1159–1164.
 11. Baserga, R. (1998). The IGF-I receptor in normal and abnormal growth. In "Hormones and Growth Factors in Development and Neoplasia" (R. B. Dickson and D. S. Salomon, Eds.), pp. 269–287. Wiley-Liss, New York.
 12. Sepp-Lorenzino, L. (1998). Structure and function of the insulin-like growth factor I receptor. *Breast Cancer Res. Treat.* **47**, 235–253.
 13. Yenush, L., and White, M. F. (1997). The IRS-1-signaling system during insulin and cytokine action. *BioEssays* **19**, 491–500.
 14. Yonemura, S., Itoh, M., Nagafuchi, A., and Tsukita, S. (1995). Cell-to-cell adherens junction formation and actin filament organization: Similarities and differences between non-polarized fibroblasts and polarized epithelial cells. *J. Cell Sci.* **108**, 127–142.
 15. Kadowaki, T., Koyasu, S., Nishida, E., Sakai, H., Takaku, F., Yahara, I., and Kasuga, M. (1986). Insulin-like growth factors, insulin, and epidermal growth factor cause rapid cytoskeletal reorganization in KB cells. *J. Biol. Chem.* **261**, 16141–16147.
 16. Izumi, T., Saeki, Y., Akanuma, Y., Takaku, F., and Kasuga, M. (1988). Requirement for receptor-intrinsic tyrosine kinase activities during ligand-induced membrane ruffling of KB cells. *J. Biol. Chem.* **263**, 10386–10393.
 17. Leventhal, P. S., Shelden, E. A., Kim, B., and Feldman, E. L. (1997). Tyrosine phosphorylation of paxillin and focal adhesion kinase during insulin-like growth factor-I-stimulated lamellipodia advance. *J. Biol. Chem.* **272**, 5214–5218.
 18. Jones, J. L., Royall, J. E., Critchley, D. R., and Walker, R. A. (1997). Modulation of myoepithelial-associated $\alpha_6\beta_4$ integrin in a breast cancer cell line alters invasive potential. *Exp. Cell Res.* **235**, 325–333.
 19. Konstantopoulos, N., and Clark, S. (1996). Insulin and insulin-like growth factor-1 stimulate dephosphorylation of paxillin in parallel with focal adhesion kinase. *Biochem. J.* **314**, 387–390.
 20. Baron, V., Calléja, V., Ferrari, P., Alengrin, F., and van Obberghen, E. (1998). p125^{Fak} focal adhesion kinase is a substrate for the insulin and insulin-like growth factor-I tyrosine kinase receptors. *J. Biol. Chem.* **273**, 7162–7168.
 21. Guvakova, M. A., and Surmacz, E. (1997a). Overexpressed IGF-I receptors reduce estrogen growth requirements, enhance survival, and promote E-cadherin-mediated cell-cell adhesion in human breast cancer cells. *Exp. Cell Res.* **231**, 149–162.
 22. Knight, J. B., Yamauchi, K., and Pessin, J. E. (1995). Divergent insulin and platelet-derived growth factor regulation of focal adhesion kinase (pp125^{Fak}) tyrosine phosphorylation, and rearrangement of actin stress fibers. *J. Biol. Chem.* **270**, 10199–10203.
 23. Noguchi, T., Matozaki, T., Horita, K., Fujioka, Y., and Kasuga, M. (1994). Role of SH-PTP2, a protein-tyrosine phosphatase with Src homology 2 domains, in insulin-stimulated Ras activation. *Mol. Cell. Biol.* **14**, 6674–6682.
 24. Retta, S. F., Barry, S. T., Critchley, D. R., Defilippi, P., Silengo, L., and Tarone, G. (1996). Focal adhesion and stress fiber formation is regulated by tyrosine phosphatase activity. *Exp. Cell Res.* **299**, 307–317.
 25. Kohn, E. C., and Liotta, L. A. (1995). Molecular insights into cancer invasion: Strategies for prevention and intervention. *Cancer Res.* **55**, 1856–1862.
 26. Burtneck, L. D., Koepf, E. K., Grimes, J., Jones, E. Y., Stuart, D. I., McLaughlin, P. J., and Robinson, R. C. (1997). The crystal structure of plasma gelsolin: Implication for actin severing, capping, and nucleation. *Cell* **90**, 661–670.
 27. Bornfeldt, K. E., Raines, E. W., Nakano, T., Graves, L. M., Krebs, E. G., and Ross, R. (1994). Insulin-like growth factor-I and platelet-derived growth factor-BB induce directed migration of human arterial smooth muscle cells via signaling pathways that are distinct from those of proliferation. *J. Clin. Invest.* **93**, 1266–1274.
 28. Aspenström, P. (1999). The Rho GTPases have multiple effects on the actin cytoskeleton. *Exp. Cell Res.* **246**, 20–25.
 29. Keely, P. J., Westwick, J. K., Whitehead, I. P., Der, C. J., and Parise, L. V. (1997). Cdc42 and rac1 induce integrin-mediated cell motility and invasiveness through PI(3)K. *Nature* **390**, 632–636.
 30. He, H., Watanabe, T., Zhan, X., Huang, C., Schuurin, E., Fukami, K., Takenawa, T., Kumar, C. C., Simpson, R. J., and Maruta, H. (1998). Role of phosphatidylinositol 4,5-bisphosphate in Ras/Rac-induced disruption of the cortactin-actomyosin II complex and malignant transformation. *Mol. Cell. Biol.* **18**, 3829–3837.
 31. Guvakova, M. A., and Surmacz, E. (1997b). Tamoxifen interferes with the insulin-like growth factor I receptor (IGF-IR) signaling pathway in breast cancer cells. *Cancer Res.* **57**, 2606–2610.
 32. Lange, K., Brandt, U., Gartzke, J., and Bergmann, J. (1998). Action of insulin on the surface morphology of hepatocytes: Role of phosphatidylinositol 3-kinase in insulin-induced shape change of microvilli. *Exp. Cell Res.* **239**, 139–151.
 33. Wennström, S., Hawkins, P., Cooke, F., Hara, K., Yonezawa, K., Kasuga, M., Jackson, T., Claesson-Welsh, L., and Stephens, L. (1994). Activation of phosphoinositide 3-kinase is required for PDGF-stimulated membrane ruffling. *Curr. Biol.* **4**, 385–393.
 34. Boyer, B., Dufour, S., and Thiery, J. P. (1992). E-cadherin expression during the acidic FGF-induced dispersion of a rat bladder carcinoma cell line. *Exp. Cell Res.* **201**, 347–357.
 35. Potempa, S., and Ridley, A. J. (1998). Activation of both MAP kinase and phosphatidylinositol 3-kinase by Ras is required for hepatocyte growth factor/scatter factor-induced adherens junction disassembly. *Mol. Biol. Cell* **9**, 2185–2200.

36. Couchman, J. R., and Rees, D. A. (1979). The behaviour of fibroblasts migrating from chick heart explants: Changes in adhesion, locomotion and growth, and in the distribution of actomyosin and fibronectin. *J. Cell Sci.* **39**, 149–165.
37. Turner, C. E., and Miller, J. T. (1994). Primary sequence of paxillin contains putative SH2 and SH3 domain binding motifs and multiple LIM domains: Identification of a vinculin and pp125Fak-binding region. *J. Cell Sci.* **107**, 1583–1591.
38. Casamassima, A., and Rozengurt, E. (1998). Insulin-like growth factor I stimulates tyrosine phosphorylation of p130^{Cas}, focal adhesion kinase, and paxillin. *J. Biol. Chem.* **273**, 26149–26156.
39. Machesky, L. M., and Hall, A. (1996). Rho: a connection between membrane receptor signalling and the cytoskeleton. *Trends Cell Biol.* **6**, 304–310.
40. Polte, T. R., and Hanks, S. K. (1997). Complexes of focal adhesion kinase (FAK) and Crk-associated substrate (p130 (Cas)) are elevated in cytoskeleton-associated fractions following adhesion and Src transformation: Requirements for Src kinase activity and FAK proline-rich motifs. *J. Biol. Chem.* **272**, 5501–5509.
41. Tachibana, K., Urano, T., Fujita, H., Ohashi, Y., Kamiguchi, K., Iwata, S., Hirai, H., and Morimoto, C. (1997). Tyrosine phosphorylation of Crk-associated substrates by focal adhesion kinase. *J. Biol. Chem.* **272**, 29083–29090.
42. Tamura, M., Gu, J., Matsumoto, K., Aoto, S.-I., Parsons, R., and Yamada, K. M. (1998). Inhibition of cell migration, spreading, and focal adhesions by tumor suppressor PTEN. *Science* **280**, 1614–1617.
43. Liu, F., Hill, D. E., and Chernoff, J. (1996). Direct binding of the proline-rich region of protein tyrosine phosphatase 1B to the Src homology 3 domain of p130 (Cas). *J. Biol. Chem.* **271**, 31290–31295.
44. Shen, Y., Schneider, G., Cloutier, J.-F., Veillette, A., and Schaller, M. D. (1998). Direct association of protein-tyrosine phosphatase PTP-PEST with paxillin. *J. Biol. Chem.* **273**, 6474–6481.
45. Rocchi, S., Tartare-Deckert, S., Sawka-Verhelle, D., Gamha, A., and van Obberghen, E. (1996). Interaction of SH2-containing protein tyrosine phosphatase 2 with the insulin receptor and the insulin-like growth factor-I receptor: Studies of the domains involved using the yeast two-hybrid system. *Endocrinology* **137**, 4944–4952.
46. Ouwens, D. M., Mikkers, H. M. M., van der Zon, G. C. M., Stein-Gerlach, M., Ullrich, A., and Maassen, J. A. (1996). Insulin-induced tyrosine dephosphorylation of paxillin and focal adhesion kinase requires active phosphotyrosine phosphatase 1D. *Biochem. J.* **318**, 609–614.
47. Yu, D.-H., Qu, C.-K., Henegariu, O., Lu, X., and Feng, G.-S. (1998). Protein-tyrosine phosphatase Shp-2 regulates cell spreading, migration, and focal adhesion. *J. Biol. Chem.* **273**, 21125–21131.

Received February 11, 1999

Revision received May 21, 1999

INSULIN RECEPTOR SUBSTRATE 1 IS A TARGET FOR THE PURE ANTIESTROGEN ICI 182,780 IN BREAST CANCER CELLS

Michele SALERNO^{1,2}, Diego SISI^{1,2}, Loredana MAURO^{1,2}, Marina A. GUVAKOVA¹, Sebastiano ANDO^{2,3} and Ewa SURMACZ^{1*}

¹Kimmel Cancer Center, Thomas Jefferson University, Philadelphia, PA, USA

²Department of Cellular Biology, University of Calabria, Cosenza, Italy

³Faculty of Pharmacy, University of Calabria, Cosenza, Italy

The pure antiestrogen ICI 182,780 inhibits insulin-like growth factor (IGF)-dependent proliferation in hormone-responsive breast cancer cells. However, the interactions of ICI 182,780 with IGF-I receptor (IGF-IR) intracellular signaling have not been characterized. Here, we studied the effects of ICI 182,780 on IGF-IR signal transduction in MCF-7 breast cancer cells and in MCF-7-derived clones overexpressing either the IGF-IR or its 2 major substrates, insulin receptor substrate 1 (IRS-1) or src/collagen homology proteins (SHC). ICI 182,780 blocked the basal and IGF-I-induced growth in all studied cells in a dose-dependent manner; however, the clones with the greatest IRS-1 overexpression were clearly least sensitive to the drug. Pursuing ICI 182,780 interaction with IRS-1, we found that the antiestrogen reduced IRS-1 expression and tyrosine phosphorylation in several cell lines in the presence or absence of IGF-I. Moreover, in IRS-1-overexpressing cells, ICI 182,780 decreased IRS-1/p85 and IRS-1/GRB2 binding. The effects of ICI 182,780 on IGF-IR protein expression were not significant; however, the drug suppressed IGF-I-induced (but not basal) IGF-IR tyrosine phosphorylation. The expression and tyrosine phosphorylation of SHC as well as SHC/GRB binding were not influenced by ICI 182,780. In summary, downregulation of IRS-1 may represent one of the mechanisms by which ICI 182,780 inhibits the growth of breast cancer cells. Thus, overexpression of IRS-1 in breast tumors could contribute to the development of antiestrogen resistance. *Int. J. Cancer* 81:299–304, 1999.

© 1999 Wiley-Liss, Inc.

ICI 182,780, an alpha-alkylsulfinylamide, is a new-generation pure antiestrogen (Wakeling *et al.*, 1991). The drug has shown great promise as a second-line endocrine therapy agent in patients with advanced breast cancer resistant to the non-steroidal antiestrogen tamoxifen (Tam). Indeed, in several *in vitro* and *in vivo* studies, the antitumor effects of ICI 182,780 were greater than those of Tam (Nicholson *et al.*, 1996; Osborne *et al.*, 1995; de Cupis *et al.*, 1995; Chander *et al.*, 1993; Wakeling *et al.*, 1991). Moreover, unlike Tam, ICI 182,780 lacks agonist (estrogenic) activity and its administration does not appear to be associated with deleterious side effects such as induction of endometrial cancer or retinopathy (Osborne *et al.*, 1995; Chander *et al.*, 1993). ICI 182,780 antagonizes multiple cellular effects of estrogens by impairing the dimerization of the estrogen receptor (ER) and by reducing ER half-life (de Cupis and Favoni, 1997; Chander *et al.*, 1993). ICI 182,780 also interferes with growth factor-induced growth, but it is not clear whether this activity is mediated exclusively through the ER, or if some ER-independent mechanism is implicated (de Cupis *et al.*, 1995). Despite their great antitumor effects, pure antiestrogens do not circumvent the development of antiestrogen resistance, as most breast tumor cells initially sensitive to ICI 182,780 eventually become unresponsive to the drug (de Cupis and Favoni, 1997; Pavlik *et al.*, 1996; Nicholson *et al.*, 1995). The mechanism of this resistance is not clear, but it has been suggested that both mutations of the ER as well as alterations in growth factor-dependent mitogenic pathways may be involved (de Cupis and Favoni, 1997; Larsen *et al.*, 1997; Pavlik *et al.*, 1996; Wiseman *et al.*, 1993).

The insulin-like growth factor (IGF) system [IGFs, IGF-I receptor (IGF-IR) and IGF binding proteins (IGFBP)] plays a critical role in the pathobiology of hormone-responsive breast

cancer (reviewed in Surmacz *et al.*, 1998). In the experimental setting, IGF-IR has been shown to stimulate growth and transformation, improve survival, as well as regulate cell-cell and cell-substrate interactions in breast cancer cells (Surmacz *et al.*, 1998). Moreover, overexpression of different elements of the IGF system, such as IGF-II, IGF-IR or insulin receptor substrate 1 (IRS-1), provides breast cancer cells with growth advantage and reduces or abrogates estrogen growth requirements (Surmacz *et al.*, 1998). On the other hand, downregulation of IGF-IR expression, inhibition of IGF-IR signaling and reduced bioavailability of the IGFs have all been demonstrated to block proliferation and survival as well as to interfere with motility or intercellular adhesion in breast cancer cells (Surmacz *et al.*, 1998).

Clinical studies confirm the role of the IGF-I system in breast cancer development. First, IGF-IR has been found to be up to 14-fold overexpressed in breast cancer compared with its levels in normal mammary epithelium (Surmacz *et al.*, 1998; Resnik *et al.*, 1998; Turner *et al.*, 1997). Moreover, cellular levels of IGF-IR or its substrate IRS-1 correlate with cancer recurrence at the primary site (Rocha *et al.*, 1997; Turner *et al.*, 1997). The ligands of IGF-IR, IGF-I and IGF-II, are often present in the epithelial and/or stromal component of breast tumors, indicating that an autocrine or a paracrine IGF-IR loop may be operative and involved in the neoplastic process (Surmacz *et al.*, 1998). In addition, endocrine IGFs probably also contribute to breast tumorigenesis since the levels of circulating IGF-I correlate with breast cancer risk in premenopausal women (Hankinson *et al.*, 1998).

ICI 182,780 interferes with the IGF-I system in breast cancer cells. The antiestrogen has been shown to attenuate IGF-I-stimulated growth, modulate expression of IGFBPs and downregulate IGF binding sites (Surmacz *et al.*, 1998; de Cupis and Favoni, 1997; de Cupis *et al.*, 1995). The interactions of ICI 182,780 with the IGF-IR signaling pathways, however, have not been characterized.

Our previous work demonstrated that in breast cancer cells, Tam interferes with the IGF-IR signaling acting upon IGF-IR substrates IRS-1 and src/collagen homology proteins (SHC) (Guvakova and Surmacz, 1997). Normally, activation of IGF-IR results in the recruitment and tyrosine phosphorylation of IRS-1 and SHC, followed by their association with several downstream effector proteins and induction of various signaling pathways (Surmacz *et al.*, 1998). For instance, association of either IRS-1 or SHC with GRB-2/SOS complexes activates the Ras/MAP pathway, whereas binding of IRS-1 with p85 stimulates PI-3 kinase. Tam treatment blocks IGF-dependent growth, which coincides with decreased tyrosine phosphorylation of IRS-1 and IGF-IR and with hyperphos-

Grant sponsor: NIH; Grant number: DK 48969; Grant sponsor: U.S. Department of Defense; Grant numbers: DAMD 17-96-1-6250 and DAMD 17-97-1-7211; Grant sponsors: NCR Italy, M.U.R.S.T. Italy 60% and P.O.P. 1998, Italy.

*Correspondence to: Kimmel Cancer Center, Thomas Jefferson University, 233 S. 10th Street, BLSB 606, Philadelphia, PA 19107, USA. Fax: (215) 923-0249. E-mail: surmacz1@jefflin.tju.edu.

Received 17 August 1998; revised 5 November 1998

phorylation of SHC (Guvakova and Surmacz, 1997). Here, we demonstrate the interactions of ICI 182,780 with IGF-IR signaling and discuss the relevant similarities and differences in the modes of action of the 2 antiestrogens.

MATERIAL AND METHODS

Cell lines and cell culture conditions

We used MCF-7 cells and several MCF-7-derived clones overexpressing either IGF-IR (MCF-7/IGF-IR cells), IRS-1 (MCF-7/IRS-1 cells) or SHC (MCF-7/SHC cells). MCF-7/IGF-IR clone 17 and MCF-7/IRS-1 clones 9, 3 and 18 were developed by stable transfection of MCF-7 cells with expression vectors encoding either IGF-IR or IRS-1 and have been characterized previously (Guvakova and Surmacz, 1997; Surmacz and Burgaud, 1995). MCF-7/SHC cells are MCF-7-derived cells transfected with the plasmid pcDNA3/SHC; compared with MCF-7 cells, the level of p55^{SHC} and p47^{SHC} overexpression in MCF-7/SHC cells is approximately 5-fold (data not shown). The above MCF-7-derived clones express ERs and respond to E2, similar to MCF-7 cells (Guvakova and Surmacz, 1997; Surmacz and Burgaud, 1995). The levels of IRS-1 in MCF-7/IGF-IR and MCF-7/SHC cells are similar to those in MCF-7 cells (see Fig. 2b and data not shown).

MCF-7 cells were grown in DMEM:F12 (1:1) containing 5% calf serum (CS). MCF-7-derived clones were maintained in DMEM:F12 plus 5% CS plus 200 µg/ml G418. In the experiments requiring E2-free conditions, the cells were cultured in phenol red-free DMEM containing 0.5 mg/ml BSA, 1 µM FeSO₄ and 2 mM L-glutamine (PRF-SFM) (Guvakova and Surmacz, 1997; Surmacz and Burgaud, 1995).

Cell growth assay

Cells were plated at a concentration 2×10^5 in 6-well plates in a growth medium; the following day (day 0), the cells were shifted to PRF-SFM containing different doses of ICI 182,780 (1–300 nM) with or without 50 ng/ml IGF-I and incubated for 4 days. The increase in cell number from day 0 to day 4 in PRF-SFM was designated as 100% growth increase.

IP and WB

The expression and tyrosine phosphorylation of IGF-I signaling proteins were measured by IP and WB, as described previously (Guvakova and Surmacz, 1997; Surmacz and Burgaud, 1995). Protein lysates (500 µg) were immunoprecipitated with the following antibodies (Abs): for the IGF-IR: anti-IGF-IR monoclonal Ab (MAb) alpha-IR3 (Oncogene Science, Cambridge, MA); for IRS-1: anti-C-terminal IRS-1 polyclonal Ab (pAb) (UBI, Lake Placid, NY); for SHC: anti-SHC pAb (Transduction Laboratories, Lexington, KY). Tyrosine phosphorylation was probed by WB with an antiphosphotyrosine MAb PY20 (Transduction Laboratories). The levels of IRS-1, IGF-IR and SHC expression were determined by stripping the phosphotyrosine blots and reprobing them with the following Abs: for IRS-1: anti-IRS-1 pAb (UBI); for IGF-IR: anti-IGF-IR mAb (Santa Cruz Biotechnology, Santa Cruz, CA); for SHC: anti-SHC MAb (Transduction Laboratories). The association of GRB2 or p85 with IRS-1 or SHC was visualized in IRS-1 or SHC blots using an anti-GRB2 MAb (Transduction Laboratories) or an anti-p85 MAb (UBI), respectively. The intensity of bands was measured by laser densitometry scanning.

Northern blotting

The levels of IRS-1 mRNA were detected by Northern blotting in 20 µg of total RNA using a 631 bp probe derived from a mouse IRS-1 cDNA (nt 1351–2002). This fragment (99.8% homology with the human IRS-1 sequence) hybridizes with both human and mouse IRS-1 mRNA (Nishiyama and Wands, 1992).

Statistical analysis

The results in cell growth experiments were analyzed by analysis of variance (ANOVA) or Student's *t*-test, where appropriate.

RESULTS

ICI 182,780 inhibits growth of MCF-7 cells with amplified IGF-IR signaling. Sensitivity to ICI 182,780 is determined by the cellular levels of IRS-1

All cell lines used in this study secrete autocrine IGF-I-like mitogens and are able to proliferate in PRF-SFM (Guvakova and Surmacz, 1997; Surmacz and Burgaud, 1995). The basal (autocrine) growth of the cells was enhanced in the presence of IGF-I (Fig. 1a,b). Short (1–2 days) treatments with ICI 182,780 were not sufficient to inhibit cell growth (data not shown), but a 4-day culture in the presence of the antiestrogen produced evident cytostatic effects (Fig. 1a,b). In general, the response to ICI 182,780 was dose dependent (Fig. 1a,b), however, compared with the other cell lines, the cells highly overexpressing IRS-1 (MCF-7/IRS-1 clones 3 and 18) were more resistant to the drug (Fig. 1b,c). Specifically, 1 nM ICI 182,780 inhibited the basal growth by 80, 55 and 50% in MCF-7, MCF-7/IGF-IR and MCF-7/SHC cells, respectively, but the same dose produced only a 20–30% growth inhibition in MCF-7/IRS-1 clones 3 and 18 (Fig. 1a,b). Higher concentrations of ICI 182,780 (10 and 100 nM) effectively suppressed the autocrine growth, or even induced cell death in all cell lines, except MCF-7/IRS-1 clone 18, where the maximal reduction (32%) of the basal growth occurred with a 100 nM dose (Fig. 1b).

In the presence of IGF-I, the effects of ICI 182,780 were attenuated; 1 nM ICI 182,780 was never cytostatic (data not shown), while the 10 and 100 nM doses inhibited (by 30–50% and 47–78%, respectively) IGF-I-dependent proliferation of cells with low IRS-1 levels (Fig. 1a,b). The same doses, however, were less efficient in MCF-7/IRS-1 clones 3 and 18, where growth reduction was 20–25% for 10 nM and 41–47% for 100 nM. Similarly, 300 nM ICI 182,780 produced a prominent cytostatic effect in all cell lines with low IRS-1 expression, but was less active in the clones highly overexpressing IRS-1 (70–93% vs. 45–60% growth inhibition) (Fig. 1a–c).

The above results suggested that IRS-1 may be an important target for ICI 182,780 action. Consequently, in the next set of experiments we studied the effects of ICI 182,780 on the expression and function of IRS-1.

ICI 182,780 reduces IRS-1 levels and impairs IRS-1 signaling in MCF-7/IRS-1, MCF-7 and MCF-7/IGF-IR cells

In MCF-7/IRS-1 cells grown under basal conditions, IRS-1 was tyrosine phosphorylated for up to 4 days (Fig. 2a). IGF-I induced a rapid and marked (5-fold) increase of IRS-1 phosphorylation which persisted for up to 1 day and declined thereafter reaching close to the basal phosphorylation status at day 4. A short (≤ 1 day) treatment with ICI 182,780 had no consequences on IRS-1 expression or tyrosine phosphorylation. (Fig. 2a, panels a and b). However, p85/IRS-1 association was approximately 30% reduced under the basal conditions at day 1 of the treatment (Fig. 2a, panel c).

The evident effect of ICI 182,780 action on IRS-1 expression and signaling occurred at day 4, and was especially pronounced in the absence of IGF-I. Specifically, without IGF-I, the drug suppressed IRS-1 protein expression by 60%, which was paralleled by a 60% reduction of IRS-1 tyrosine phosphorylation, and coincided with an almost complete (approximately 95%) inhibition of p85/IRS-1 and GRB2/IRS-1 binding. The addition of IGF attenuated ICI 182,780 action, however, the effects of the treatment remained well detectable: IRS-1 levels were downregulated by 30%, IRS-1 tyrosine phosphorylation by 20% and p85/IRS-1 binding by 30%. Under IGF-I conditions, GRB2/IRS-1 binding was not appreciably affected (Fig. 2a, panels a–d).

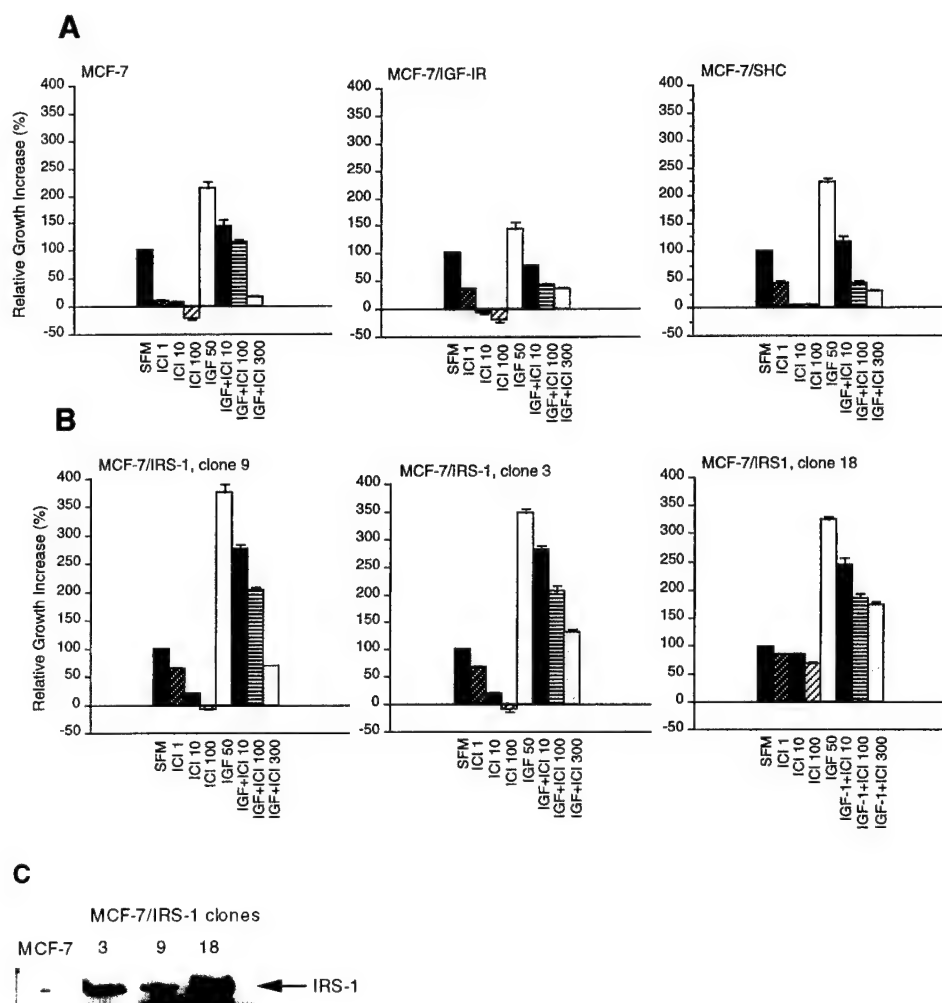


FIGURE 1 – ICI 182,780 inhibits the growth of MCF-7 cells overexpressing different elements of IGF-IR signaling. IRS-1 levels determine ICI 182,780 sensitivity. (a) ICI 182,780-induced growth inhibition in the parental MCF-7 cells (8×10^4 IGF-IR/cell), MCF-7/IGF-IR clone 17 (1×10^6 IGF-IR/cell) and MCF-7/SHC (5-fold SHC overexpression over the level in MCF-7 cells). (b) Growth reduction in MCF-7/IRS-1 clone 9 (3-fold IRS-1 overexpression over the levels in MCF-7 cells), clone 3 (7-fold overexpression) and clone 18 (9-fold overexpression). The cells were treated with different doses of ICI 182,780 in the presence or absence of 50 ng/ml IGF-I, as described in Material and Methods. The increase in cell number between day 0 and day 4 is taken as 100%. The results are means from at least 4 experiments. Bars indicate standard error. (c) Levels of IRS-1 protein in different MCF-7/IRS-1 cell lines. IRS-1 levels were determined by IP and WB as described in Material and Methods. Representative results from 3 experiments are shown.

Importantly, analogous action of ICI 182,780 on IRS-1 expression and tyrosine phosphorylation was seen in other cell lines studied (Fig. 2b). In both MCF-7/IGF-IR and MCF-7 cells containing only endogenous IRS-1, ICI 182,780 inhibited the IRS-1 expression under basal conditions by approximately 60%, which was paralleled by the reduced IRS-1 tyrosine phosphorylation (by approximately 90–95%). In the presence of IGF-I, the antiestrogen suppressed the IRS-1 levels by approximately 50% and IRS-1 tyrosine phosphorylation by approximately 40%.

ICI 182,780 attenuates IRS-1 mRNA expression

ICI 182,780 reduced the levels of 5 kb IRS-1 mRNA (Nishiyama and Wands, 1992) in MCF-7 and MCF-7/IGF-IR cells in the absence or presence of IGF-I, by 50 and 70%, respectively (Fig. 3). Moreover, the 5 kb message transcribed from the CMV-IRS-1 plasmid was downregulated (by approximately 70%) in MCF-7/IRS-1 cells treated with both IGF-I and ICI 182,780 (data not shown).

ICI 182,780 inhibits IGF-I-induced but not basal tyrosine phosphorylation of IGF-IR

In MCF-7/IGF-IR cells, IGF-I moderately increased the expression of IGF-IR. This effect was slightly (by 20%) blocked in the presence of ICI 182,780. Under the same conditions, the drug significantly (by 80%) reduced tyrosine phosphorylation of IGF-IR (Fig. 4). ICI 182,780 had no effect on the basal expression of IGF-IR, however, it produced a 30% increase in the basal tyrosine phosphorylation of IGF-IR (Fig. 4). The latter peculiar effect of the antiestrogen occurred in several repeat experiments. Short treatments with ICI 182,780 (≤ 1 day) were not associated with any significant changes in IGF-IR expression (data not shown).

Long-term ICI 182,780 treatment does not affect SHC signaling

In the presence of IGF-I, SHC tyrosine phosphorylation was moderately induced, with the maximum seen at 1 hr upon stimulation. On the other hand, GRB2/SKC binding peaked at 15 min after IGF-I addition and declined thereafter with the minimal

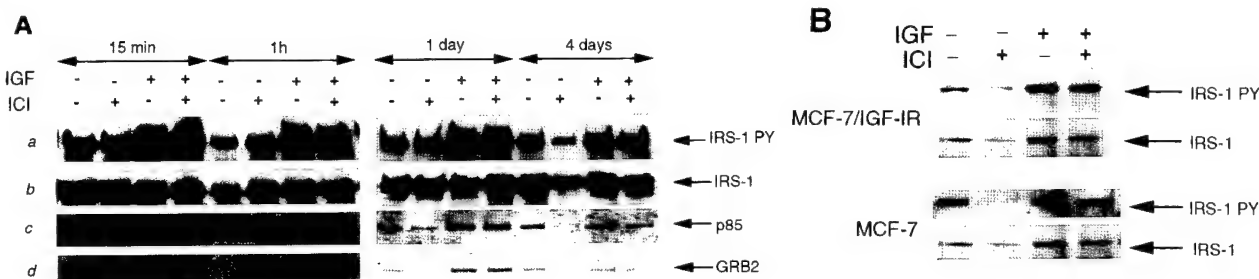


FIGURE 2 – ICI 182,780 inhibits IRS-1-mediated signaling. (a) Effects of ICI 182,780 in MCF-7/IRS-1 clone 3. IRS-1 tyrosine phosphorylation (IRS-1 PY) (panel a), protein levels (IRS-1) (panel b), as well as IRS-1-associated p85 of PI-3 kinase (panel c) and GRB2 (panel d) were determined in cells treated for 15 min, 1 hr, 1 day or 4 days with 100 nM ICI 182,780 in the presence or absence of 50 ng/ml IGF-I. In the 1 hr treatment, lane IGF (–) ICI (–) is underloaded. Representative results from 5 experiments are shown. (b) Effects of ICI 182,780 on IRS-1 in MCF-7/IGF-IR and MCF-7 cells. IRS-1 tyrosine phosphorylation (IRS-1 PY) and protein levels (IRS-1) were examined in cells treated with 100 nM ICI 182,780 for 4 days. Representative blots of 5 experiments are shown.

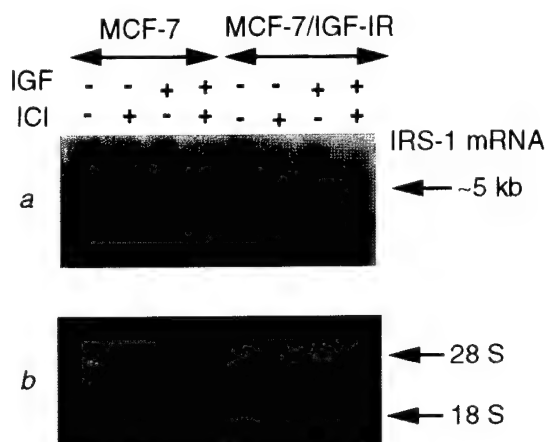


FIGURE 3 – ICI 182,780 attenuates the expression of IRS-1 mRNA levels in MCF-7 and MCF-7/IGF-IR cells. The expression of IRS-1 mRNA was determined in cells treated with 100 nM ICI 182,780 for 4 days in the presence or absence of IGF-I. Panel a. IRS-1 mRNA of approximately 5 kb. Panel b. Control RNA loading: 28S and 18S RNA in the same blot.

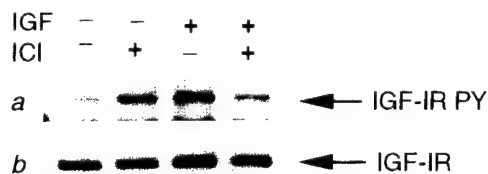


FIGURE 4 – Effects of ICI 182,780 on IGF-IR. IGF-IR tyrosine phosphorylation (IGF-IR PY) (panel a) and protein levels (IGF-IR) (panel b) in MCF-7/IGF-IR clone 17 treated for 4 days with 100 nM ICI 182,780 in the presence or absence of 50 ng/ml IGF-I. Representative results of 3 different experiments are shown.

binding found at day 4 (Fig. 5). ICI 182,780 treatment, in the presence or absence of IGF-I, failed to induce significant changes in the levels or tyrosine phosphorylation of SHC proteins, except a transient stimulation of the basal SHC tyrosine phosphorylation at 15 min (Fig. 5). Importantly, at all time points, SHC/GRB2 association was not influenced by the drug.

Interestingly, at day 4, SHC tyrosine phosphorylation and SHC/GRB2 binding were suppressed in the presence of IGF-I (Fig. 5). This characteristic regulation of SHC by IGF-I, documented by

us previously in MCF-7 cells and MCF-7-derived clones, was not affected by ICI 182,780 (Guvakova and Surmacz, 1997).

Similar lack of ICI 182,780 effects on SHC expression and signaling was noted in MCF-7 and MCF-7/IGF-IR cells (data not shown).

DISCUSSION

Pure antiestrogens have been shown to interfere with one of the most important systems regulating the biology of hormone-dependent breast cancer cells, namely, the IGF-I system (de Cupis and Favoni, 1997; Nicholson *et al.*, 1996). The compounds inhibit IGF-induced proliferation, which is associated with, *i.e.*, downregulation of IGF binding sites and reduction of IGF availability. Similar action has been ascribed to non-steroidal antiestrogens such as Tam or 4-OH-Tam (Chander *et al.*, 1993).

The effects of pure antiestrogens on the IGF signal transduction have been unknown. Here, we studied if and how ICI 182,780 modulates the IGF-IR intracellular pathways in breast cancer cells. We focused on the relationship between drug efficiency and signaling capacities of IGF-IR or IRS-1 since these molecules appear to control proliferation and survival in breast cancer cells (Surmacz *et al.*, 1998; Rocha *et al.*, 1997; Turner *et al.*, 1997).

Previously we found that the cytostatic action of Tam involves its interference with IGF signaling pathways. In particular, Tam suppressed tyrosine phosphorylation of IRS-1 and caused hyperphosphorylation of SHC (Guvakova and Surmacz, 1997). The most important conclusion of the present work is that inhibition of IRS-1 expression is an important element of ICI 182,780 mode of action. The first observation was that amplification of IGF signaling did not abrogate sensitivity to ICI 182,780. Next, ICI 182,780 appeared to affect a specific IGF signaling pathway, as the efficiency of the drug was dictated by the cellular levels of IRS-1, but not that of SHC or IGF-IR. For instance, MCF-7/IGF-IR clone 17 was very sensitive to ICI 182,780 despite a 12-fold IGF-IR overexpression, whereas MCF-7/IRS-1 clones 3 and 18 (7- and 9-fold IRS-1 overexpression, respectively) were quite resistant to the drug (Fig. 1). Moreover, ICI 182,780 reduced IRS-1 levels and tyrosine phosphorylation in several cell lines in the presence or absence of IGF-I, while its action on IGF-IR was limited to the inhibition of IGF-I-induced tyrosine phosphorylation and its effects on SHC were none.

The reduction of IRS-1 expression by ICI 182,780 occurred in all cell lines studied, however, it was clearly more pronounced in the cells expressing lower (endogenous) levels of the substrate (*i.e.*, MCF-7 and MCF-7/IGF-IR cells) (Fig. 2). This suggests that downregulation of IRS-1 by ICI 182,780 is a saturable process, and overexpression of IRS-1 may provide resistance to the drug. Indeed, although we did not notice a strict correlation between

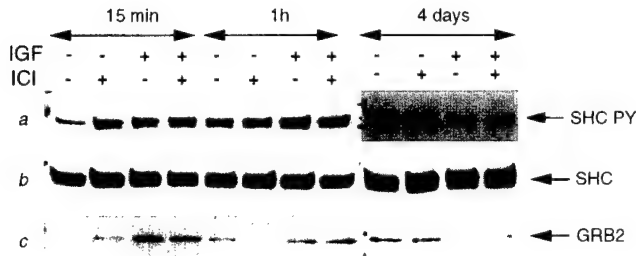


FIGURE 5 – Effects of ICI 182,780 on SHC signaling. SHC tyrosine phosphorylation (SHC PY) (panel a), protein levels (SHC) (panel b) and SHC-associated GRB2 (panel c) were studied in MCF-7/SHC cells treated for 4 days with 100 nM ICI 182,780 in the presence or absence of 50 ng/ml IGF-I. Representative results of 5 experiments are shown.

IRS-1 levels or IRS-1 tyrosine phosphorylation and ICI 182,780-dependent growth inhibition, IRS-1-overexpressing cells tended to be more resistant to the cytostatic action of the antiestrogen (Fig. 1). Interestingly, overexpression of IRS-1 clearly had a greater impact on the response to high doses of ICI 182,780 (≥ 100 nM) than on the effects of low drug concentrations. This suggests that ICI 182,780 action is multiphased, with the initial inhibition being IRS-1 independent (but perhaps, ER-dependent) and the strong growth reduction associated with the blockade of IRS-1 function (Figs. 1, 2).

ICI 182,780 affected IRS-1 expression not only on the level of protein but also on the level of mRNA. In our experiments, the antiestrogen reduced the expression of IRS-1 mRNA in the presence or absence of IGF-I. However, the mechanism by which ICI 182,780 interferes with IRS-1 mRNA expression was not studied here and it remains speculative. Regarding transcriptional regulation, no estrogen-responsive elements have been mapped in the IRS-1 promoter, but it cannot be ruled out that ICI 182,780 acts indirectly through some other regulatory sequences in the 5' untranslated region of *IRS-1* gene, such as AP1, AP2, Sp1, C/EBP, E box (Araki *et al.*, 1995; Matsuda *et al.*, 1997). A post-transcriptional component may be argued by the fact that the inhibition of IRS-1 mRNA by ICI 182,780 was evident in IGF-I-treated MCF-7/IRS-1 cells, in which the majority of IRS-1 message originated from the expression plasmid devoid of any IRS-1 promoter sequences (CMV-driven IRS-1 cDNA) (Surmacz and Burgaud, 1995) (data not shown). In addition, the finding that ICI 182,780 similarly inhibited IRS-1 mRNA levels under the basal and IGF-I conditions, but IRS-1 protein was significantly more reduced in the absence of IGF-I (Fig. 3 vs. Fig. 2a) could suggest that the drug acts upon some IGF-I-dependent mechanism controlling mRNA stability, translation, or post-translational events. In fact, in other experimental systems, IGF-I or insulin regulated

various messages, including IRS-1 mRNA, on the post-transcriptional level (Araki *et al.*, 1995).

In its action on IRS-1, ICI 182,780 appeared more potent than Tam, which decreased tyrosine phosphorylation of IRS-1 but did not cause any detectable changes in IRS-1 expression. Our results with Tam suggested that this antiestrogen may influence the activity of tyrosine phosphatases (PTPases) (Guvakova and Surmacz, 1997). Indeed, both Tam and ICI 182,780 interfere with IGF-I-dependent growth by upregulating PTPases LAR and FAP-1 (Freiss *et al.*, 1998). In the present work, ICI 182,780 effects on phosphatases acting on IRS-1 were impossible to assess, since the drug also affected IRS-1 expression (Fig. 3). However, some interference of ICI 182,780 with the phosphorylation/dephosphorylation events could be indicated, for instance, by our experiments with IGF-IR, where, under basal conditions, the compound induced IGF-IR phosphorylation without evident modifications of the receptor expression (Fig. 4).

Other important observations stemming from our results concern similarities and differences between the effects of ICI 182,780 and Tam on the IGF-IR and SHC. While Tam did not modulate the expression of IGF-IR protein (Guvakova and Surmacz, 1997), ICI 182,780 moderately decreased IGF-IR levels in the presence of IGF-I. The action of ICI 182,780 and Tam on IGF-IR tyrosine phosphorylation was similar, namely, both compounds inhibited IGF-I-induced but not basal tyrosine phosphorylation of IGF-IR. The effects of ICI 182,780 and Tam on SHC were different. With Tam, we observed elevated tyrosine phosphorylation of SHC proteins and increased SHC/GRB2 binding in growth-arrested cells, while ICI 182,780 did not affect SHC phosphorylation or expression (Guvakova and Surmacz, 1997). Thus, induction of non-mitogenic SHC signaling is a peculiarity of Tam but not a ICI 182,780 mechanism of action.

In summary, cytostatic effects of ICI 182,780, similar to Tam, are associated with the inhibition of IGF-IR signaling. The mitogenic/survival IRS-1 pathway is a target for both antiestrogens. Both drugs reduce the levels of tyrosine phosphorylated IRS-1, but only ICI 182,780 clearly inhibits expression of the substrate. High cellular levels of IRS-1 hinder the response to higher doses of ICI 182,780, thus overexpression of IRS-1 in breast tumors may represent an important mechanism of antiestrogen resistance.

ACKNOWLEDGEMENTS

This work was supported by NIH grant DK 48969 to E.S., U.S. Department of Defense grants DAMD 17-96-1-6250 to E.S. and DAMD 17-97-1-7211 to M.A.G., NCR Italy grants to D.S. and M.S., a M.U.R.S.T. Italy 60% grant to M.S. and a P.O.P. 1998, Italy grant to S.A. ICI 182,780 used in this project was generously provided by Dr. A. Wakeling (ZENEGA, Macclesfield, UK).

REFERENCES

- ARAKI, E., HAAG, B.L., MATSUDA, K., SHICHI, M. and KAHN, C.R., Characterization and regulation of the mouse insulin receptor substrate gene promoter. *Mol. Endocrinol.*, **9**, 1367–1379 (1995).
- CHANDER, S.K., SAHOTA, S.S., EVANS, T.R.J. and LUQMANI, Y.A., The biological evaluation of novel antiestrogens for the treatment of breast cancer. *Crit. Rev. Oncol. Hematol.*, **15**, 243–269 (1993).
- DE CUPIS, A. and FAVONI, R.E., Oestrogen/growth factor cross-talk in breast carcinoma: a specific target for novel antiestrogens. *Trends Pharmacol. Sci.*, **18**, 245–251 (1997).
- DE CUPIS, A., NOONAN, D., PIRANI, P., FERRERA, A., CLERICO, L. and FAVONI, R.E., Comparison between novel steroid-like and conventional nonsteroidal antioestrogens in inhibiting oestradiol- and IGF-I-induced proliferation of human breast cancer-derived cells. *Brit. J. Pharmacol.*, **116**, 2391–2400 (1995).
- FREISS, G., PUECH, C. and VIGNON, F., Extinction of insulin-like growth factor-I mitogenic signaling by antiestrogen-stimulated FAS-associated protein tyrosine phosphatase-1 in human breast cancer cells. *Mol. Endocrinol.*, **12**, 568–579 (1998).
- GUVAKOVA, M.A. and SURMACZ, E., Tamoxifen interferes with the insulin-like growth factor I receptor (IGF-IR) signaling pathway in breast cancer cells. *Cancer Res.*, **57**, 2606–2610 (1997).
- HANKINSON, S., WILLET, W.C., COLDITZ, G., HUNTER, D.J., MICHAUD, D.S., DEROO, B., ROSNER, B., SPEIZER, F. and POLLAK, M., Circulating concentrations of insulin-like growth factor I and risk of breast cancer. *Lancet*, **351**, 1393–1396 (1998).
- LARSEN, S.S., MADSEN, M.W., JENSEN, B.L. and LYKKESFELDT, A.E., Resistance of human breast cancer cells to the pure steroidal antiestrogen ICI 182,780 is not associated with a general loss of estrogen-receptor expression or lack of estrogen responsiveness. *Int. J. Cancer*, **72**, 1129–1136 (1997).
- MATSUDA, K., ARAKI, E., YOSHIMURA, R., TSURUZOE, K., FURUKAWA, N., KANEKO, K., MOTOSHIMA, H., YOSHIZATO, K., KISHIKAWA, K. and SHICHI, M., Cell-specific regulation of IRS-1 gene expression: role of E box and

- C/EBP binding site in HepG2 cells and CHO cells. *Diabetes*, **46**, 354-362 (1997).
- NICHOLSON, R.I., GEE, J.M., BRYANT, S., FRANCIS, A.B., MCCLELLAND, R.A., KNOWLDEN, J., WAKELING, A.E. and OSBORNE, C.K., Pure antiestrogens. The most important advance in the endocrine therapy of breast cancer since 1896. *Ann. N.Y. Acad. Sci.*, **784**, 325-335 (1996).
- NICHOLSON, R.I., GEE, J.M., MANNING, D.L., WAKELING, A.E., MONTANO, M.M. and KATZENELLENBOGEN, B.S., Responses to pure antiestrogens (ICI 164,384, ICI 182,780) in estrogen-sensitive and -resistant experimental and clinical breast cancer. *Ann. N.Y. Acad. Sci.*, **761**, 148-163 (1995).
- NISHIYAMA, M. and WANDS, J.R., Cloning and increased expression of an insulin receptor substrate 1-like gene in human hepatocellular carcinoma. *Biochem. biophys. Res. Comm.*, **183**, 280-285 (1992).
- OSBORNE, C.K., CORONADO-HEINSOHN, E.B., HILSENBECK, S.G., MCCUE, B.L., WAKELING, A.E., MCCLELLAND, R.A., MANNING, D.L. and NICHOLSON, R.I., Comparison of the effects of a pure antiestrogen with those of tamoxifen in a model of human breast cancer. *J. nat. Cancer Inst.*, **87**, 746-750 (1995).
- PAVLIK, E.J., NELSON, K., SRINIVASAN, S., DEPRIEST, P.D. and KENADY, D.E., Antiestrogen resistance in human breast cancer. In E.J. Pavlik (ed.), *Estrogens, progestins, and their antagonists*, Vol. 1, pp. 116-159, Birkhauser, Boston (1996).
- RESNIK, J.L., REICHART, D.B., HUEY, K., WEBSTER, N.J.G. and SEELY, B.L., Elevated insulin-like growth factor I receptor autophosphorylation and kinase activity in human breast cancer. *Cancer Res.*, **58**, 1159-1164 (1998).
- ROCHA, R.L., HILSENBECK, S.G., JACKSON, J.G. and YEE, D., Insulin-like growth factor binding protein-3 (IGFBP3) and insulin receptor substrate (IRS1) in primary breast cancer: correlation with clinical parameters and disease-free survival. *Clin. Cancer Res.*, **3**, 103-109 (1997).
- SURMACZ, E. and BURGAUD, J.-L., Overexpression of insulin receptor substrate 1 (IRS-1) in the human breast cancer cell line MCF-7 induces loss of estrogen requirements for growth and transformation. *Clin. Cancer Res.*, **1**, 1429-1436 (1995).
- SURMACZ, E., GUVAKOVA, M.A., NOLAN, M.K., NICOSIA, R. and SCIACCA, L., Type I insulin-like growth factor receptor function in breast cancer. *Breast Cancer Res. Treat.*, **47**, 255-267 (1998).
- TURNER, B.C., HAFFTY, B.G., NAYARANNAN, L., YUAN, J., HAVRE, P.A., GUMBS, A., KAPLAN, L., BURGAUD, J.-L., CARTER, D., BASERGA, R. and GLAZER, P., IGF-IR and cyclin D1 expression influence cellular radiosensitivity and local breast cancer recurrence after lumpectomy and radiation. *Cancer Res.*, **57**, 3079-3083 (1997).
- WAKELING, A.E., DUKES, M. and BOWLER, J., A potent specific pure antiestrogen with clinical potential. *Cancer Res.*, **51**, 3867-3873 (1991).
- WISEMAN, L.R., JOHNSON, M.D., WAKELING, A.E., LYKKESFELDT, A.E., MAY, F.E. and WESTLEY, B.R., Type I IGF receptor and acquired tamoxifen resistance in oestrogen-responsive human breast cancer. *Europ. J. Cancer*, **29A**, 2256-2264 (1993).

SHC- α 5 β 1 INTEGRIN INTERACTIONS IN BREAST CANCER CELL ADHESION AND MOTILITY

Loredana Mauro^{1,2#}, Diego Sisci^{1,2#}, Michele Salerno^{1,2}, Jerry Kim¹,
Timothy Tam¹, Marina A. Guvakova¹, Sebastiano Ando^{'2},
and Ewa Surmacz^{1*}

¹Kimmel Cancer Institute, Thomas Jefferson University, Philadelphia, PA 19107, and ²Department of Cellular Biology, Faculty of Pharmacy, University of Calabria, Cosenza, Italy

L.M and D.S. contributed equally to this work

Running title: SHC in adhesion and motility

Key words: SHC, α 5 β 1 integrin, fibronectin, motility, breast cancer

*Corresponding Author:

Ewa Surmacz, Ph.D.
Kimmel Cancer Institute
Thomas Jefferson University
233 S. 10th Street, BLSB 606
Philadelphia, PA 19107
tel. 215-503-4512, fax 215-923-0249
e-mail: surmacz1@jefflin.tju.edu

ABSTRACT

The oncogenic SHC proteins are signaling substrates for most receptor and cytoplasmic tyrosine kinases (TKs) and are implicated in diverse processes, including growth, transformation and differentiation. In tumor cells overexpressing TKs, the levels of tyrosine phosphorylated SHC are chronically elevated. The significance of the amplification of SHC signaling in breast tumorigenesis remains unknown. This study demonstrates that the overexpression of SHC (3 and 8-fold) in MCF-7 breast cancer cells resulted in chronic hyperphosphorylation of the substrate, but only moderately improved responsiveness of cells to growth factors and did not enhance monolayer or anchorage-independent growth in serum. Amplification of SHC, however, significantly altered interactions of cells with fibronectin (FN). Specifically, in SHC overexpressing cells (MCF-7/SHC cells), association of SHC with $\alpha 5 \beta 1$ integrin (FN receptor) was increased, spreading on FN accelerated, and basal growth on FN reduced. These effects coincided with an early decline of adhesion-dependent MAP kinase activity. Basal motility of MCF-7/SHC cells on FN was inhibited relative to that in several cell lines with normal SHC levels. However, when EGF or IGF-I were used as chemoattractants, the locomotion of MCF-7/SHC cells was greatly (~5-fold) stimulated, while it was only minimally altered in the control cells. The spreading of MCF-7/SHC cells on FN was paralleled by dissociation of tyrosine phosphorylated $p46^{SHC}$ from $\alpha 5 \beta 1$ integrin, whereas EGF treatment stimulated $p46^{SHC}/\alpha 5 \beta 1$ integrin binding. These data suggest that SHC is a mediator of the dynamic regulation of cell adhesion and motility on FN in breast cancer cells.

INTRODUCTION

The ubiquitous SH2 homology/collagen homology (SHC) proteins (p46, p52, and p66) are overlapping SH2-PTB adapter proteins that are targets and downstream effectors of most transmembrane and cytoplasmic tyrosine kinases (TKs) (Pelicci et al., 1992, 1995a). Consequently, overexpression of p52^{SHC} and p46^{SHC} (referred to as SHC hereinafter) amplifies various cellular responses; for instance, induces mitogenic effects of growth factors in NIH 3T3 mouse fibroblasts and myeloid cells (Pelicci et al., 1992; Lafrancone et al., 1995), stimulates differentiation in PC12 rat pheochromocytoma (Rozakis-Adcock et al. 1992), and augments hepatocyte growth factor (HGF)-induced proliferation and migration in A549 human lung adenocarcinoma (Pelicci et al., 1995b). Overexpressed SHC is oncogenic in NIH 3T3 mouse fibroblasts, but amplification of p66^{SHC} isoform does not induce transformation (Pelicci et al., 1992; Salcini et al., 1994; Migliaccio et al., 1997) and may even inhibit growth pathways (Okada et al., 1997). Importantly, increased tyrosine phosphorylation of SHC, which has been noticed in different tumor cell lines, is a marker of receptor or cytoplasmic TKs overexpression (Pelicci et al., 1995a). In breast cancer, for instance, SHC is hyperphosphorylated in cells overexpressing ERB-2 and c-Src (Biscardi et al., 1998; Stevenson and Frackelton, 1998). Whether such an amplification of SHC signaling contributes to the development of a more aggressive phenotype of breast tumor cells remains unknown.

The downstream effector pathways emanating from SHC are partially known. Upon tyrosine phosphorylation by TKs, SHC associates with the GRB2/SOS complex and subsequently stimulates the canonical Ras-MAPK (p42

and p44 Mitogen-Activated Protein Kinases) signal transduction cascade (Pelicci et al., 1992; Salcini et al., 1994; Migliaccio et al., 1997). SHC/GRB2 binding and the activation of Ras are prerequisites for SHC-induced mitogenesis and transformation in NIH mouse fibroblasts (Salcini et al., 1994). In addition, SHC has been described to associate with adapters Crk II (Matsuda et al., 1994) and GRB7 (Stein et al., 1994), a signaling protein p145 (Liu et al., 1994, Kavanaugh and Williams, 1994), and PEST tyrosine phosphatase (Habib et al., 1994) in various experimental systems. However, SHC pathways incorporating these signaling intermediates and biological significance of these signals are not well understood.

There is substantial evidence suggesting that in addition to its role in mitogenesis and transformation, SHC also regulates non-growth processes, such as cell adhesion and motility. For instance, overexpressed SHC improved motility in HGF-stimulated melanoma cells (Pelicci et al., 1995b), and downregulation of SHC reduced epidermal growth factor (EGF)-dependent migration in MCF-7 breast cancer cells (Nolan et al., 1997). SHC was also essential for kidney epithelial cells scattering mediated by the receptors c-met, c-ros, and c-neu (Sacks et al., 1996). The mechanisms by which SHC signals may regulate cell adhesion and motility are still obscure.

Recent data demonstrated that in several cell types (Jurkat, HUVEC, MG-63 and A431 cells), SHC couples with a class of ECM receptors, specifically with the integrins $\alpha 1\beta 1$, $\alpha 5\beta 1$, $\alpha v\beta 3$, and $\alpha 6\beta 4$, but not with $\alpha 2\beta 1$, $\alpha 3\beta 1$, and $\alpha 6\beta 1$ (Wary et al., 1996). In A 431 cells, the recruitment of SHC to integrins containing a $\beta 1$ subunit was induced by cell contact with ECM (Wary et al., 1996). Ligation of $\beta 1$ class integrins resulted in the activation and binding (through a protein

caveolin) of a cytoplasmic TK Fyn, which then associated with and phosphorylated SHC (Wary et al., 1998). Additional reports suggested that SHC can also be tyrosine phosphorylated by other adhesion-inducible TKs, such as the p125 focal adhesion kinase (FAK) or FAK-associated kinases of the Src family (Schlaepfer & Hunter, 1997; Schlaepfer et al., 1998). Tyrosine phosphorylation of SHC activates Ras and subsequently induces MAPK activity (Wary et al. 1996). This SHC-mediated pathway has been suggested as a major contributor of integrin-stimulated MAPK activity (Giancotti, 1997; Pozzi et al., 1998). However, an alternative way of adhesion-dependent MAPK induction, relying on the direct binding of GRB2/SOS to tyrosine phosphorylated FAK and subsequent stimulation of Ras, has also been proposed (Schlaepfer et al., 1994; Schlaepfer et al., 1998). The biological significance of integrin-stimulated MAPK activity is not well understood, however, recent data indicated that it positively regulates cell growth and survival (Wary et al., 1996; Pozzi et al. 1998), but is not required for cell migration (Cary et al., 1998).

This work addressed the consequences of amplified SHC signaling on proliferation, transformation, adhesion and motility in breast cancer MCF-7 cells. In these cells, SHC is an important intermediate of different signaling pathways. Growth factors present in serum, such as IGF-I or EGF can induce SHC through their cognate receptors (Pelicci, 1992; Giorgetti et al., 1994; Nolan et al., 1997). Estrogens (also contained in serum) may elevate tyrosine phosphorylation of SHC via cytoplasmic TKs of the Src family (Migliaccio et al., 1996). In addition, SHC can be stimulated by cytoplasmic TKs as a result of cell spreading on ECM (Wary et al., 1996). MCF-7 cells express several integrin receptors: $\alpha 2\beta 1$, $\alpha 3\beta 1$, $\alpha 5\beta 1$, $\alpha v\beta 5$ (Doerr and Jones, 1996). Of those, only $\alpha 5\beta 1$, a FN receptor, is a SHC

binding integrin (Wary et al., 1996). Interestingly, in MCF-7 cells, the levels of c-Src are increased compared with that in normal breast epithelial cells (Biscardi et al., 1998), which may result in the amplification of integrin-mediated activation of SHC.

The interactions of cells with FN have been reported to influence or control different processes regulating the behavior of cancer cells, namely cell migration, invasion, and metastasis as well as survival and proliferation (Akiyama et al., 1995). Highly metastatic cell lines seem to overexpress FN receptors and exhibit good adhesion to the substrate (Tawil et al., 1996). In experimental breast metastasis, inhibition of $\alpha 5 \beta 1$ integrin with a specific blocking antibody abrogated cell spread in nude mice (Newton et al. 1995). The importance of SHC signaling in the interactions of breast cancer cells with FN has not been studied and is a subject of this work.

RESULTS

SHC overexpression improves mitogenic response to IGF-I or EGF. To investigate the implications of increased SHC signaling in breast cancer cells, we developed several MCF-7-derived clones stably overexpressing p46^{SHC} and p52^{SHC}. Out of 20 G418 resistant clones, 7 exhibited SHC overexpression. Two representative clones, MCF-7/SHC, 1 and MCF-7/SHC, 9, with a 3- and 8-fold SHC amplification, respectively, were used in subsequent experiments (Fig. 1 A). Tyrosine phosphorylation of SHC, especially p52^{SHC}, was chronically elevated in these clones, however, the extent of SHC tyrosine phosphorylation was not directly proportional to the levels of the protein. Specifically, a 3- and 8-fold SHC

overexpression increased the levels of tyrosine phosphorylated p52^{SHC} isoform by 1.5- and 2.5-fold, respectively (Fig. 1 A).

Studies on growth factor responsiveness in MCF-7/SHC clones demonstrated that the amplification of SHC only moderately (20-40%) potentiated growth response to EGF and IGF-I, growth factors that stimulate tyrosine phosphorylation of SHC (Pelicci et al., 1992; Giorgetti et al., 1994) and require SHC for their mitogenic action in MCF-7 cells (Nolan et al., 1997). This effect of SHC overexpression was more evident with higher doses of mitogens added to PRF-SFM (Fig. 1 B). However, when the cells were grown in a complete serum-containing medium, the growth rate of MCF-7/SHC clones was comparable to that of MCF-7 cells or other cell lines with normal SHC levels (data not shown).

SHC overexpression does not enhance transforming potential of MCF-7 cells.

Since SHC exhibits oncogenic properties when overexpressed in NIH mouse fibroblasts (Pelicci et al., 1992), we assessed transforming potential of MCF-7/SHC clones. Despite significant SHC overexpression in these cells, in several repeat experiments and under different growth conditions used, anchorage-independent growth of MCF-7/SHC cells was never enhanced relative to that seen in MCF-7 cells (Tab. 1). In the same assay, MCF-7 cells overexpressing insulin receptor substrate 1 (IRS-1), i.e., MCF-7/IRS-1, clone 3, exhibited typical for these cells, increased transformation in the presence of serum or IGF-I (Surmacz and Burgaud, 1995).

SHC associates with $\alpha 5\beta 1$ integrin (FN receptor) in MCF-7 cells. The abundance of SHC/ $\alpha 5\beta 1$ integrin complexes is increased in MCF-7/SHC cells.

The limited or absent effects of SHC overexpression on mitogenic and transforming potential of MCF-7 cells prompted us to assess the role of SHC in non-growth processes such as adhesion and motility. Because interactions of cells with FN have been implicated in breast cancer metastasis (Akiyama et al., 1995) and since SHC is a potential mediator of FN receptor signaling (Wary et al., 1996; Schlaepfer et al., 1998), we investigated how overexpressed SHC affects $\alpha 5\beta 1$ function in MCF-7 cells. The first observation was that the levels of SHC, especially p52^{SHC}, associated with $\alpha 5\beta 1$ were markedly increased (~ 3-fold) in MCF-7/SHC clones compared with that in MCF-7 cells or in several cell lines with normal levels of SHC, but overexpressing IRS-1 or the IGF-I receptor (IGF-IR) (Fig. 2). Interestingly, the amount of SHC associated with $\alpha 5\beta 1$ integrin was similar in both MCF-7/SHC clones, regardless of the level of SHC overexpression (Fig. 2). This suggests that the extent of SHC/ $\alpha 5\beta 1$ binding is not directly proportional to total cellular SHC levels and that $\alpha 5\beta 1$ /SHC complex formation is a saturable process, possibly limited by the expression of the integrin.

MCF-7/SHC cells exhibit increased adhesion to FN. Because of the enhanced association of SHC with $\alpha 5\beta 1$ integrin in MCF-7/SHC cells, we examined the interactions of these cells with FN and compared them with that seen in cells expressing normal or reduced SHC levels. The results demonstrated that the overexpression of SHC was associated with an accelerated cell adhesion to FN, while the reduction of SHC levels blocked cell spreading on the substrate (Fig. 3). The differences in the dynamics of cell interactions with FN were most evident at

1 h after plating (Fig. 3, panels A). Specifically, while at this time both MCF-7/SHC clones were well spread on FN, and no floating cells were observed, only ~50% of MCF-7 cells exhibited initial attachment to the substrate (cells were still rounded but with distinct membrane protrusions), and MCF-7/anti-SHC cells remained completely suspended. At 2 h after plating, MCF-7 and MCF-7/SHC clones were attached to FN and the differences in adhesion among these cell lines were, in most experiments, unremarkable. At the same time, MCF-7/anti-SHC cells were still at the stage of establishing initial contacts with FN (Fig. 3, panels C). After 24 h, MCF-7/anti-SHC cells formed small aggregates demonstrating limited contact with the substrate, but all other tested cell lines (represented here by MCF-7 cells) were fully attached (Fig. 3, panels D'). At 48 h, MCF-7/anti-SHC cells were completely detached, while MCF-7 and MCF-7/SHC cells begun proliferation on FN (data not shown).

Our experiments also indicated that the adhesion of MCF-7/SHC cells to FN was mediated by $\alpha 5 \beta 1$ integrin, since it was totally blocked with a specific anti- $\alpha 5 \beta 1$ blocking antibody (Fig. 3, panels D), but not with a control goat IgG (not shown).

In contrast with the results obtained on FN, the dynamics of cell adhesion on collagen (COL), which requires an integrin not associating with SHC ($\alpha 2 \beta 1$) (Wary et al., 1996), was similar in all tested cell lines, regardless of the levels of SHC expression. Specifically, all cells tested initiated contacts with COL at 15 min and completed attachment at 1 h after plating (data not shown).

Overexpression of SHC modulates adhesion-dependent MAP kinase activity on FN. Cell adhesion to ECM and activation of different integrin-associated

cytoplasmic TKs results in the stimulation of MAPK activity (Clark and Brugge, 1995). This process can be mediated through SHC, which, as a substrate of the TKs (e.g., Fyn, and possibly other c-Src-like kinases or FAK), is tyrosine phosphorylated, binds the GRB2/SOS complex and stimulates Ras (Wary et al., 1996, 1998). MAPKs have also been shown to be activated directly by FAK, through FAK-GRB 2/SOS-Ras pathway (Schleapfer et al., 1994, 1998, Schleapfer & Hunter, 1997). Here we studied the effect of SHC amplification on adhesion-dependent MAPK response in MCF-7 and MCF-7/SHC cells (Fig. 4). We found that overexpression of SHC significantly modulated MAPK activation in cells spread on FN, but on COL or plastic (Fig. 4 A). Specifically, in both MCF-7 cells and MCF-7/SHC clone 9, the activation of MAPK on COL was bi-phasic, with a peak between 30 min and 1 h after plating, followed by a decline of activity at 8 h, and then an increased activity between 12 and 24 h. In contrast, the dynamics of MAPK activation on FN was different in MCF-7 and MCF-7/SHC cells. Although the stimulation of MAPK was the highest at 1h after plating in both cell lines, in MCF-7 cells the kinases remained highly stimulated for up to 24 h, while in MCF-7/SHC cells their activity subsided at 4 h to reach basal levels at 24 h (Fig. 4 A). In a control experiment, where the cells were plated on plastic, the pattern of MAPK activation was similar in both cell lines, with a slightly earlier decline in MCF-7/SHC cells.

Next, we investigated whether SHC overexpression affects growth factor-induced MAPK response in cells plated on FN. We used EGF in this experiment since this mitogen stronger induces SHC phosphorylation than IGF-I in MCF-7 cells (Surmacz et al., unpublished observations). The pattern of EGF-stimulated MAPK activity was comparable (a peak between 15 min and 1 h after treatment

followed by decline to basal levels) on COL, FN and plastic in MCF-7 and MCF-7/SHC cells. However, in SHC overexpressing cells cultured on FN, the extend of MAPK activation between 15 min and 1 h of EGF was ~ 2.5-fold greater than that seen in MCF-7 cells. Such differences were not observed on COL (Fig. 4 B).

Since MAPK pathway contributes to cell growth, we investigated whether the reduced duration of adhesion-dependent MAP activity reflects mitogenicity of MCF-7/SHC cells cultured on FN (Tab. 2). Indeed, we found that overexpression of SHC coincided with a significant (~2-fold) growth inhibition (Tab. 2). Interestingly, the addition of EGF (different doses, up to 100 ng/ml) to growth medium did not improve proliferation of MCF-7/SHC or MCF-7 cells on FN. The addition of IGF-I (doses up to 100 ng/ml) only minimally (9-22%) stimulated growth under the same conditions (Tab. 2).

Overexpression of SHC inhibits basal motility on FN. IGF-I or EGF mobilize MCF-7/SHC cells. We investigated whether increased binding of SHC to $\alpha 5\beta 1$ integrin affects cell motility in FN-coated inserts. We found that basal migration of MCF-7/SHC cells was significantly (~4-fold) reduced compared with that of MCF-7 cells and several MCF-7-derived cell lines containing normal amounts of SHC (Fig. 5). In contrast, the motility of MCF-7/SHC clones in COL-coated inserts was similar ($p \geq 0.05$) to that seen with other tested cell lines (Fig. 5).

The use of EGF or IGF-I as chemoattractants dramatically (~5-7-fold, $p \leq 0.01$) improved the migration of MCF-7/SHC cells towards FN, but not to COL. The mitogens did not affect motility of other cells to COL, except some inhibition of MCF-7/IRS-1, clone 18 with 10 ng/ml EGF. Interestingly, in FN-coated inserts, 10 ng/ml EGF stimulated the migration of MCF-7/IRS-1 cells, however, the extent

of this stimulation was much lower than that of SHC overexpressing clones (Fig. 5). The increased EGF sensitivity of MCF-7/IRS-1 clones has been noticed before (Nolan et al., 1997).

SHC/ α 5 β 1 association is modulated during cell interaction with FN. The interactions of cells with FN coincided with the rearrangement of the SHC/ α 5 β 1 complex. Specifically, whereas in floating MCF-7/SHC cells, tyrosine phosphorylated forms of p46^{SHC} and p52^{SHC} were bound to the FN receptor, the attachment of cells to the substrate was paralleled by the dissociation of tyrosine phosphorylated p46^{SHC} from α 5 β 1 integrin. In contrast, EGF treatment of MCF-7/SHC cells, which induced partial detachment and migration, enhanced binding of p46^{SHC} isoform to the FN receptor (Fig. 6). Because of low SHC expression, the interactions between SHC and the FN receptor in MCF-7 cells and other control cell lines were impossible to assess.

DISCUSSION

SHC is a signaling substrate of most receptor-type and cytoplasmic TKs and therefore may amplify various cellular responses (reviewed in Pelicci et al., 1995 a). In consequence, the significance of SHC amplification must depend on the intracellular and extracellular cell context. Breast cancer cells, unlike normal breast epithelium, frequently overexpress TKs, such as c-Src (80%), or ERB2 (~20-30%), which may result in constitutive activation of SHC (Biscardi et al., 1998; Stevenson and Frackelton, 1998). The contribution of amplified SHC signaling to development and progression of breast cancer is not known. We addressed this question by examining the effects of SHC overexpression in MCF-

7 cells (representing an early stage of breast cancer and characterized by moderate c-Src amplification). Our results provide novel information on the role of SHC in proliferation, transformation, adhesion and motility in epithelial cells.

SHC in epithelial cell growth and transformation. In mouse fibroblasts, overexpression of SHC resulted in increased SHC tyrosine phosphorylation, augmented EGF-, or IGF-I-dependent MAPK response, accelerated cell cycle progression through G1 phase in the absence of growth factors, and enhanced anchorage-independent growth in soft agar and tumorigenicity in nude mice (Pelicci et al., 1992; Salcini et al., 1994; Giorgetti et al., 1994). Increased levels of SHC also potentiated growth factor response in myeloid and A549 adenocarcinoma cells (Lafrancone et al., 1995; Pelicci et al., 1995b). Consistent with these findings are our previous data demonstrating that downregulation of SHC results in reduced sensitivity to mitogenic action of EGF and IGF-I and growth inhibition in breast cancer cells. The present studies indicated that in SHC overexpressing epithelial cells, like in fibroblasts, basal SHC tyrosine phosphorylation was increased, and cell responsiveness to IGF-I and EGF was moderately augmented in monolayer culture on plastic. However, amplification of SHC did not potentiate proliferation of MCF-7 cells in complete serum-containing medium. This, again, was consistent with the effects observed in SHC overexpressing NIH 3T3 fibroblasts (Salcini et al., 1994). In addition, overexpression and constitutive hyperactivation of SHC did not enhance basal MAP activity in cells grown in complete medium.

Noteworthy, high levels of SHC did not promote transformation of MCF-7 cells, whereas overexpression (at a similar level) of another signaling substrate IRS-1 markedly augmented anchorage-independent growth (Surmacz and

Burgaud, 1995). Since anchorage-independent growth reflects tumorigenic potential of breast cancer cells (e.g., Sommers et al., 1990) and other cell types (e.g., Pelicci et al., 1992), our results indicate that SHC is not oncogenic in MCF-7 cells. This would suggest that although signaling pathways involved in growth factor response and mitogenicity are similar in fibroblasts and epithelial cells, those that control transformation are different.

SHC in cell adhesion. Pursuing the role of SHC in breast epithelial cells, we found that SHC regulates cells interactions with FN. SHC was found associated with $\alpha 5 \beta 1$ integrin, the FN receptor, and such complexes were more abundant in MCF-7/SHC cells than in other cell lines with normal levels of SHC expression. The increased SHC/ $\alpha 5 \beta 1$ binding was paralleled by accelerated cell attachment to FN, reduced basal motility, and inhibited proliferation on the substrate. These effects were absent on COL (whose receptor does not bind SHC in MCF-7 cells), which suggests a specific role of SHC- $\alpha 5 \beta 1$ interactions in increasing cell adhesion in MCF-7 cells.

The association of SHC with certain classes of integrins has been noted in several other cell systems. In A431 cells and other cell lines, binding and tyrosine phosphorylation of SHC to $\beta 1$ integrin was induced by cell contact with ECM or integrin cross-linking with a specific antibody (Wary et al., 1996). Similarly, an association of SHC with $\alpha 6 \beta 4$ integrin was observed in attached, but not suspended, A431 cells (Mainiero et al., 1996). EGF treatment resulted in dissociation of SHC from $\alpha 6 \beta 4$ integrin, and it has been suggested that the EGF receptor and $\alpha 6 \beta 4$ integrin compete for the same pool of SHC when transmitting their respective intracellular signals (Mainiero et al., 1996). In our system, SHC was tyrosine phosphorylated and complexed with $\alpha 5 \beta 1$ integrin even in

suspended cells. EGF did not affect the abundance or tyrosine phosphorylation of integrin-bound SHC. The adhesion of MCF-7/SHC cells to FN coincided with dissociation of p46^{SHC} from the FN receptor, whereas the stimulation of adherent cells with EGF induced p46^{SHC}/α5β1 binding. Thus, also in MCF-7 cells, there is a common SHC reserve used by the FN and EGF receptors.

In several cell types, ligation of SHC-binding integrins, but not other integrins, has been reported to enhance cell cycle progression (Wary et al., 1996). In our cell system, however, the increased association of SHC with α5β1 and the enhanced attachment to FN coincided with growth inhibition. On the other hand, downregulation of SHC in MCF-7 cells impaired cell interactions with FN and, eventually, resulted in cell death. These results imply that the SHC-α5β1 integrin complex indeed is involved in the dynamic regulation of cell adhesion and proliferation, and any imbalance in SHC expression (in plus or in minus) may critically affect these processes.

SHC overexpression and MAPK activation. Cell attachment and activation of integrins leads to the stimulation of MAPK through different pathways, e.g. c-Src-like TK-SHC-GRB2-SOS-Ras, FAK-SHC-GRB2-SOS-Ras, or FAK-GRB2-SOS-Ras (Schlaepfer & Hunter, 1997; Wary et al., 1998; Schlaepfer et al., 1994, 1998). This adhesion-dependent MAPK activity has been proposed to contribute to cell growth and survival (Wary et al., 1996, 1998; Clark & Brugge, 1995). In MCF-7 and MCF-7/SHC cells, the pattern and the extent of adhesion- or EGF-induced MAPK activation was similar on COL, but different on FN, which suggests that the observed differences were mediated by SHC bound to α5β1 integrin. This also implies that the potential activation of SHC by FAK or

other TKs, which theoretically could occur on COL, did not play a role in the regulation of MAPK in our experimental system.

On FN, the amplification of SHC corresponded to the reduced duration of adhesion-mediated MAPK response. Interestingly, in mouse fibroblasts, an early decline of MAPK activity coincided with growth inhibition, whereas a prolonged activity marked cell cycle progression (Reiss et al., 1998). Thus, the abbreviated MAPK response in MCF-7/SHC cells could reflect their significantly slower growth on FN. EGF-induced MAPK between 15 min and 1 h following treatment was stronger in SHC overexpressing cells, however, this early effect was sufficient to enhance growth on FN. Recent data indicate that adhesion-dependent MAPK response is a bi-phasic event, with the early phase controlled by Ras and the later step by PKC (Howe & Juliano, 1998). Our results suggest that increased SHC- $\alpha 5\beta 1$ integrin interactions may augment the first phase, but reduce the second, which in consequence interferes with cell proliferation.

SHC and motility. The levels of SHC affect cell migration. In A549 adenocarcinoma cells, overexpressed SHC potentiated cell HGF-induced cells motility. In MCF-7 cells, reduction of SHC levels impaired EGF-stimulated migration. In accordance with these results, EGF or IGF-I stronger induced motility of MCF-7/SHC clones than other control cell lines when tested in FN-coated inserts. Noteworthy, however, basal migration of SHC overexpressing clones on FN was significantly reduced compared with that of MCF-7 or MCF-7/IRS-1 cells. Most likely, this reflects stronger adhesion of MCF-7/SHC cells to the substrate.

In summary, in MCF-7 cells, the impact of the amplified SHC on cell growth and transformation is not significant, however, SHC plays an important

role in the regulation of cell adhesion and motility on FN. The significance of SHC-mediated interactions with FN in breast cancer metastasis are not known and will be pursued in an animal model.

MATERIALS AND METHODS

Cell Lines and Cell Culture Conditions. MCF-7 cells are estrogen receptor positive cells of a low tumorigenic and metastatic potential. The growth of MCF-7 cells is controlled by estrogens, such as estradiol (E2), and growth factors, such as IGF-I and EGF (Surmacz and Burgaud, 1995; Guvakova and Surmacz, 1997). MCF-7 cells express several integrins, including $\alpha 5 \beta 1$ (FN receptor), $\alpha 2 \beta 1$ (COL receptor), $\alpha 3 \beta 1$ (COL/FN/laminin 5 receptor) and $\alpha v \beta 3$ (vitronectin receptor) (Doerr and Jones, 1996).

MCF-7/SHC clones 1 and 9 are MCF-derived cells stably transfected with the expression plasmid pcDNA3/SHC containing a human SHC cDNA encoding p55^{SHC} and p47^{SHC}. The clones expressing the transgene were selected in 2 mg/ml G418, and the levels of SHC expression in 20 G418-resistant clones were determined by Western blotting (WB).

As control cells, we used several MCF-7-derived clones with modified growth factor signaling pathways, specifically, MCF-7/IRS-1, clones 3 and 18 that are MCF-7 cells overexpressing IRS-1 (Surmacz and Burgaud, 1995); MCF-7/IGF-IR, clone 17 that is an MCF-7-derived clone overexpressing the IGF-IR (Guvakova and Surmacz, 1997), and MCF-7/anti-SHC, clone 2 with SHC levels decreased by 50% due to the stable expression of an anti-SHC RNA (Nolan et al., 1997).

MCF-7 cells were grown in DMEM:F12 (1:1) containing 5% calf serum (CS). MCF-7-derived clones were maintained in DMEM:F12 plus 5% CS plus 200 ug/ml G418. In the experiments requiring E2- and serum-free conditions, the cells were cultured in phenol red-free DMEM containing 0.5 mg/ml BSA, 1 uM FeSO₄ and 2 mM L-glutamine (referred to as PRF-SFM).

Monolayer Growth Assay. Cells were plated at a concentration 2×10^5 in 6-well plates in the growth medium; the following day (day 0), the cells were shifted to PRF-SFM containing 1 or 20 ng/ml IGF-I or 1 or 10 ng/ml EGF. After 4 days, the number of cells was determined by direct counting.

Anchorage-Independent Growth Assay. Transforming potential of the cells (anchorage-independence) were measured by their ability to form colonies in soft agar. The cells, 1×10^3 /35 mm plate, were grown in a medium solidified with 0.2% agarose. The solidified medium contained either (i) DMEM:F12 supplemented with 10% FBS or 5% CS, or (ii) PRF-SFM with either 200 ng/ml IGF-I, 50 ng/ml EGF, or 200 ng/ml IGF-I plus 50 ng/ml EGF. After 21 days of culture, the colonies greater than 100 um in diameter were counted using an inverted phase-contrast microscope.

Adhesion Assay. Cells synchronized for 24 h in PRF-SFM were plated in 60 mm plates coated with FN (50 ug/ml). To inactivate $\alpha 5 \beta 1$ integrin, the cells were incubated with a blocking $\alpha 5 \beta 1$ Ab 10 ug/ml (Chemicon) for 30 min before plating. Cell morphology was recorded using an inverted phase-contrast microscope with a camera.

Growth on FN. Cells (0.5×10^5 /ml) were seeded in 12-well plates coated with FN (50ug/ml) in normal growth medium with or without EGF (10, 50 or 100 ng/ml) or IGF-I (20 or 100 ng/ml). The cells were counted after 4 days of culture.

Motility Assay. Motility was tested in modified Boyden chambers containing porous (8 mm) polycarbonate membranes. The underside of membranes was coated with either 200 ug/ml COL IV or 50 ug/ml FN, as described by Mainiero et al., 1996. According to this protocol, COL or FN cover not only the underside of the membrane, but also diffuse into the pores where cell contact with ECM is initiated. 2×10^4 of synchronized cells suspended in 200 ul of PRF-SFM were plated into upper chambers. Lower chambers contained 500 ul of PRF-SFM with EGF (1 and 10 ng/ml) or IGF-I (20 ng/ml). After 12 h, the cells in the upper chamber were removed, while the cells that migrated to the lower chamber were fixed with Coomassie Blue and counted under the microscope.

Immunoprecipitation and Western Blotting. The expression of SHC was assessed in 500 ug of protein lysate by immunoprecipitation (IP) with an anti-SHC polyclonal antibody (pAb) (Transduction Laboratories), followed by Western Blotting (WB) with an anti-SHC mAb (Transduction Laboratories). Tyrosine phosphorylation of SHC was measured by WB using an anti-phosphotyrosine mAb PY20 (Transduction Laboratories). The levels of $\alpha 5 \beta 1$ integrin were assessed in 1 mg of protein lysate by IP and WB using an anti- $\alpha 5 \beta 1$ pAb (Chemicon). The amounts of integrin-associated SHC were measured in $\alpha 5 \beta 1$ immunoprecipitates with an anti-SHC pAb (Chemicon). The intensity of

bands representing relevant proteins was measured by laser densitometry scanning.

MAPK Activity. The tyrosine phosphorylated forms of p42 and p44 MAPK were identified by WB in 50 ug of whole cell lysates with an anti-active ERK mAb (Promega). Adhesion-induced MAP kinase activity was assessed in cells plated either on plastic, COL IV or FN and then lysed at different times after plating (0-24h). To determine EGF-induced MAP activity, the cells were plated on different substrates, allowed to attach for 1h, and then treated with 10 ng/ml EGF. The cells were lysed at different times (0-24h) of the treatment and MAP activity was measured as described above.

Statistical Analysis. The results of cell growth experiments were analyzed by Student t-test.

ACKNOWLEDGMENTS

This work was supported by the following grants and awards: NIH DK 48969 (E.S.); U.S. Department of Defense DAMD17-96-1-6250 (E.S.) and DAMD 17-97-1-7211 (M.A.G.); CNR Italy fellowships (D.S and M.S.), University of Calabria postdoctoral fellowship in Animal Biology (L.M.) and POP 1998 grant from Regione Calabria (S.A.).

REFERENCES

- Akiyama, S. K., Olden, K. & Yamada, K. M. (1995). *Cancer Metast. Rev.*, **14**, 173-189.
- Biscardi, J. S., Belsches, A. P. & Parsons, S. J. (1998). *Mol. Carcinogen.*, **21**, 261-272.
- Cary, L. A., Han, D. C., Polte, T. R., Hanks, S. K. & Guan, J-L. (1998). *J. Cell Biol.*, **140**, 211-221.
- Clark, E. A. & Brugge, J. S. (1995). *Science*, **268**, 233-239.
- Dedhar, S. (1995). *Cancer Metast. Rev.* **14**, 165-172.
- Doerr, M. E. & Jones, J. I. (1996). *J. Biol. Chem.*, **271**, 2443-2447.
- German, N. S. & Johanning, G. L. (1997). *Cancer Let.*, **118**, 95-100.
- Giancotti, F. G. (1997). *Cur. Opin. Cell Biol.*, **9**, 691-700.
- Giorgetti, S., Pelicci, P. G., Pelicci, G. & Van Oberghen, E. (1994). *Eur. J. Bioch.*, **223**, 195-202.
- Gui, G. P., Puddefoot, J. R., Vinson, G., P., Wells, C. A. & Carpenter, R. (1997). *Br. J. Cancer*, **75**, 623-633.
- Guvakova, M. A. & Surmacz, E. (1997). *Exp. Cell Res.* **231**, 149-162.
- Habib, T., Herrera, R. & Decker, S. J. (1994). *J. Biol. Chem.*, **269**, 25243-25246.
- Howe, A. & Juliano, R. L. (1998). *J. Biol. Chem.*, **273**, 27268-27274.
- Kavanaugh, W. M. & Williams, L. T. (1994). *Science*, **266**, 1862-1865.
- Lafrancone, L., Pelicci, G., Brizzi, M. F., Aronica, M. G., Casciari, C., Giuli, S., Pegoraro, L., Pawson, T. & Pelicci, P. G. (1995). *Oncogene*, **10**, 907-917.
- Liu, L., Damen, J. E., Cutler, R. L. & Krystal, G. (1994). *Mol. Cell. Biol.* **14**, 6926-6935.

- Mainiero, F., Pepe, A., Wary, K. K., Spinardi, L., Mohammadi, M., Schlessinger, J. & Giancotti, F. G. (1995). *EMBO J.*, **14**, 4470-4481.
- Mainiero, F., Pepe, A., Yeon, M., Ren, Y. & Giancotti, F. G. (1996). *J. Cell Biol.*, **134**, 241-253.
- Matsuda, M., Ota, S., Tanimura, R., Nakamura, H., Matuoka, K., Takenawa, T., Nagashima, K. & Kurata, T. (1996). *J. Biol. Chem.*, **271**, 14468-14472.
- Migliaccio, A., Di Domenico, M., Castoria, G., de Falco, A., Bontempo, P., Nola, E. & Auricchio, F. (1996). *EMBO J.*, **15**, 1292-1300.
- Migliaccio, E., Mele, S., Salcini, A. E., Pelicci, G., Lai, K. M., Supreti-Furga, G., Pawson, T., Di Fiore, P. P., Lafrancone, L. & Pelicci, P. G. (1997). *EMBO.*, **16**, 706-716.
- Nolan, M., Jankowska, L., Prisko, M., Xu, S., Guvakova, M. & Surmacz, E. (1997). *Int. J. Cancer*, **72**, 828-834.
- Okada, S., Kao, A. W., Ceresa, B. P., Blaikie, P., Margolis, B. & Pessin, J. E. (1997). *J. Biol. Chem.*, **272**, 28042-28049.
- Pelicci, G., Giordano, S., Zhen, Z., Salcini, A. E., Lafrancone, L., Bardeli, A., Panayotou, G., Waterfield, M. D., Ponzetto, C. Pelicci, P. G. & Comoglio, P. M. (1995b) *Oncogene*, **10**, 1631-1638.
- Pelicci, G., Lafrancone, L., Grignani, F., McGlade, J., Cavallo, F., Forni, G., Nicoletti, I., Grignani, F., Pawson, T. & Pelicci, P. G. (1992). *Cell*, **70**, 93-104.
- Pelicci, G., Lafrancone, L., Salcini, A. E., Romano, A., Mele, S., Borrello, M. G., Segatto, O., Di Fiore, P. P. & Pelicci, P. G. (1995a). *Oncogene*, **11**, 899-907.
- Pozzi, A., Wary, K. K., Giancotti, F. G. & Gardener, H. A. (1998). *J. Cell Biol.*, **142**, 587-594.

- Reiss, K., Valentinis, B., Tu, X., Xu, S. & Baserga, R. (1998). *Exp. Cell Res.*, **242**, 361-372.
- Sachs, M., Weidner, K. M., Brinkmann, V., Walther, I., Obermeier, A., Ullrich, A. & Birchmeier, W. (1996). *J. Cell Biol.* **133**, 1095-1107.
- Salcini, A. E., McGlade, J., Pelicci, G., Nicoletti, I., Pawson, T., & Pelicci, P.G. (1994). *Oncogene*, **9**, 2827-2836.
- Sasaoka, T., Rose, D. W., Jhun, B. H., Saltiel, A., R., Draznin, B. & Olefsky, J. M. (1994). *J Biol. Chem.*, **269**, 13689-13694.
- Schlaepfer, D. D. & Hunter, T. (1997). *J. Biol. Chem.*, **272**, 13189-13195.
- Schlaepfer, D. D., Jones, K. C. & Hunter, T. (1998). *Mol. Cell. Biol.*, **18**, 2571-2585.
- Sommers, C. L., Papagerge, A., Wilding, G., & Gelmann, E. P. (1990). *Cancer Res.*, **50**, 67-71.
- Stein, D., Wu, J., Fuqua, S. A., Roonprapunt, C., Yajnik, V., D'Eustachio, P., Moskow, J. J., Buchberg, A. M., Osborne, K. & Margolis, B. (1994). *EMBO J.*, **13**, 1331-1340.
- Stevenson, L. E. & Frackelton, A. R. (1998). *Breast Cancer Res. Treatm.*, **49**, 119-128.
- Surmacz, E. & Burgaud, J-L. (1995). *Clin. Cancer Res.* **1**, 1429-1436.
- Tawil, N. J., Gowri, V., Djoneidi, M., nip., J., Carbonetto, S. & Brodt. P. (1996). *Int. J. Cancer*, **66**, 703-710.
- Wary, K. K., Mainiero, F., Isakoff., S. J., Marcantonio, E. E., & Giancotti, F. G. (1996). *Cell*, **87**, 733-743.
- Wary, K. K., Mariotti, A., Zurzolo, C. & Giancotti, F. G. (1998). *Cell*, **94**, 625-634.

Yamada, K. M. & Geiger, B. (1997). *Current Opin. Cell Biol.*, **9**, 76-85.

TABLES

Tab. 1. Anchorage-Independent Growth of MCF-7/SHC Cells

| Number of Colonies | | | | | |
|--------------------|---------|-------|---------------|-------------|-----------------------|
| Cell Line | 10% FBS | 5% CS | SFM+ IGF-I | SFM+ EGF | SFM+ IGF-I +EGF |
| MCF-7 | 172 | 105 | 2 | 1 | 12 |
| MCF-7/SHC, 1 | 164 | 90 | 0 | 0 | 9 |
| MCF-7/SHC, 9 | 155 | 88 | 0 | 0 | 10 |
| MCF-7/IRS-1, 3 | 213 | 131 | 25 | 10 | 22 |

The cells were tested in soft agar as described under Materials and Methods. The agar-solidified medium was either DMEM:F12 with 10% FBS, or 5% CS, or PRF-SFM with EGF (200 ng/ml), IGF-I (50 ng/ml), or EGF plus IGF-I (50 ng/ml plus 200 ng/ml, respectively). MCF-7/IRS-1, clone 3, characterized by an increased transforming potential (Surmacz and Burgaud, 1995), was used as a positive control. The experiment was repeated 7 times. Average number of colonies of the size at least 100 μ m in diameter is given.

Tab. 2. Growth of MCF-7/SHC cells on FN

| Cell Number | | | |
|--------------|-------------------|-------------------|-------------------|
| Cell Line | 5%CS | 5% CS +EGF | 5% CS+ IGF-I |
| MCF-7 | 2.2×10^5 | 2.2×10^5 | 2.4×10^5 |
| MCF-7/SHC, 1 | 1.1×10^5 | 1.0×10^5 | 1.3×10^5 |
| MCF-7/SHC, 9 | 0.9×10^5 | 0.8×10^5 | 1.1×10^5 |

The growth of cells on FN in either normal growth medium (DMEM:F12 + 5% CS) or growth medium containing EGF (100 ng/ml) or IGF-I (100 ng/ml) was tested as described under Materials and Methods. The cells were plated at the concentration 0.5×10^5 cells/ml and counted after 4 days of culture. The values represent cell number/ml, and are average results from 3 independent experiments.

FIGURE LEGENDS

Fig. 1. MCF-7/SHC cells. A. SHC expression and tyrosine phosphorylation.

The protein levels and tyrosine phosphorylation of SHC in two selected MCF-7/SHC clones 1 and 9 were determined by IP and WB with specific antibodies as detailed under Materials and Methods. Cell lysates were isolated from logarithmic cultures maintained in normal growth medium. **B. Growth response of MCF-7/SHC cells to IGF-I and EGF.** The cells were synchronized in PRF-SFM and stimulated with mitogens for 4 days as described in Materials and Methods.

Abscissa, cell lines; ordinate, the percentage of growth increase over that in PRF-SFM. Dotted bars, low doses: IGF-I 1 ng/ml or EGF 1 ng/ml; striped bars, high doses, IGF-I 20 ng/ml or EGF 10 ng/ml. High doses of IGF-I or EGF are the EC₅₀ concentrations in these cells. SD is marked by solid bars; asterisks indicate statistically significant differences ($p \leq 0.05$) between the growth responses of MCF-7/SHC cells and identically treated MCF-7 cells. The results are average of 4 experiments.

Fig. 2. SHC associates with $\alpha 5\beta 1$ integrin. The amounts of SHC associated with $\alpha 5\beta 1$ in MCF-7/SHC cells, MCF-7 cells, and several control clones with normal SHC levels but increased levels of IRS-1 (MCF-7/IRS-1, clones 3 and 18) or the IGF-IR (MCF-7/IGF-IR, clone 17) were determined by IP with an anti- $\alpha 5\beta 1$ pAb and WB with an anti-SHC pAb (a). The expression of $\alpha 5\beta 1$ integrin in the cells tested was determined after stripping the above blot and reprobing with the anti- $\alpha 5\beta 1$ pAb (b).

Fig. 3. Adhesion of MCF-7/SHC clones on FN. MCF-7/SHC clones 1 and 9 (amplified SHC), MCF-7 cells (normal SHC levels) and MCF-7/anti-SHC, clone 2 (reduced SHC levels) were synchronized for 24h in PRF-SFM and plated on FN (50 ug/ml) in PRF-SFM. The cells were photographed at times 0 (A), 1h (B), and 2h (C). The role of $\alpha 5\beta 1$ integrin in the adhesion of MCF-7/SHC clones 1 and 9 was assessed by blocking the FN receptor with a specific antibody 30 min before cell plating (D), as described in Materials and Methods. The long-term (24 h) adhesion of MCF-7 and MCF-7/anti-SHC, clone 2 is shown in panels D'.

Fig. 4. Adhesion-induced (A) and EGF-dependent (B) MAPK activity in MCF-7/SHC cells. To measure adhesion-induced MAP kinase activity (A), MCF-7 and MCF-7/SHC cells were plated on plastic, COL IV or FN. The cells were lysed at the indicated times after plating. The tyrosine phosphorylated forms of p42 and p44 MAPK were determined as described under Materials and Methods. EGF-induced MAP kinase activity (B) was determined in MCF-7 and MCF-7/SHC cells. The cells were plated on plastic, COL IV or FN, allowed to attach for 1h, and then treated with 10 ng/ml EGF. The cells were lysed at different times (0-24h) of the treatment. In (A) and (B), representative results demonstrating MAPK response in MCF-7 cells and MCF-7/SHC, clone 1 are shown.

Fig. 5. Motility of MCF-7/SHC cells in FN or COL inserts. The motility of MCF-7/SHC cells and several control cell lines with normal SHC levels was tested as described under Materials and Methods. The upper and lower chambers contained PRF-SFM. Growth factor-induced motility was assessed by

supplementing PRF-SFM in lower chambers with either EGF (1 or 10 ng/ml) or IGF-I (20 ng/ml). The percentage of cells that migrated to the underside of inserts (relative to the number of cells plated) is designated as % Motility.. The experiments were repeated 4 times. Average values are given. Asterisks indicate statistically significant (*, $p \leq 0.05$, **, $p \leq 0.01$) differences between the basal and growth factor induced migration of a given cell line.

Fig. 6. SHC/ $\alpha 5\beta 1$ association is modulated during attachment to FN. The association of SHC with $\alpha 5\beta 1$ integrin was determined in 1 mg of protein lysate of MCF-7/SHC, clones 1 and 9. The lysates were IP with an anti- $\alpha 5\beta 1$ pAb and immunoblotted with an anti-phosphotyrosine antibody PY20 (a). Subsequently, the blots were stripped and reprobed with an anti-SHC pAb (b). SHC/ $\alpha 5\beta 1$ associations are shown in cells either before plating on FN (Floating), spread on FN for 1 h (Attached) or partially detached upon the treatment with 10 ng/ml EGF for 1 h (Detached). The experiment was repeated 3 times; a representative blot demonstrating the SHC/ $\alpha 5\beta 1$ complex in MCF-7/SHC, 1 cells is shown.

probes, have been conducted to examine the expression of β_2 and β_1 mRNA in fetal hamster pancreas from untreated and ethanol treated dams. This project has been funded by grant #RO1CA42829.

#1156 The α_7 nicotinic acetylcholine receptor is expressed in normal and neoplastic lung cells. Plummer III, H.K., and Schuller, H.M. *Experimental Oncology Laboratory, Department of Pathology, University of Tennessee, Knoxville, TN 37996.*

In previous research, we have demonstrated that the growth of small cell lung cancer (SCLC) cell lines is regulated by neuronal nicotinic receptors with high affinity to α -bungarotoxin, and that the nicotine derived nitrosamine, 4(methylnitrosamino)-1-(3-pyridyl)-1-butanone (NNK), a potent lung carcinogen, bound to this receptor with high affinity (Biochem. Pharmacol. 55:1377, 1998). Molecular cloning by Couturier et al. (1990) has demonstrated that the binding domain for α -bungarotoxin is the α_7 nicotinic acetylcholine receptor (Neuron 5:847). We are now investigating this receptor in normal and neoplastic lung cells by molecular methods. Using reverse transcription-polymerase chain reaction (RT-PCR), we have screened several cell lines for the presence of α_7 . Two SCLC cell lines, H-69 and H-82, show expression of α_7 . In addition, normal hamster fetal neuroendocrine lung cells and a fresh tissue sample from an atypical human lung carcinoma also express α_7 . We are currently investigating the effects of nicotine and nitrosamines on the expression and function of α_7 by RT-PCR and ribonuclease protection assays. Supported by PHS grant RO1CA51211.

#1157 Epidermal growth factor receptor (EGFR) is involved in normal urothelial regeneration. Daher, A., El-Marjou, A., De Boer, W., Abbou, C., Thiery, J.P., Van Der Kwast, T., Chopin, D., and Radvanyi, F. *Centre de recherches chirurgicales, Hôpital Henri Mondor, Créteil and Unité 144 CNRS, Institut Curie, Paris, France.*

Introduction: Previous studies established that EGF family of growth factor receptors are expressed in human urothelium. Our group previously reported the functional effects of EGF family of growth factors on the proliferation of normal human urothelial cells (De Boer, 1996). In the current study, we investigated the implication of EGFR on urothelial regeneration using an *in vitro* culture model.

Materials and methods: Using the previously reported organoid-like culture model of urothelium, six 4 mm holes were performed using a biopsy puncher on confluent cultures. Urothelial regeneration was measured at different time intervals after the wounding (4h, 24h and 48h) on fixed stained membranes using an image analyser. We studied the effect of several inhibitors of the EGFR: 1) a specific tyrosine kinase inhibitor (AG1478) and a similar compound which is not an EGFR inhibitor (AG63) 2) a blocking EGFR antibody (LA22) 3) an anti-EGF antibody (10825.1), on the proliferation and the migration of urothelial cells.

Results: In this model, the regeneration of a 12,56 mm² defect is obtained in 48h. The regeneration is inhibited by the AG1478, the blocking anti-EGFR antibody and to a lesser extent by the EGF antibody. Urothelium wound repair involved both migration and proliferation. We showed that both proliferation and migration were affected by the EGFR inhibitors. These results indicate that the EGFR signalling pathways is involved in urothelial regeneration.

#1158 The effect of IGF-I on proliferation and secretion of IGFBP-2 in human breast cancer cell lines. P. Maxwell and H.W. van den Berg, *Dept. Oncology, The Queen's University of Belfast, Belfast BT9 7BL, Northern Ireland.*

IGF-I binding proteins (IGFBP's) are important modulators of IGF-I action. We have previously shown that development of anti-estrogen resistance and estrogen independence in human breast cancer cells *in vitro* is associated with a reduction in the level of secretion of IGFBP-2, and have suggested a growth inhibitory role for this binding protein. In this study we have investigated the effects of IGF-I on proliferation and IGFBP-2 secretion together with the modulating effect of exogenous IGFBP-2 on IGF-I mediated effects on cell proliferation. IGF-I (1–75 ng ml⁻¹) stimulated the proliferation of ZR-75-1 and MCF-7 cells in serum-free medium (SFM) in a dose dependent manner, with maximal effects being observed at approximately 20 ng ml⁻¹. The proliferation of an estrogen independent variant of ZR-75-1, ZR-PR-LT, and a tamoxifen resistant variant of MCF-7, LY2, was also stimulated by IGF-I. These stimulatory effects of IGF-I on cell proliferation were accompanied in all cell lines by a reduction in the levels of IGFBP-2 recovered in conditioned SFM, with maximal effects being again observed at approximately 20 ng ml⁻¹ IGF-I. Exogenous IGFBP-2 (4–32 nM) reversed the growth stimulatory effects of IGF-I (3.29 nM) and a degree of dose-dependency was also observed. IGFBP-2 alone exhibited variable IGF-I independent effects on cell proliferation, being either without effect (ZR-75-1), growth inhibitory (ZR-PR-LT) or growth stimulatory (MCF-7 and LY2). These data provide further evidence for a growth inhibitory role for IGFBP-2 via inhibition of the actions of IGF-I, but also suggest more complex cell specific effects independent of IGF-I.

#1159 Tyrosine kinase activity of the IGF-IR is required for the development of breast cancer cell aggregates in three-dimensional culture. Guvakova, M. A., Surmacz, E. *Kimmel Cancer Institute, Thomas Jefferson University, Philadelphia, PA 19107.*

In human breast carcinomas, the expression and tyrosine kinase activity of the insulin-like growth factor type I receptor (IGF-IR) is increased relative to normal

breast epithelium. However, the consequences of such IGF-IR amplification in the development and progression of breast cancer are yet to be fully defined. To further explore the functional role of the IGF-IR kinase in breast cancer biology, we developed stable clones of MCF-7 breast cancer cells overexpressing kinase-deficient mutants of the human IGF-IR. IGF-IR-mediated signaling and three-dimensional (3-D) cell growth on the extracellular matrix (ECM) were investigated using the clones with the highest levels of mutant IGF-IRs. The overexpression of the IGF-IR/YF3 mutant, containing a triple tyrosine mutation in the kinase domain, abolished several IGF-I-dependent effects, including tyrosine phosphorylation of the IGF-IR and its substrates IRS-1 and SHC, formation of downstream signaling complexes of IRS-1/PI-3-kinase and SHC/Grb-2, and activation of MAP kinases (ERK1/ERK2). The overexpression of the IGF-IR/KR, with an inactive tyrosine kinase ATP-binding site, abrogated SHC signaling, reduced IGF-IR and IRS-1 tyrosine phosphorylation, and attenuated MAP kinase activity. In 3-D culture, the clones expressing the dominant-negative IGF-IR mutants demonstrated significantly reduced compared to MCF-7 cells ability to form large multicellular aggregates ($\geq 300 \mu\text{m}$): 57% and 97% inhibition in cells overexpressing IGF-IR/YF3 and IGF-IR/KR, respectively. The kinase-deficient IGF-IR mutants, however, retained the ability to localize at cell-cell contacts and associate with adherence junction proteins E-cadherin, α - and β -catenins. We conclude that IGF-IR tyrosine kinase activity is required for the development of the large aggregates of breast tumor cells growing on ECM in 3-D culture. (Supported by DAMD 17-97-1-7211 and NIH DK 48969)

#1160 Mitogenic functions of Insulin-like growth factor-1 (IGF-I) require MAP kinase pathway activation in CNS primitive neuroectodermal tumor (PNET) / medulloblastoma (MB). Patti, R., Reddy, C.D., Georger, B., Grotzer, M., Sutton, L. and Phillips, P. *Department of Neuroscience and Neurosurgery, Children's Hospital of Philadelphia, Philadelphia PA 19104.*

IGF-I supports cell survival and growth in normal neuronal cells. To assess the role of IGF-I mediated cell proliferation in CNS neuroectodermal tumors, we examined mitogenic effects of IGF-I and signaling pathways associated with IGF-I stimulation in DAOY PNET/MB cells. RT-PCR analysis confirmed that IGF-I is an autocrine factor for 7/7 PNET/MB cell lines studied. Treatment of DAOY with recombinant IGF-I increased tumor cell growth rates. IGF-I mitogenic effects are mediated by rapid phosphorylation of IGF-I receptor and is inhibited by blocking antibody (1H7). Binding of IGF-1 to IGF-1R increases ERK kinase activity, evidenced by histone phosphorylation. Inhibition of MAP kinase pathway by a MEK inhibitor (PD 98059) blocked IGF-I mitogenic effects and inhibited DAOY cell growth. These results demonstrate that IGF-I is an autocrine growth factor in PNET cell lines whose mitogenic effects are mediated by the MAP kinase pathway.

#1161 Downregulation of the insulin-like growth factor I receptor by antisense can reverse transformed phenotypes of HPV positive and negative human cervical cancer cell lines. Hongo, A., Nakamura, K., Yoshinouchi, M., and Kudo, T. *Okayama University Medical School, Okayama 700-8558, Japan.*

Insulin-like Growth Factor I Receptor (IGF-IR) plays an essential role in the establishment and maintenance of transformed phenotype, and blockage of IGF-IR pathway by antisense or dominant negatives causes reversal of transformed phenotypes in many rodent and human tumor cell lines. It was reported that expression of both E6 and E7 proteins of human papilloma virus (HPV) transformed R-cells that were generated from mouse embryo fibroblast by targeted disruption of IGF-IR gene. We transfected IGF-IR antisense mRNA expression plasmid into HPV18 positive Hela S3 cell line and HPV negative C33a cell line to figure out that IGF-IR could be a target for cervical cancer cells especially in the presence of HPV. Stable clones were selected under G418 and used for the study. Approximately 30–80% downregulation of IGF-IR level was observed by western blot in antisense clones. There was little difference in monolayer growth. In C33a cells, wild type and sense clones formed 92–146 colonies in soft agar after 3 weeks, antisense clones formed less than 12 colonies. In Hela S3 cells, wild type and sense clones formed 238–291 colonies in soft agar after 2 weeks, antisense clones formed 14–160 colonies. There was a good correlation between IGF-IR downregulation level and inhibition of transformation in soft agar. This result indicates that downregulation of IGF-IR by antisense can reverse transformed phenotype of human cervical cancer cells even in the presence of HPV proteins.

#1162 Construction of a TGF- β 1 carrying vector which induces growth inhibition in epithelial cancer cells. Zeinoun, Z., Teugels, E., Vermeij, J., Neyns, B., De Grève, J. *Laboratory of Medical Oncology & Department of Medical Oncology, Oncologisch Centrum, Akademisch Ziekenhuis Vrije Universiteit Brussel, Belgium.*

Transforming Growth Factor β 1 is a secreted polypeptide which has the capacity to induce an autocrine growth suppression in many epithelial cells. The loss of the autocrine growth suppressive circuit of TGF- β 1 may be an important step in cancer formation since many cancer cells lose their sensitivity to TGF- β 1's growth inhibition and many others retain the responsiveness but do not produce enough active peptide to sustain the autocrine growth suppressive loop (Zeinoun et al, Anticancer Res. *in press*). For the latter kind of cancer cell types, it would be a good idea to introduce a DNA sequence which codes for the bioactive peptide. Therefore TGF- β 1 cDNA has been point mutated by site directed mutagenesis to

129 Modulation of platelet-derived growth factor β -receptor signalling by CIs/SOCS proteins

Eva Grönroos, Sigridur Valgeirsdóttir, Carl-Henrik Heldin, Akihiko Yoshimura* and Ivan Dikic

Ludwig Institute for Cancer Research, Uppsala, Sweden, *Institute of Life Science Kurome University, Kurume, Japan

CIS (Cytokine Inducible SH2-containing Proteins) or as they are also known, SOCS proteins (Suppressors of Cytokine Signalling) belong to a recently cloned group of proteins acting as negative regulators of cytokine induced STAT signalling. In CIS/SOCS proteins, the N-terminal region is followed by a SH2 domain and a C-terminal motif called the CIS homology (CH) domain or SOCS box. CIS/SOCS proteins have been found to interact with different cytosolic kinases such Jak2, Tec and Pyk2, but also with receptors such as the FGF receptor, c-kit receptor and EPO receptor. Since Platelet-derived growth factor (PDGF) β -receptor has been shown to activate different STAT proteins, we investigated if CIS/SOCS proteins also can interact with PDGF β -receptor and suppress PDGF-induced STAT activation.

HA-tagged PDGF β -receptor and the Myc-tagged CIS1, JAB/SOCS1 or CIS3/SOCS3 were transiently transfected into Cos1 or 293T cells and probed for interaction by immunoprecipitation. All three proteins co-precipitated with the β -receptor as revealed by immunoblotting. Interestingly, co-expression of CIS/SOCS proteins reduced the total tyrosine phosphorylation of the PDGF β -receptor. *In vitro*, PDGF β -receptor kinase activity was reduced in cells over-expressing CIS/SOCS proteins as compared to control cells. To investigate the role of CIS/SOCS proteins in PDGF-induced STAT activation, the transcriptional activity of STAT5 was measured in transiently transfected cells. In comparison to control cells, PDGF-induced STAT5 activation was reduced by 40-60% in the presence of CIS/SOCS proteins. In all the mentioned results, PDGF β -receptor function was most affected by CIS3 over expression. These results indicate that CIS/SOCS proteins may act as negative regulators of PDGF-induced signalling. The mechanism of this modulation *in vivo* is currently under investigation.

131 IGF-IR Tyrosine Kinase is Required for Breast Cancer Epithelial Cell Motility. Marina A. Guvakova and Ewa Surmacz. Kimmel Cancer Institute, Thomas Jefferson University, Philadelphia, PA 19107, USA.

Insulin-like growth factor (IGF-I) is known to promote the motility of different cell types. We investigated the role of IGF-I receptor (IGF-IR) signaling in motility of MCF-7 breast epithelial cells over-expressing either the wild type or kinase-inactivated mutants of the IGF-IR. The elevated level of the wild type IGF-IR correlated with augmented migration of cells *in vitro*, whereas migration was not increased in cells over-expressing the similar level of the catalytically inactive IGF-IR. IGF-I stimulation of subconfluent wild type IGF-IR over-expressing cells induced rapid morphological transition towards mesenchymal phenotype and resulted in disruption of polarized cell monolayer. Immunofluorescence staining of IGF-I-treated cells with rhodamine-phalloidin revealed dynamic changes in the actin cytoskeleton marked by disassembly of long actin fibers within 5 min, followed by development of meshwork of short actin bundles localized to multiple membrane protrusions. In parallel, IGF-I induced transient dephosphorylation of focal adhesion-associated proteins: p125 focal adhesion kinase (FAK), p130 Crk-associated substrate (Cas) and paxillin. Pretreatment of cells with 5 μ M phenylarsine oxide (PAO), an inhibitor of phosphotyrosine phosphatases, rescued FAK and its associated proteins Cas and paxillin from IGF-I-induced tyrosine dephosphorylation. PAO also inhibited development of IGF-I-induced membrane protrusions and blocked cell migration. Our results suggest that IGF-IR tyrosine kinase directly or indirectly activates a putative tyrosine phosphatase acting upon focal adhesion proteins. IGF-IR signaling is required for dynamic remodeling of the actin cytoskeleton and focal adhesion contacts during IGF-I-induced motility in MCF-7 cells. (DAMD 17-97-1-7211, NIH DK 48969)

130 IGF-I but not GH regulates Insulin-like Growth factor Binding Protein-3 gene expression in MG-63 human osteosarcoma cells: underlying mechanisms.André GROVER^{1,4}, Roberto ROSATO¹, Katia GERLAND¹, Hélène JAMMES², Nelly BATAILLE¹, Berta SEGOVIA¹, Mohammed Rahmani¹ & Louis MERCIER¹. ¹Inserm U142 & ²U327, Paris, France, ³Laboratoire d'Endocrinologie Moléculaire, INRA, Jouy en Josas, France, and ⁴LHEA, UFR des Sciences Médicales et Pharmaceutiques, Angers, France.

Bone remodeling is closely regulated by hormones and locally expressed growth factors (e.g. Growth Hormone, Insulin-like Growth Factors -IGFs- and their binding proteins -IGFBPs). Using MG-63 human osteosarcoma cells as a model system, we have further investigated the molecular mechanism(s) underlying the control of IGFBP-3 gene expression by IGF-I.

Treatment of MG-63 cells with physiological concentrations of IGF-I (6-20 nM) led to a dose-dependent increase in IGFBP-3 mRNA, with a maximal stimulation of ~9-10-fold over unstimulated cells. RT-PCR analysis showed that this increase in IGFBP-3 mRNA was detectable as soon as 3 hours after the onset of IGF-I treatment, the steady-state amount of IGFBP-3 transcripts being then progressively increased over a 24 hours period, and remaining elevated until at least 30 hours. IGFBP-3 mRNA stability ($t_{1/2}$ ~20 hours) was identical, irrespective of the absence or presence of IGF-I treatment ($p > 0.2$, Student's *t* test; Actinomycin-D experiments). Altogether, the results support the notion that in MG-63 cells the induction of IGFBP-3 mRNA by IGF-I may not be regulated at the level of mRNA turnover.

Consistent with the increase in IGFBP-3 mRNA, Western ligand- and immuno-blot analysis of MG-63 cells conditioned medium showed that IGF-I induced a dose-dependent increase in IGFBP-3 secretion (~40-50-fold at 16 nM IGF-I and above). Its kinetics was similar to that observed for IGFBP-3 transcripts.

Although RT-PCR analysis showed that the GH receptor (hGH-R) gene is transcribed in MG-63 cells, treatment of the cells with hGH for up to 72 hours did not increase secretion of IGFBP-3 in the conditioned medium, nor induced *c-fos* (an acknowledged GH-responsive gene) gene transcription. Furthermore, transfection and co-transfection experiments have demonstrated that overexpression of recombinant hGH-R was a pre-requisite for GH-enhanced expression of GH-responsive reporter genes (GHRE-I-CAT or GHRE-II-CAT or LHRE-Luc). This increase was specific since it was abolished when the GH-responsive elements (pGHRE-I-mut, pGHRE-II-mut) were mutated. Altogether, these data suggest that the transduction pathways involved in the transcriptional activation of GH-responsive promoters by GH are functional in MG-63 osteosarcoma cells.

132 A crucial role for intact FRS2 in FGF signal transduction pathway.

Yaron R. Hadari, Arnold Lee, Irit Lax and Joseph Schlessinger. Department of Pharmacology New York University Medical Center, New York, NY, 10016, USA.

FRS2 and IRS1 are two docking proteins that link activated FGF and insulin receptors, respectively, with the Ras/MAPK signaling pathway. Each protein contains an N-terminal domain that mediate interactions with the cell membrane and with a subfamily of receptors, and C-terminal domain with numerous tyrosine phosphorylation residues that serve as docking sites for signaling proteins. Two chimeric proteins were generated and expressed in PC12 cells. One composed of the N-terminal domain of FRS2 fused to the C-terminal domain of IRS1, and a second chimera composed of the N-terminal domain of IRS1 fused to the C-terminal domain of FRS2. The chimeric protein containing the N-terminal domain of FRS2 is tyrosine phosphorylated in response to FGF stimulation, while the chimeric protein containing the N-terminal domain of IRS1 is phosphorylated only in response to insulin stimulation. Ligand stimulation leads to tyrosine phosphorylation and recruitment of Grb2 and Shp2. While overexpression of FRS2 in PC12 cells leads to enhanced MAPK activation and neurite outgrowth in response to FGF stimulation, stimulation of MAPK activation was not detected in cells expressing the chimeric proteins in response to FGF or insulin stimulation. Enhanced neurite outgrowth was detected in response to FGF stimulation in cells overexpressing the chimeric protein composed of the N-terminal domain of FRS2 fused to the C-terminal domain of IRS1. These experiments demonstrate that the amino terminal domains of FRS2 and IRS1 are essential for specific interactions with FGF and insulin receptors, and underscore the central role of FRS2 in signaling downstream of FGF receptors.

(Y. R. Hadari was supported by Long Term Fellowship from the International Human Frontier Science Program Organization (HFSP)).

IGF-IR Stimulates Breast Epithelial Cell Motility via Reorganization of the Actin Cytoskeleton, Remodeling of Focal Contacts, and Modulation of the Phosphorylation Status of Focal Adhesion Proteins: FAK, Cas and Paxillin. M. A. Guvakova, E. Surmacz. Kimmel Cancer Institute, Thomas Jefferson University, Philadelphia, PA 19107.

Insulin-like growth factor (IGF-I) is known to promote the motility of different cell types. We investigated the role of IGF-I receptor (IGF-IR) signaling in motility of MCF-7 breast epithelial cells overexpressing the wild type IGF-IR. The elevated level of the IGF-IR correlated with augmented migration of cells *in vitro*. The treatment of subconfluent serum-starved cells with 50 ng/ml IGF-I induced rapid morphological transition towards mesenchymal phenotype and resulted in disruption of polarized cell monolayer. Immunofluorescence staining of IGF-I-treated cells with rhodamin-phalloidin revealed dynamic changes in the actin cytoskeleton marked by disassembly of long actin fibers within 5-15 min, followed by development of meshwork of short actin bundles localized to multiple membrane protrusions. In parallel, IGF-I induced transient dephosphorylation of focal adhesion-associated proteins: p125 focal adhesion kinase (FAK), p130 Crk-associated substrate (Cas) and paxillin. Pretreatment of cells with 5 μ M phenylarsine oxide (PAO), an inhibitor of phosphotyrosine phosphatases, rescued FAK and its associated proteins Cas and paxillin from IGF-I-induced tyrosine dephosphorylation. PAO-pretreated cells were refractory to morphological transition and did not develop cellular protrusion in response to IGF-I. Additionally, PAO inhibited migration of MCF-7/IGF-IR cells in a time and concentration dependent manner. Our results suggest that in MCF-7 cells stimulation of the IGF-IR activates a putative tyrosine phosphatase acting upon focal adhesion proteins and promoting the reorganization of focal contacts. This process is associated with dynamic remodeling of the actin cytoskeleton. Coordinated regulation of these events is required for induction of MCF-7 cell motility.

THE SRC FAMILY KINASES FUNCTION IN THE DYNAMIC CONTROL OF EPITHELIAL ADHESIONS: IMPLICATIONS FOR CANCER CELL INVASION.

MC Frame, DW Owens, GW McLean AW Wyke and VG Brunton. The Beatson Institute for Cancer Research, Garscube Estate, Switchback Road, Bearsden, Glasgow G61 1BD, UK.

Epithelial cells are held in tight association in tissues by homophilic interactions between the cadherin family of Ca^{++} -dependent transmembrane receptors. Despite their obvious importance as biological modulators, we still lack a detailed understanding of the assembly and disassembly of cadherin-mediated cell-cell adhesions.

Here we report that, c-Yes and c-Src, and their putative substrate p120^{CTN}, undergo Ca^{++} -induced, actin-dependent, translocation to regions of cell-cell contact in keratinocytes, where they co-localise with E- and P-cadherin. Furthermore, a Src-selective tyrosine kinase inhibitor and a kinase-defective, dominant-inhibitory c-Src protein, induce epithelial cell-cell adhesion and re-distribution of E-cadherin to cell-cell contacts, even in low Ca^{++} concentrations that do not normally support stable cell-cell adhesion. Time-lapse microscopy demonstrated that Src inhibition induces stabilization of adhesions formed between randomly contacting cells, an effect also stimulated by high Ca^{++} . Consequently, cells in which the Src kinases are inhibited are unable to dissociate from an epithelial sheet. In addition, hepatocyte growth factor-induced dispersion and invasion of E-cadherin-expressing colon cancer cells into Matrigel *in vitro*, conditions under which c-Yes and c-Src localise at cell-cell adhesions and co-immunoprecipitates with E-cadherin, is also blocked by Src inhibition.

Our results demonstrate that the activity of the endogenous cellular Src family kinases disrupts epithelial cell-cell adhesions during their dynamic regulation *in vitro* and is also required to free cells from the constraints of their epithelial connections during invasion of cancer cells that retain E-cadherin. Thus, as epithelial adhesions are formed, there is recruitment of the components that both stabilize the adhesions, and also the components that induce their destabilization and disassembly.

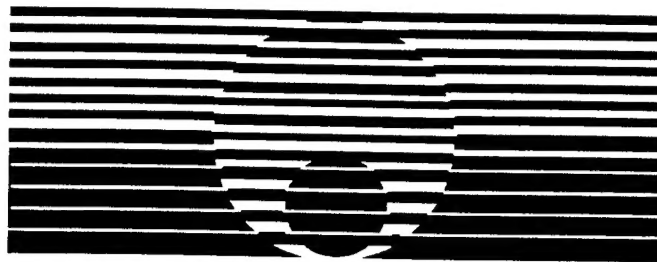
PROGRAM AND ABSTRACTS

Presented at

Fourteenth International Symposium on Cellular Endocrinology

"CELL SIGNALING AND THE CYTOSKELETON"

Sponsored By:
Adirondack Biomedical Research Institute



SEPTEMBER 24 - 27, 1998

at the
Lake Placid Resort
Lake Placid, New York

ORGANIZING COMMITTEE

Dr. Susan Jaken
Adirondack Biomedical Research Institute

and

Dr. Alan Aderem
University of Washington